



Underwater Acoustics Propagation Analysis and Modelling of Sound Emitting Devices

BY

OSHOKE WIL IKPEKHA (B.Eng., M.Sc.)

A THESIS SUBMITTED IN PARTIAL FULFILMENT OF THE
REQUIREMENT FOR THE DEGREE OF

DOCTOR OF PHILOSOPHY

SUPERVISED BY DR. STEPHEN DANIELS

SCHOOL OF ELECTRONIC ENGINEERING
DUBLIN CITY UNIVERSITY

FEBRUARY 2017

Declaration

I hereby certify that this material, which I now submit for assessment on the programme of study leading to the award of Doctor of Philosophy is entirely my own work, and that I have exercised reasonable care to ensure that the work is original, and does not to the best of my knowledge breach any law of copyright, and has not been taken from the work of others save and to the extent that such work has been cited and acknowledged within the text of my work.

Signed: _____

ID No.: 56711111

Oshoke Wil Ikpekha

Date: _____

*THIS THESIS IS DEDICATED TO GOD ALMIGHTY
AND
TO THE LOVING MEMORY OF MY BEAUTIFUL
MOTHER
MRS ANGELA EKE IKPEKHA (RIP)*

Acknowledgement

First and foremost, I would like to thank God for seeing me through to the end of this wonderful journey. I would like to thank my Supervisor Dr Stephen Daniels for his endless support, encouragement and assistance through all the tough times, without him I simply wouldn't have made it this far. I would like to thank the Irish Research Council (IRC) for the scholarship fund for the entirety of my PhD, and also the Marine and Environmental Sensing Technology Hub (MESTECH) for their assistance. I would like to thank Dr. Marissa Condon for helping to read-proof my thesis and for her support and guidance when I most needed it. I would be ungrateful not to mention my colleagues and friends Dr Asmaa Eltayeb, Dr Dhruv Gandhi, Dr Alan Armstrong and Dr Oladipupo Olaitan for their numerous help, support and comradery throughout this journey. I would also like to thank my colleagues in the energy design laboratory, plasma laboratory and all my DCU friends for all their time and support, and for making my time in DCU very sweet and bearable. I would like to acknowledge my siblings, aunties, uncles and my friends including Ms Sikirat Sanusi Smith, Mr Emmanuel Ikpekha, Fr Patrick Carroll, Mr Gbenga Oluwasanmi, Mr Rilwan Jayeola and everyone (as I can't mention every individual here) outside of academia for their love, support and belief in me, even if they didn't understand much of my work, but somehow bore the burden which I shared with them. Finally, I'll like to sign out with one of my favourite quotes from the bible:

“I returned, and saw under the sun, that the race is not to the swift, nor the battle to the strong, neither yet bread to the wise, nor yet riches to men of understanding, nor yet favour to men of skill; but time and chance happeneth to them all”, Ecclesiastes 9:11.

Abbreviations

| | |
|-------|---|
| ABC | Absorbing Boundary Condition |
| A/D | Analogue/Digital |
| AE | Acoustic Emitting |
| ANL | Ambient Noise Level |
| CODAR | Coastal Ocean Dynamics Applications Radar |
| DAQ | Data Acquisition System |
| dB | Decibel |
| DAT | Digital Audio Tape |
| DSP | Digital Signal Processing |
| ESH | End Stop Hit |
| FFT | Fast Fourier Transform |
| FEA | Finite Element Analysis |
| FEM | Finite Element Method |
| km | kilometres |
| kW | kilowatt |
| MT | Moving Translator |
| MW | megawatt |
| NM | Normal Mode |
| OWC | Oscillating Water Column |
| OWEC | Offshore Wave Energy Converter |
| PDE | Partial Differential Equation |
| PDS | Power Spectral Density |
| PE | Parabolic Equation |
| PML | Perfectly Matched Layer |
| PTO | Power Take Off |
| rms | Root Mean Squared |
| SSH | Sea Surface Height |
| STFT | Short Time Fourier Transform |

| | |
|-------|-----------------------------------|
| SONAR | Sound Navigation and Ranging |
| SPL | Sound Pressure Level |
| SWH | Significant Wave Height |
| USEV | Underwater Sound Emitting Vessels |
| UWSN | Underwater Sensor Network |
| UA | Underwater Acoustics |
| WEC | Wave Energy Converter |

Table of Contents

| | |
|---|------|
| Declaration | ii |
| Dedication | iii |
| Acknowledgement..... | iv |
| Abbreviations | v |
| List of Figures | x |
| List of Tables..... | xiv |
| Author’s Conferences & Conference Presentations..... | xv |
| Author’s Publications..... | xvi |
| Abstract | xvii |
| Chapter 1 | 1 |
| 1 Introduction..... | 1 |
| 1.1 Research Objectives | 4 |
| 1.2 Thesis Organisation | 5 |
| Chapter 2 | 7 |
| 2 Marine Energy Devices/Monitoring Systems..... | 7 |
| 2.1 WEC System and Energy Conversion..... | 7 |
| 2.2 WEC Types and Classifications | 16 |
| 2.2.1 Oscillating Water Column..... | 22 |
| 2.2.2 Point Absorber | 25 |
| 2.2.3 Attenuator..... | 26 |
| 2.2.4 Overtopping | 26 |
| Chapter 3 | 27 |
| 3 Sound Signals and Underwater Acoustics | 27 |
| 3.1 Fundamentals of Sound | 27 |
| 3.2 Underwater Acoustics | 38 |
| 3.3 Physics of Underwater Acoustics..... | 43 |
| 3.4 Underwater Acoustic Recording and Monitoring Systems..... | 46 |
| 3.5 Underwater Acoustic Modelling and Simulation..... | 48 |
| 3.6 Finite Element Modelling and Comsol | 53 |

| | |
|--|-----|
| Chapter 4 | 54 |
| 4 Marine Energy Devices and Marine Mammals | 54 |
| 4.1 Introduction | 55 |
| 4.2 Marine Mammals, Energy Devices & Noise..... | 55 |
| 4.3 Model Description | 56 |
| 4.4 Results and Discussions | 61 |
| 4.5 Conclusion..... | 65 |
| Chapter 5 | 66 |
| 5 Noise from Ferries and the Potential Effect of Sea State on their Propagation: A Dublin Bay Port Area Study | 66 |
| 5.1 Introduction | 67 |
| 5.2 Methodology | 68 |
| 5.3 Results & Discussion..... | 74 |
| 5.4 Conclusion, Recommendations & Future Work | 84 |
| Chapter 6 | 86 |
| 6 Modelling and Analysis of Underwater Acoustic Signals Emitted by Marine Energy Devices | 86 |
| 6.1 Introduction | 87 |
| 6.2 Wave Energy Converter and Noises | 88 |
| 6.3 Finite Element Modelling and Simulation | 89 |
| 6.4 Results | 94 |
| 6.4.1 Analysis of FE Models..... | 94 |
| 6.4.2 Analysis of Data from Literature | 96 |
| 6.5 Conclusion..... | 99 |
| 6.6 Limitations of Modelling..... | 99 |
| Chapter 7 | 100 |
| 7 Conclusion & Future Work..... | 100 |
| 7.1 Summary | 101 |
| 7.2 Contribution of Thesis..... | 102 |
| 7.3 Future Work..... | 103 |
| Chapter 8 | 105 |
| 8 Appendices..... | 105 |

| | | |
|-----|------------------|-----|
| 8.1 | Appendix 1 | 105 |
| 8.2 | Appendix 2 | 106 |
| 8.3 | Appendix 3 | 107 |
| | References | 108 |

List of Figures

| | |
|--|----|
| Figure 1 - Underwater acoustics applications. Note that some application areas overlap..... | 3 |
| Figure 2 - Cost of energy generating technologies | 8 |
| Figure 3 - Schematic of an Oscillating Water Column (OWC) WEC device with its turbine [22]..... | 9 |
| Figure 4 - Result of damping and wave height on the power output of OWC WEC [21]..... | 11 |
| Figure 5 - Influence of damping and frequency ratio on the OWC WEC [21]..... | 12 |
| Figure 6 - Wells turbine principle of operation [21]..... | 13 |
| Figure 7 - Non dimensional efficiency versus flow coefficient for the monoplane and biplane Wells turbines [21]..... | 14 |
| Figure 8 - Non dimensional pressure drop versus flow coefficient for monoplane and biplane Wells turbines [21]..... | 15 |
| Figure 9 - Pictorial schematic of WECs showing their scale and orientation..... | 16 |
| Figure 10 - Schematic of a simple point absorber WEC device [20]..... | 17 |
| Figure 11 - Photograph of the Wavebob WEC device in Ireland [32]..... | 17 |
| Figure 12 - Schematic of the attenuator WEC device [20]..... | 18 |
| Figure 13 - Picture of the Pelamis WEC device [33]..... | 18 |
| Figure 14 - Schematic of an Oscillating Water Column (OWC) WEC device [34].. | 19 |
| Figure 15 - Picture of the Oceanlinx Greenwave WEC device [35]..... | 20 |
| Figure 16 - Schematic of an Overtopping (Terminator) WEC Device [36] | 20 |
| Figure 17 - Picture of the Wave Dragon WEC device in Denmark [37]..... | 21 |
| Figure 18 - Schematic of the Limpet OWC WEC [38]..... | 23 |
| Figure 19 - Wells turbine of the Limpet OWC [39]..... | 23 |
| Figure 20 - Schematic of the Pico OWC WEC Power Plant [40]..... | 24 |
| Figure 21 - Posterior view of the Pico power plant [41]..... | 24 |
| Figure 22 - Schematic (left) and Picture (right) of the AWS Point Absorber Device [42]..... | 25 |

| | |
|--|----|
| Figure 23 - Schematic of a representation of sound pressure variation. At the maximum deviation of sound from the equilibrium pressure there is compression and vice versa in the case of rarefaction. | 28 |
| Figure 24 - The Fletcher-Munson equal-loudness contours showing the threshold of human audibility and threshold of pain for various frequency components [45]. | 29 |
| Figure 25 - Schematic of two waveforms. The initial coherent waves are in phase adding up to increase sound level. The subsequent incoherent waves are out of phase adding up and cancelling out each other to reduce sound levels. | 33 |
| Figure 26 - Typical ocean background noise at different frequency components (Wenz curve). Underwater sound levels are given in dB re $1\mu\text{Pa}^2/\text{Hz}$ [12]. | 37 |
| Figure 27 - Sound Level Weighting Curves A, B, C and D [49]..... | 38 |
| Figure 28 - Depth profiles from the open ocean of temperature, salinity and density. Courtesy: University of Rhode Island..... | 46 |
| Figure 29 - Waveguide models with pressure release surface (a), and solid bottom surface (b)..... | 58 |
| Figure 30 - Truncated acoustic-aquatic domain mesh. | 60 |
| Figure 31 - Sound pressure level values from sound source of model without bottom surface interface influence | 61 |
| Figure 32 - SPL value from sound source of model with bottom surface influence . | 62 |
| Figure 33 - Models with and without bottom surface influences..... | 63 |
| Figure 34 - Schematic showing configuration of multiple deployed WEC..... | 64 |
| Figure 35 - SPL values from multiple sound sources of model (b) with bottom surface influence | 64 |
| Figure 36 - Map of the Dublin bay region in Ireland showing the hydrophone deployment area and the ship docking area in relation to the lower Liffey..... | 69 |
| Figure 37 - Schematic of the Data Acquisition System | 70 |
| Figure 38 - Schematic of the hydrophone system (left) and the actual system on the pontoon (right) with the hydrophone submerged in water..... | 71 |
| Figure 39 - Tidal states at the site. Data were collected during spring and neap tides, at low and high water levels..... | 72 |
| Figure 40 - Graph of (a) narrowband PSD and (b) 1/3 octave band centred frequencies SPL of vessel departing the Dublin Poolbeg marina..... | 76 |

| | |
|--|----|
| Figure 41 - Normalised data for vessel departure against the absence of vessel | 77 |
| Figure 42 - Spectrogram of the short-time Fourier transform of the (a) ambient noise when the vessel is absent from the site and (b) noise radiated as the vessel pulls away from the dock for 350 s. | 78 |
| Figure 43 - Graph of (a) narrowband PSD and (b) 1/3 octave band centre frequencies SPL of vessel arriving and berthing the Dublin Poolbeg marina..... | 79 |
| Figure 44 - Normalised data for vessel arrival against the absence of vessel..... | 80 |
| Figure 45 - Graph of (a) narrow-band PSD and (b) 1/3 octave band centre frequencies SPL of vessel activities during spring and neap seasons. Here, the variations in the tidal heights of both seasons show an insignificant effect on the sound signal amplitudes; this might be attributed to the use of a static hydrophone system..... | 82 |
| Figure 46 - Underwater 1/3 octave band centre frequencies SPL, for low tidal conditions, during the presence and absence of vessels. Similar values are obtained at high tidal conditions. Overall SPL values for low frequency components increases significantly during the presence of these vessels as supposed during their absence. | 83 |
| Figure 47 - Geometry showing the absorbing boundary condition (ABC), perfectly matched layer (PML). | 91 |
| Figure 48 - Computational domain depicting bottom surface and pressure release surface. | 91 |
| Figure 49 - Theoretical propagation loss - $PL = -20 \log R - \alpha R$ of (a) frequencies as a function of range from 0.1 – 100 km and frequencies of 0.1 – 100 kHz, and (b) 0.1 – 3.1 km and frequencies 0.1 – 1 kHz. Using Francois and Garrison absorption coefficient (α) with conditions: Temperature = 10 ⁰ C, Salinity = 35 p.s.u. and depth = 24 m..... | 93 |
| Figure 50 - Solid bottom Surfaces of Models. Four types of rough surfaces used with roughness values equal to fractions of the RMS wavelength values. | 93 |
| Figure 51 - Attenuation of sound as a function of frequency and range for the different models. Models exhibit the same characteristics as theoretical models with respect to frequency against range. | 95 |

Figure 52 - Propagation loss of 1/3 Octave band centred frequency from a point absorber WEC. Sound source is at a depth of 24 m and the dominant frequency amplitudes are in the 100 Hz to 1000 Hz frequency range. 97

Figure 53 - Propagation loss of models 1, 2 & 4 against estimated values from literature (Haikonen *et al.*). Model 4 with rough surface interface exhibits more attenuation of sound signals and gives closer results to actual experimental values estimated from the literature. 98

Figure 54 - Representation of a direct driven linear WEC [57]..... 105

Figure 55 - Spectrums of the ESH noise from the L12 and WESA. Frequency (Hz) on the x-axis and sound pressure level root mean square (dB re 1 μ Pa) on the y-axis. (a) L12 ESH noise in SWH 1.5m (blue line) and ANLs in SWH 1.5m (green line). b) WESA ESH noise in Low (SWH 1.5 \pm 0.15m) (yellow line) and ANLs in Low (green line). (c) WESA ESH noise in High (SWH 2.5 \pm 0.5m) (red line) and ANLs in High (green line). (d) Comparison between all ESH: L12: SWH 1.5 (blue line), WESA: Low (yellow line) and WESA: High (red line) [57]..... 107

List of Tables

| | |
|---|-----|
| Table 1 - Octave and 1/3 octave band centre, upper and lower frequency values | 34 |
| Table 2 - Assessment criteria used in studies to assess potential impact of underwater noise on marine species..... | 40 |
| Table 3 - Sound propagation models and their respective application domain. Table is an adaptation of Paul C. Etter’s professional development short course on underwater acoustics modelling and simulation. | 52 |
| Table 4 - Parameters of the acoustic medium used in the simulation..... | 58 |
| Table 5 - Acoustic parameters and properties used in the models..... | 92 |
| Table 6 - Summary of WEC and ambient noise measurements. Shown are noise type: Moving Translator (MT) and End Stop Hit (ESH), Significant Wave Height (SWH), overall sound pressure level (SPL), noise duration, ambient noise level (ANL), estimate range for the noise to reach ambient noise levels [57]. | 106 |

Author's Conferences & Conference Presentations

- Ikpekha, O.W. and Daniels, S. Modelling and Analysis of Underwater Acoustic Signals Emitted by Marine Energy Device. *Presentation of work at the Fifth Annual Asian Conference on Sustainability, Energy and the Environment*, 11 - 14th June 2015, Kobe, Japan.
- Ikpekha, O.W. and Daniels, S. Modelling the Propagation of Underwater Acoustic Signals of a Marine Energy Device Using Finite Element Method. *Presentation of work at the Twelfth International Conference on Sustainability, Energy and the Environment*, 8 - 10th April 2014, Cordoba, Spain.
- Ikpekha, O.W. and Daniels, S. Condition Monitoring of Marine Devices. *Presentation of work at the Smart Ocean Forum*, 5 - 6th November 2013, Belfast Northern Ireland.
- Ikpekha, O.W. and Daniels, S. *Fourth International Conference on Ocean Energy*, 17 - 19th October 2012, Dublin, Ireland.

Author's Publications

The following publications stem from this research. All publications are full length papers and each describes a particular aspect of this research.

- Ikpekha, O.W. and Daniels, S. (2015). Modelling and Analysis of Underwater Acoustic Signals Emitted by Marine Energy Device. *Proceedings of the Asian Conference on Sustainability, Energy & the Environment, ACCESS*. Kobe, Japan. Submitted for journal publication with the IAFOR Journal of Sustainability, Energy and the Environment (2015).
- Ikpekha, O.W. and Daniels, S. (2015). Effect of Water Conditions on the Analysis of Underwater Vessel Noise: Dublin Bay Port Area Survey. *Journal of Marine Science and Technology*. Revised manuscript under review.
- Ikpekha, O.W. and Daniels, S. (2014). Modelling the Propagation of Underwater Acoustic Signals of a Marine Energy Device Using Finite Element Method. *Proceedings of International Conference on Renewable Energies and Power Quality*. Cordoba, Spain. Accepted for a journal publication with Renewable Energy & Power Quality Journal (Vol. 12. 2014).

Abstract

Electro-Mechanical devices such as Wave Energy Converters (WECs) are potentially an important technology for the generation of renewable ocean energy. These underwater Acoustic Emitting (AE) machines are liable to experience certain failure modes such as damaged bearings, hydraulic faults, electrical arcs, vibration, etc. during their operation. This can lead to catastrophic failure of components of an overall ocean based system if necessary preventative measures are not taken. It is important therefore to create a robust condition monitoring process of rapid detection and classification of faults in these machines, to reduce costs and increase lifetime and reliability. This will assist companies involved in the deployment of these systems, particularly companies involved in the renewable ocean energy and marine technology sectors, to improve on the operational and management costs of ocean based systems, specifically impacting on efficiency and yield, reliability, and maintenance costs. Underwater sound around AE machines and vessels is often monitored for environmental impact assessment studies, and could be used to monitor the health of AE machines and vessels. This thesis illustrates the acquisition and visualization of acoustic signals produced by underwater AE machinery/vessels. It illustrates the technique involved in the deployment of an acquisition system and the subsequent conditioning, processing and presentation of the acquired underwater acoustic data. The work presented in this thesis also involves numerical modelling and simulation of low frequency component sound signals of underwater AE machines and vessels. It illustrates the effect of the interaction of sound signals with varied surfaces and boundaries, and their influences on the propagation of these underwater sound signals. A brief study of the effect of acoustic signals on marine fauna is also discussed in this thesis.

Chapter 1

1 Introduction

Our world today is faced with huge environmental problems including global warming, climate change and ozone layer depletion. These problems stem from activities like the burning of fossil fuel and the release of harmful gases into the atmosphere. These activities are also related to other environmental concerns such as air pollution, acid precipitation, and deforestation [1].

The world's population is expected to double by the middle of the 21st century, and economic development will grow simultaneously with it. Global demand for energy services is thus expected to increase by as much as an order of magnitude by 2050, with energy demands expected to increase by 1.5 - 3 times [1]. A key goal therefore is to create a means of “development that meets the needs of the present without compromising the ability of future generations to meet their own needs” [2]. These aforementioned challenges require long-term efficient and sustainable development solutions, and one such solution is to maximise the use of renewable energy sources and technology available to us.

The world's oceans offer a potentially huge largely untapped natural renewable energy resource [3] as they possess high power density and high utility factor, in the sense that much of this energy could be captured and used compared to what is currently being used [4]. Research today greatly focuses on power generation from these renewable resources including wave energy.

Generally, wave energy is harnessed from the oceans by the operation of marine based electro-mechanical devices such as Wave Energy Converter (WEC). These devices capture the wave energies from the ocean and then convert them mechanically into electrical energy using a number of working principles [4]. The assessment of the ‘health’ of these marine based electro-mechanical devices is

therefore very important, with the utilization of a non-invasive means to predict failure mode in these devices paramount in the marine industry.

The overall future application and ultimate aim of the work carried out is to create a methodology to acoustically monitor the ‘health’ of these devices using their acoustic emissions. Using the acoustic spectrum information, fingerprints of devices over a range of conditions during normal operation can be established. Deviations from the baseline fingerprint, or ‘special cause variations’ are highlighted and communicated as a fault, or used as an indicator that a fault is likely to occur if corrective action(s) is not taken. Classification of the type of fault that is about to occur in these devices is useful in assisting remote diagnosis and in the decision making process.

Certain types of failure modes such as damaged bearings, hydraulic faults, electrical arcs, vibrations etc. have unique spectral signatures which can be detected, analysed and reported in real-time to a remote location. Analysis of these acoustic data in both the time and frequency domains are employed to extract the relevant information from these acquired acoustic spectra. A crucial aspect of the overall project is the strong engineering design element. This includes the choice of sensor specifications and the underwater systems network communication, together with the actual deployment of the system.

Condition monitoring for renewable energy systems is a growing research area with much work currently focussed on the wind energy market, in particular using vibration analysis to determine the condition of turbine systems [5, 6]. In mainstream manufacturing, condition monitoring is also well established [7-9], and there are a lot of activities in signature analysis and low-cost non-invasive sensor development for more complex systems. In the semiconductor manufacturing industry in particular, there is a major emphasis on condition monitoring for high capital-value complex electro-mechanical equipment [10, 11]. In this industry, rapid detection and classification of faults is essential from a manufacturing cost perspective. There is a substantial body of knowledge in this field which has a direct parallel with the large equipment in the marine sector.

There are various applications of underwater acoustics as depicted in Figure 1 [12]. In the research world today, there is a considerable amount of literature on acoustics in the marine environment for applications going from sound navigation and ranging (SONAR) to seismic exploration [13]. However, there is little to no literature on the application of acoustic emission condition monitoring for marine based devices which is a primary focus of this thesis.

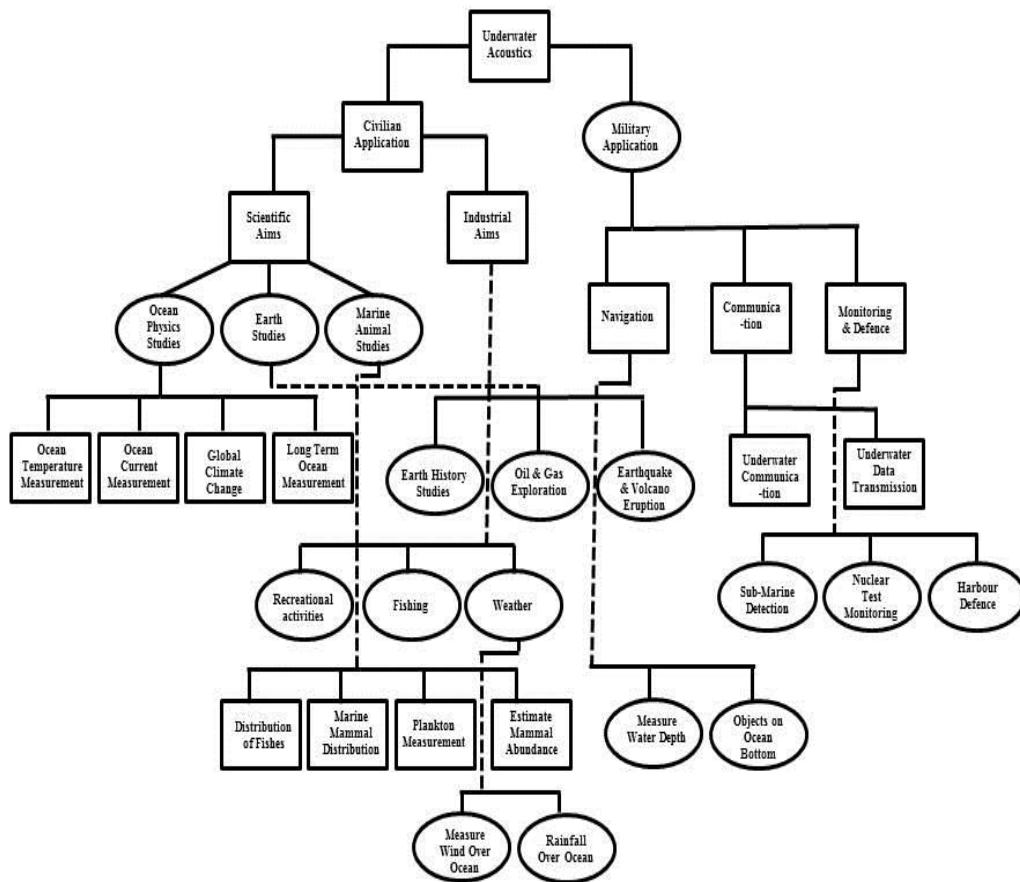


Figure 1 - Underwater acoustics applications. Note that some application areas overlap.

The area of condition monitoring is rapidly growing based on the need to reduce costs, and increase lifetime and reliability. The output directly impacts on the operational and management (O&M) costs of ocean based systems, specifically impacting on efficiency / yield, reliability, and maintenance costs. The ability to

predict and possibly prevent catastrophic failure of an ocean based system such as a wave energy device makes a significant impact on its overall return on investment and risk profile. A conservative estimate for the maintenance costs of marine based energy systems, based on similar land-based systems such as wind-turbines, is 26% of the overall costs [14]. For the less established ocean energy sector, this number is likely to be much higher.

This research impacts the cost and reliability of maintaining marine based electro-mechanical systems. Companies involved in the renewable ocean energy and marine technology sectors could greatly benefit. The primary application focuses on predictive fault detection and classification systems for marine devices. This in turn minimises catastrophic failure of components by informing the operator of the likelihood of a fault occurring. It is very important to note that the commercial opportunity involved is very significant.

1.1 Research Objectives

The overall aim of this work is to adopt a methodology for assessing the ‘health’ of marine based electro-mechanical devices, with future focus on WEC devices. Fingerprints acquired from these devices over a range of conditions during normal operation are established. Deviations from the baseline fingerprint, is thus highlighted as a fault, or can be used as an indicator that a fault is likely to occur if corrective action is not taken. Classification of the type of fault that is about to occur is useful to assist the remote diagnosis and decision making process. The objectives in this thesis therefore include:

- Investigate the state of the art electro-mechanical underwater acoustic-emitting devices especially WECs and their operational techniques.
- Use underwater sensor to actively monitor acoustic emissions from underwater acoustic emitting devices/vessels.

- Analysis of acoustic data to optimise the robustness of the methodology, and signal processing techniques employed in order to extract the relevant information from the acoustic spectra.
- Simulation of numerical models which involves the propagation of underwater sound from sound source to receiver, together with the influences of bottom surfaces on these sound signals in terms of SPL amplitudes. There is also a brief introduction of the effect on a certain species of fauna. This aids in further optimization of the overall robustness of the methodology and the processes involved.
- A preliminary study to identify effect of acoustic signal on marine fauna.

1.2 Thesis Organisation

The thesis is organised and laid out as follows: Chapter 2 outlines a review of the types of WEC devices currently available in the world today. It gives a description of the state of the art of technological concepts behind each innovative model. The chapter also describes the operational techniques behind these models and how they differ from each other, including their respective power ratings and capacities. It proceeds to give an account of the ‘scale’ of different models in operation today, be it a fractioned scale test model or a fully scaled operational model. It goes on to give examples of these devices and where they have or are planned to be deployed. Pictorial and schematic references of several types of WEC devices are also given to provide the reader with a clear understanding of the images and principles of functionality of these devices.

Chapter 3 introduces the principles of sound propagation in water. It provides the reader with knowledge on the various techniques involved in the modelling and simulation of sound, with emphasis on underwater sound and its propagation properties. It describes the important estimable parameters of underwater sound, together with the effects caused as a result of changes in these parameters. It is important to note that the first two chapters give the reader a clear insight into, and

understanding of the experiments, modelling & simulation, and data analysis of subsequent chapters.

Chapter 4 presents a study of the propagation of acoustic signals in water from source to receiver. It also implicitly presents a study of the effect of WEC devices on marine fauna. It presents a prequel to the modelling of WEC, together with the effect of sound signals produced by WECs on a marine mammal species. This chapter incorporates the effect of the bathymetry (features of underwater terrain) of the acoustic domain on the propagation of sound signals, and its influences on the reception of these signals by marine animals as receivers. This chapter precludes the optimisation of the acoustic technique employed in a more robust technique that is described in a subsequent chapter.

Chapter 5 presents acoustic signal measurement from sound emitting vessels. This chapter is paramount to the overall scope of the thesis as it gives a clearly defined methodology on how to collect acoustic data (and their subsequent signatures) from sound emitting machineries with minimum impact on the quality of the data collected. This technique is theorized to be successfully applied in the case of WECs. This chapter presents underwater acoustic measurements from noise emitting vessels under different oceanographic and operational conditions. It gives a comprehensive explanation of the techniques involved in not only the methodology of acquisition of the acoustic data, but also the conditioning, processing, analysis and presentation techniques involved in the communication of sensible data to the reader.

Chapter 6 of this thesis is a sequel to the modelling and simulation of underwater acoustic signals carried out in chapter 4. It provides a more robust acoustic modelling environment and gives scientific reasons for each step. It also incorporates data analysis from the experiment in chapter 5, and the use of this data to improve on any shortcomings from previous modelling and simulation of the acoustic domain.

Chapter 7 concludes the work of the entire thesis in form of a summary of the work carried out, and it lays out a blueprint for further work to achieve the overall aim, and advancement on the work carried out in this thesis.

Chapter 2

2 Marine Energy Devices/Monitoring Systems

This chapter presents a study of marine energy devices around the world's coastal areas. It gives an overview of the types of marine energy devices including wave energy devices that have and are been deployed today. It is important to note that the marine energy sector is a fast growing economic, engineering and design sector that is still in its infancy when compared to other established sectors such as the wind energy sector. Some of the models presented are scaled models which are in the development and testing phase, while some others are at the design phase.

2.1 WEC System and Energy Conversion

Research and discussions on the harnessing of wave energy has been going on since the 18th century [15]. However, the modern focus on the generation of power from renewable sources stems from the emergence of the oil crisis in the 1970s [16], recent global climate change issues, rising levels of CO₂ and the depletion of the ozone layer.

Research in the area of ocean wave energy is relatively immature when compared to other types of renewable energy technologies [3]. Research in this area is mainly driven by the need to meet renewable energy targets, as they are a hugely, largely untapped energy resources.

Wave energy devices offer one of the highest energy density amongst all other renewable energy sources [17], and they also typically have very limited environmental impact when it comes to cycle emissions of these devices. Figure 2

shows the projected estimated costs for different energy technologies in USD per kilowatt hour by the year 2020 by Delucchi *et al.* [18]. This graph shows wave energy production cost to be very competitive compared to other production techniques.

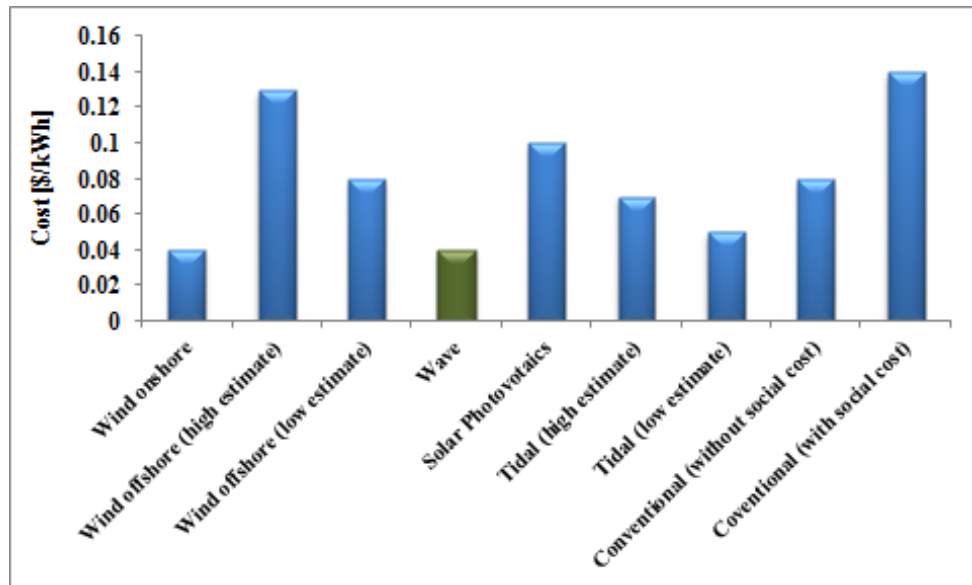


Figure 2 - Cost of energy generating technologies

Worldwide, there were over 1000 WEC devices reported in 2002 [17]. Recently (2009 - 2013) the global level of patent activity with regards to ocean energy technology devices averaged well over 150 patent activities [19]. These devices can be distinguished by their respective operational principles, their orientation relative to the direction of the wave motion and their deployment site. Their various design considerations are subject to their deployment site (water depth conditions) and their intended resource characteristics [20]. They are deployed in deep waters (50 - 100 m), intermediate waters (20 - 50 m) or shallow waters (< 20 m) depending on their designs. All WEC devices are prone to develop failure modes and have potential acoustic emission profiles.

The total mean power absorbed by a three dimensional WEC device at a given frequency per unit crest wave (of the incident wave) is used to qualify its performance. This quantity is known as its capture or absorption width with a dimension of length [21]. This quantity is also referred to as its efficiency in some

cases. The efficiency is the ratio of output power to input power in a two dimensional scenario (as supposed to the 3-D capture width), having a maximum value of unity. Device performance is usually quantified using the non-dimensional ratio of the capture width to the length of the device. This quantity is maximised for a given geometry and frequency by optimising parameters of the power take off (PTO) mechanisms. This is the mechanism for conversion of ocean wave energy into mechanical and/or electrical energy by WECs, and it simply relates to the device having its maximum mean absorbed power at a certain frequency.

The Oscillating water column (OWC) is a very common type of WEC deployed around the world which operates on a very simple principle of air compression and decompression. It generates energy from the rise and fall of water caused by waves and tides in the ocean as depicted in Figure 3, including the integral turbine. Energy is captured from a turbine placed at the opening of an inverted chamber into which air goes in and out depending on the level of the water on the floor of the chamber.

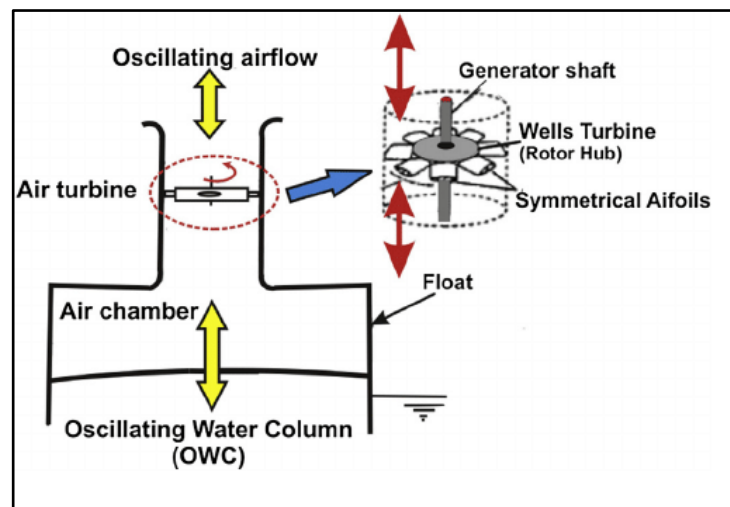


Figure 3 - Schematic of an Oscillating Water Column (OWC) WEC device with its turbine [22]

Since OWC WECs are characterised by conversion systems utilizing air turbines, these turbines usually include the Wells or Impulse turbines PTO system. An entire OWC WEC system comprises of a capture device (including an electrical generator) connected to an air turbine. The performance of the capture device and the

generator are affected by the physical environment, and the impact on the torque/speed of the turbine. To maximise the potential for energy conversion the core interdependence between the OWC capture unit and the turbine has to be optimised. To achieve this optimised potential, two matching principles need to be addressed. These principles include the ability of the turbine to provide a damping level that restricts the air flow exiting the system. This maximises the conversion of wave energy to kinetic energy by the OWC system, and thus the pneumatic energy produced as a result of the air excitation immediately above the OWC. The second principle involves the optimisation of the conversion of pneumatic energy to mechanical energy in the system, and subsequently to electrical energy over the range of flow rates as air exits the OWC.

The OWC WEC interface performance is modelled using the generic mass-spring-damper eqn. (2.1.1) of an oscillating body with a single degree of freedom as a result of a time varying force $F(t)$.

$$F(t) = m \frac{d^2}{dt^2} + B \frac{dy}{dt} + Ky \quad (2.1.1)$$

From eqn. (2.1.1) F is the applied force at time t , m is the mass of the body, B is the damping, y is the displacement and K which is the spring restoring constant due to the OWC buoyancy. $K = A_c \rho_w g$, where A_c is the OWC's surface area, ρ_w the water density and g the gravitational acceleration. This morphs into the established solution (eqn. 2.1.2) [23] of the equation of motion for sinusoidal excitation which is analogous to the mechanical mass-spring-damper system, and is given as:

$$W_{OWC} = \frac{\frac{1}{2} B_A \omega^2_{OWC} |F|^2}{(K - M_E \omega^2_{OWC})^2 + (B_A + B_2)^2 \omega^2_{OWC}} \quad (2.1.2)$$

In eqn. (2.1.2) W_{OWC} is the average power output of the OWC WEC device, and ω_{OWC} is the angular frequency of oscillation. This eqn. (2.1.2) is slightly different from the generic one (mass-spring-damper) by the addition of two terms which account for the wave generated by the body as it oscillates. These additional terms are the frequency dependent effective mass M_E which is the entrained mass together with the added mass, and the two component damping. The component

damping includes the applied damping B_A provided by the turbine extracting energy from the system, and the secondary damping B_2 which in itself consists of the radiation and loss damping due to wave generation by the column, and energy losses due to incident wave power, respectively. Therefore to maximise the applied damping of the turbine and thus the power output of the OWC WEC eqn. (2.1.3) is utilized.

$$B_{A_{OPT}} = \sqrt{B_2^2 + \left[\frac{K - M_E \omega_{OWC}^2}{\omega_{OWC}} \right]^2} \quad (2.1.3)$$

From eqn. (2.1.3) (where $B_{A_{OPT}}$ is the optimum applied damping value), tweaking the parameters to adjust the wave height and the damping of the OWC influences the power output and bandwidth response, respectively. This is depicted in Figure 4 and Figure 5 which are results of a series of hydraulic tests on damping of an OWC's power output and bandwidth, respectively.

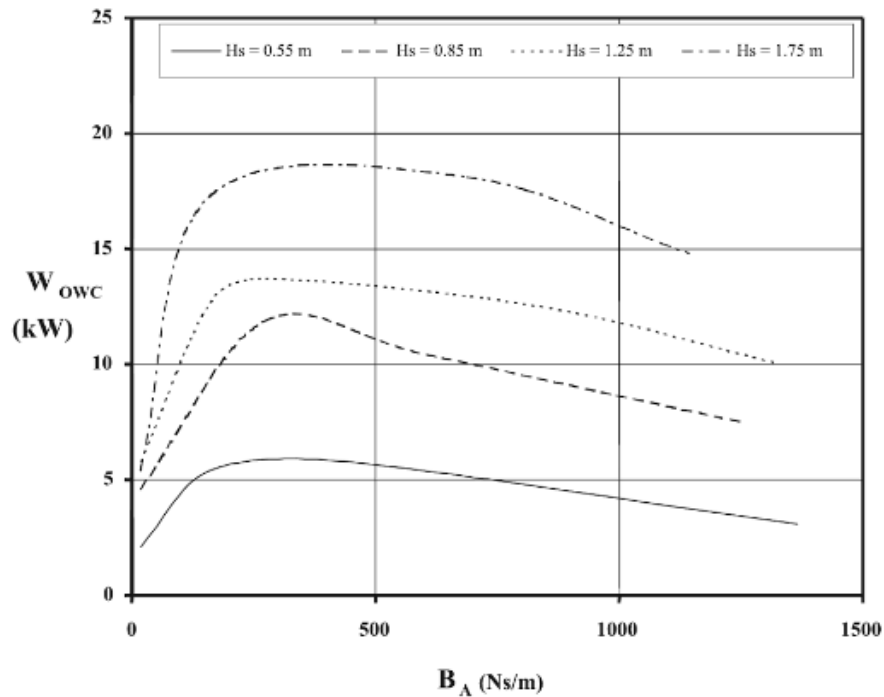


Figure 4 - Result of damping and wave height on the power output of OWC WEC [21]

Figure 4 illustrates that the power output of an OWC decreases as the damping is increased. Underdamping immensely reduces the efficiency of the OWC to an

extent which over-damping does not, thus providing a further incentive to over-damp the system [21]. Figure 5 shows the performance bandwidth response for three different damping levels initially at a value of $B_A 1$, and for double and quadruple the initial level. It can be deduced that performance must be optimised over a wide range of frequency values to maximise output for any particular set of wave conditions. Conclusively, the optimal applied damping is subject to wave period, incident wave power and tidal level [24].

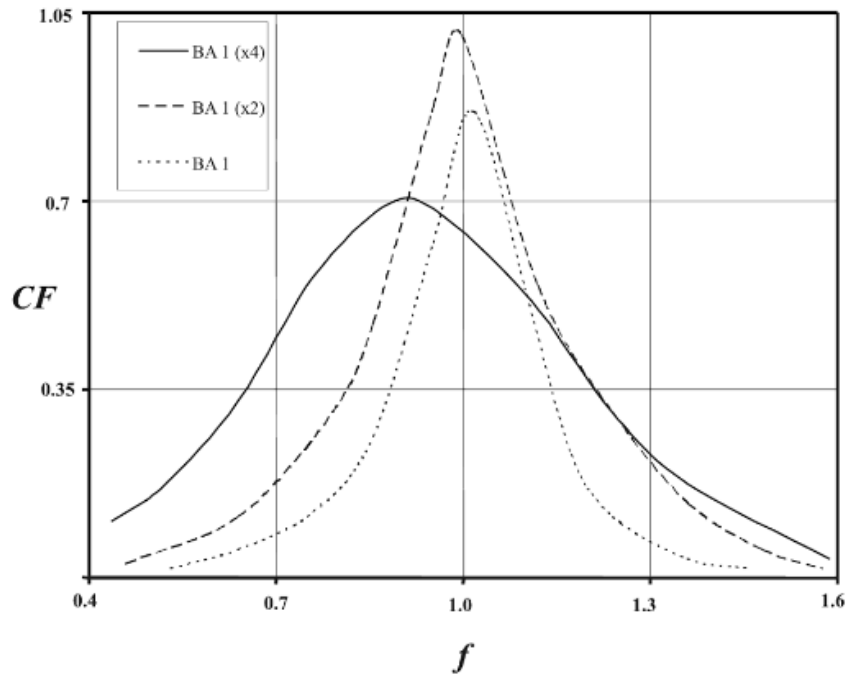


Figure 5 - Influence of damping and frequency ratio on the OWC WEC [21]

Wells turbines as a main component of an OWC WEC system's configuration commonly have symmetrical aerofoil blades located peripherally on a rotor at 90 degrees stagger to the airflow. An alternating airflow drives the rotor predominately in one direction of rotation [25-27]. The symmetrical blades of the Wells Turbine are set around the hub at a 90 degree angle with their chord lines normal to the axis of rotation as shown in Figure 6.

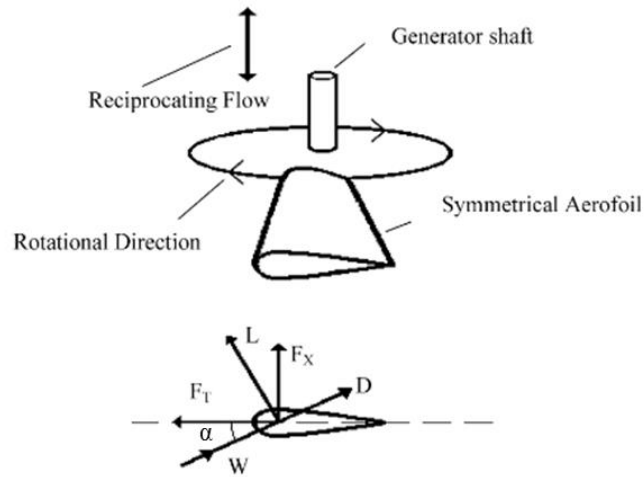


Figure 6 - Wells turbine principle of operation [21]

The velocity W at an angle of incidence α to the blade chord is relative to absolute air flow velocity V_a which is axial at the inlet, and tangential rotor velocity U_t at radius r from the axis of rotation. This generates the lift force L and drag force D normal and parallel to the relative velocity W respectively (shown in Figure 6), and can be resolved into tangential and axial directions to the rotor as shown in eqn. 2.1.1 and 2.1.2.

$$F_T = L \sin\alpha - D \cos\alpha \quad 2.1.1$$

$$F_X = L \cos\alpha + D \sin\alpha \quad 2.1.2$$

It is important to note that the magnitude of F_T and F_X vary during a cycle for a symmetrical aerofoil in an oscillating airflow, but the direction of F_T remains independent of the reciprocating flow. However, at the lowest flow rate F_T will be negative because of aerodynamic drag on the blades and also at the highest flow rates because lift will be lost due to boundary layer separation [21]. If a turbine is well matched to the sea distribution, F_T results in the generation of positive torque and power for much of the wave cycle. During extreme wave conditions the aerofoils stall and this act as a limiter. The normal component F_X results in an axial thrust force which is supposed to be borne by suitable bearings. F_T and F_X are given in dimensionless coefficients C_τ and C_X , and they are given as:

$$C_\tau = C_L \sin\alpha - C_D \cos\alpha \quad 2.1.3$$

$$C_x = C_L \cos\alpha + C_D \sin\alpha \quad 2.1.4$$

Lift and drag are subject to 3-D flow [28], and studies show that blade performance depends on the corresponding single aerofoil data as a result of interference effects between turbine blades [21]. At the lowest angle of attack drag dominates over lift initially, before lift prevails to a maximum value at the stalling incidence. At this point the boundary layer separates from the blade surfaces leading to loss of lift and a rapid increase in the dominance of the performance due to drag. From Figure 7 it can be deduced that the operational region of Wells turbines are poor at low angles (0 - 18 degrees) of incidence [21], and aerodynamic characteristic performance of the turbine blades hugely depends on the incidence of the airflow onto the blades. This is demonstrated by the experimental results in Figure 7 and Figure 8.

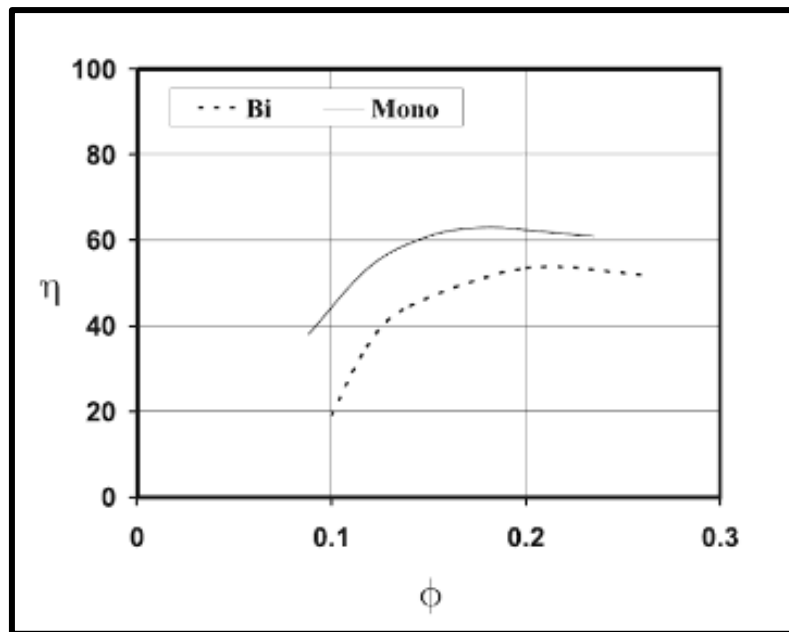


Figure 7 - Non dimensional efficiency versus flow coefficient for the mono and biplane Wells turbines [21]

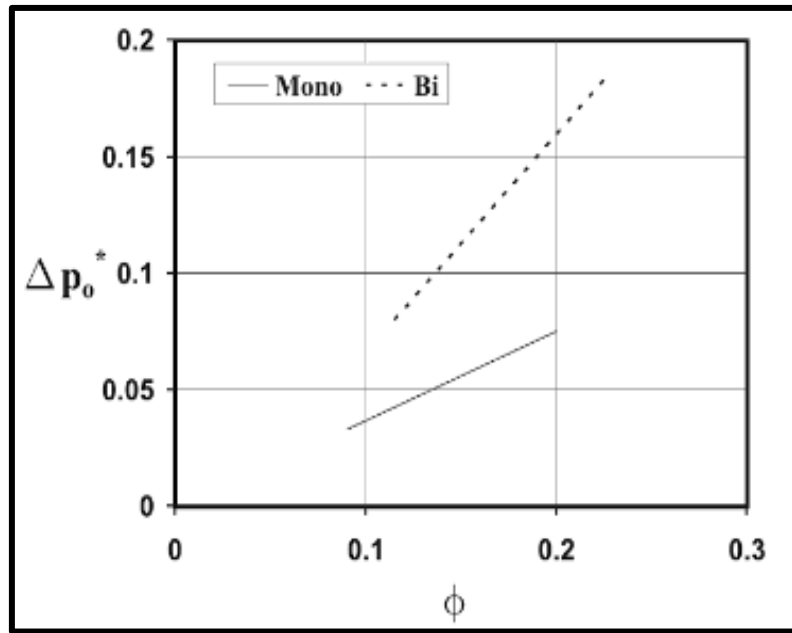


Figure 8 - Non dimensional pressure drop versus flow coefficient for monoplane and biplane Wells turbines [21]

The frequency of bi-directional and random air flow in a WEC device is very low, and thus the air flow through the device is usually assumed to be quasi-steady. Figure 7 and Figure 8 show the usual variation of efficiency (η) and pressure drop (Δp_0^*) with flow coefficient (ϕ), pressure (p^*) is found to be proportional to the pressure drop across the rotor for a given rotor speed and Δp and ϕ is proportional to the flow rate Q .

It is therefore important that the turbine design in this region is optimal in terms of performance. These performance characteristics include efficiency, torque and pressure drop. Generally, optimisation of the PTO of these turbine WEC systems include the development of their geometric variables, blade profiles, rotor plane numbers [29], utilization and optimisation of guide vanes [30], pitching of monoplane turbine's blade and counter-rotation of biplane's rotors [31].

2.2 WEC Types and Classifications

Conventionally WEC devices were typically floating devices and as such were classified as point absorbers, terminators or attenuators. This classification helped in providing information on the geometry of any particular device together with their principle of operation as depicted in Figure 9.

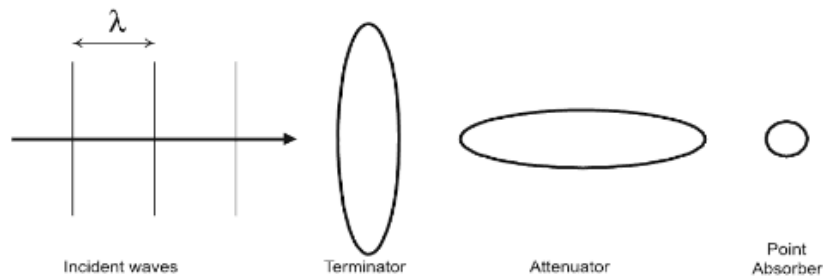


Figure 9 - Pictorial schematic of WECs showing their scale and orientation

Point absorbers are a type of WEC device that are small and are normally cylindrical in shape. They tend to be constrained to only one major degree of motion (having only two components), which is usually an upwards and downwards movement, receiving incoming waves from any angle. Figure 10 shows the schematic of an exemplary point absorber. The base component is fixed (due to gravitational forces through the large foundation mass) or can be moored to the sea bed, and the floating component is normally induced by a heaving motion with respect to the fixed base due to its buoyancy. The concept of point absorbers is very appealing when it comes to modelling, because the scattered waves can be neglected and forces on the body are only due to the incident waves [21].

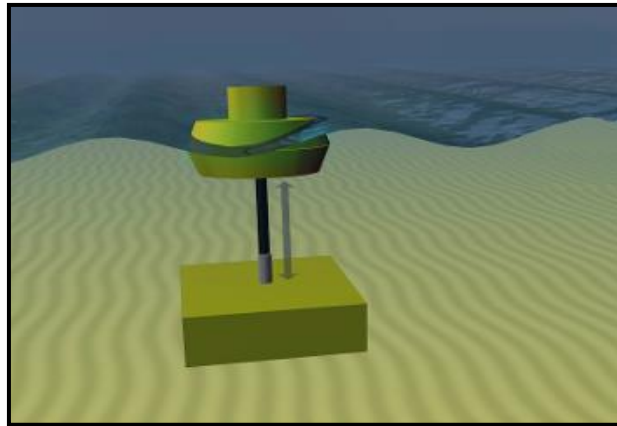


Figure 10 - Schematic of a simple point absorber WEC device [20]

There are three kinds of point absorbers. These include the *simple point absorbers* where the mobile component moves vertically with respect to the base. The second is the *oscillating wave surge converter* where the mobile component moves transversely as well as vertically to the base. And the third type of point absorber is the *submerged pressure differential* where the mobile component is completely submerged in the water. Examples of point absorber WEC devices include the Wave Bob (see Figure 11) deployed in Ireland, PowerBuoy™ developed by Ocean Power Technologies (OPT) in New Jersey USA, AquaBuOY™ WEC developed by AquaEnergy Group Ltd., and the Archimedes Waveswing.



Figure 11 - Photograph of the Wavebob WEC device in Ireland [32]

The Wavebob is a 1/4 scaled WEC model developed in Ireland and deployed in the Galway Bay area between 1999 and 2013. It is exposed to 1/3 of the expected

full energy of the Atlantic Ocean, as it is located inside a natural breakwater. Another example of a point absorber WEC is the Ocean Power Technologies (OPT) PowerBuoy which has a rated power of up to 150 kW. OPT are currently developing variant models with rated power values of up to 500 kW.

Attenuators are energy absorbing structures of high rectangular aspect ratio, and are usually placed perpendicular to the wave front as shown in Figure 12. The structures induce oscillatory motion from the energy of the oncoming waves yawing autonomously to face the dominant wave direction.

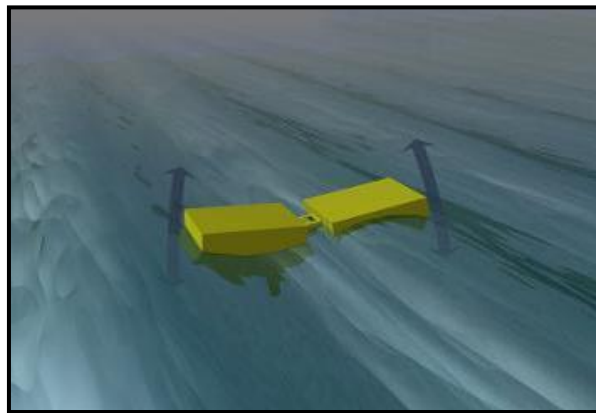


Figure 12 - Schematic of the attenuator WEC device [20]

Common attenuators are surface floating structures. However, others can be fully submerged. Examples of attenuators include the Pelamis Wave Power (shown in Figure 13), the Wavestar, Dexam-Wave and the AlbaTERN.



Figure 13 - Picture of the Pelamis WEC device [33]

The 120 m long semi submerged P2 Pelamis model in Orkney in the United Kingdom operates at depths of between 50 to 250 m and has an energy rated power of 750 kW. An interesting feature of these devices is the ‘self-referencing’ mechanism which enables them to maintain a directional heading perpendicular to the oncoming wave direction.

The Oscillating water column (OWC) operates on the principle of air compression and decompression. It generates energy from the rise and fall of water caused by waves and tides in the ocean. Energy is captured from a turbine placed at the opening of an inverted chamber into which air goes in and out depending on the level of the water on the floor of the chamber as shown in Figure 14.

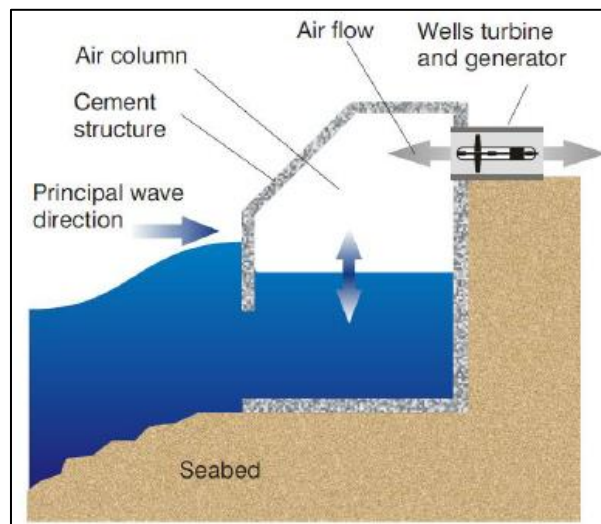


Figure 14 - Schematic of an Oscillating Water Column (OWC) WEC device [34]

The variation of the water level in the chamber acts like a large piston on the volume of air within the chamber. Examples of OWC WEC devices include Oceanlinx Greenwave (see Figure 15) and Wavegen.

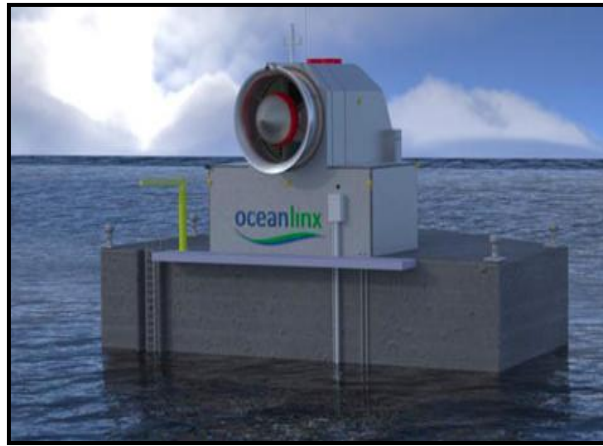


Figure 15 - Picture of the Oceanlinx Greenwave WEC device [35]

The Oceanlinx Greenwave is made of a simple flat packed prefabricated reinforced concrete that sits directly on top of the ocean floor in a 10 - 15 m ocean depth. The turbine converts wave energy to electrical energy using high pressure air. Deployed in Australia, it has an energy power rating of up to 1 MW, with a possible increase to 10 MW.

Terminators which are also known as *overtopping devices* usually have a central collection basin that fills up as the water level rises up. The water spills over a retaining wall to fill the basin creating a small elevation through a standard low-head hydro turbine as shown in Figure 16.

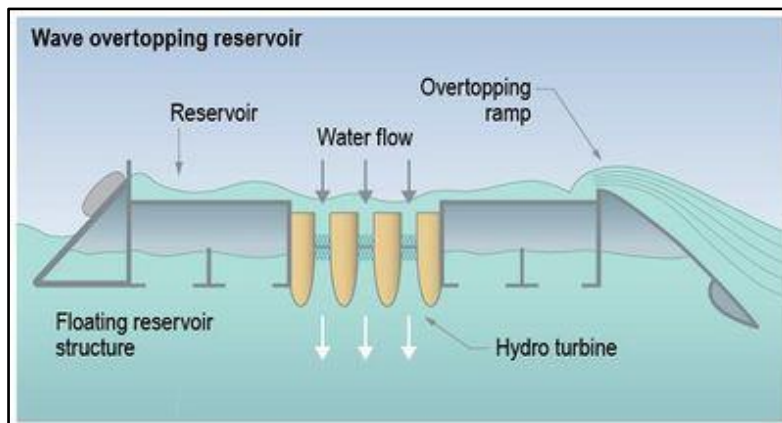


Figure 16 - Schematic of an Overtopping (Terminator) WEC Device [36]

They can be located as floating devices in deep ocean water or built as part of a shoreline structure or man-made breakwater. Examples include the Wave Dragon (shown in Figure 17), Wave Plane and WAVEnergy.



Figure 17 - Picture of the Wave Dragon WEC device in Denmark [37]

The wave dragon uses the pair of curved reflectors to gather waves into the central receiving part. The waves then flow up a ramp and over the top into a raised reservoir, from which the water is allowed to return to the ocean using several low-head turbines [3]. The wave dragon is deployed up to 25 km offshore and has a 7 MW capacity [37].

Alternate classification of WEC devices extends beyond those (floating devices) mentioned above. This is because more recent WECs cannot be classified solely based on their principle of operation. An example includes recently shore-mounted OWCs which are a type of point absorber even if it is known that point absorbers are floating devices. Now, for a full description of a WEC device type, one needs to specify its operational principle such as an OWC and where they are being deployed such as onshore or offshore. The European Union (EU) funded OWEC-1 project classification system is based on a device's present status, the development time-scale and economic investment cost. With these new considerations devices are classified as being first, second, or third generation system without the inclusion of the mode of operation.

Onshore or near shore OWC devices are considered *first generation systems*. These devices are installed presently or are under development in the UK, Japan, Portugal and India. It is important to note that these first generation devices have dominance in the industry today due to the conventional technological principal and power take-off equipment. Float-pump *second generation WECs* are designed to operate on offshore and nearshore sites where high levels of energy are available. These devices may be slack-moored or tight-moored; however they all possess a

favourable ratio between absorbed energy and volume. *Third generation systems* are large scaled offshore devices. Large in terms of energy potentials and size, and they are generally typed as point absorbers. It is important to note that any device classification cannot be entirely satisfactory. An example is the Pelamis WEC which can be classified both as an attenuator with regards to the initial classification system, and a third generation device. Below are four categories of WECs currently deployed around the world that have reached the full-scale stage, each with a particular type of power conversion mechanism. It is paramount to note that some of these devices have been mentioned previously; however more details are given here.

2.2.1 Oscillating Water Column

Current full scale models of the OWC include the Land Installed Marine Power Energy Transmitter (LIMPET) OWC and the Pico plant. Wavgen's LIMPET OWC is fitted with a pair of 250 kW self-rectifying Wells turbine rotor units with a 2.6 m diameter (few OWCs are fitted with impulse turbines instead) which have great virtues in terms of simplicity and effectiveness. The unit has seven blades with symmetrical airfoil section which are bolted via a containment ring to a plate which in turn fits directly on to the shaft of the generator hidden under a cylindrical cover. A contra-rotating biplane turbine is formed by the use of two of these assemblies back to back in the baseline configuration of the LIMPET OWC. Figure 18 and Figure 19 show the schematic of the LIMPET OWC and its turbine respectively.

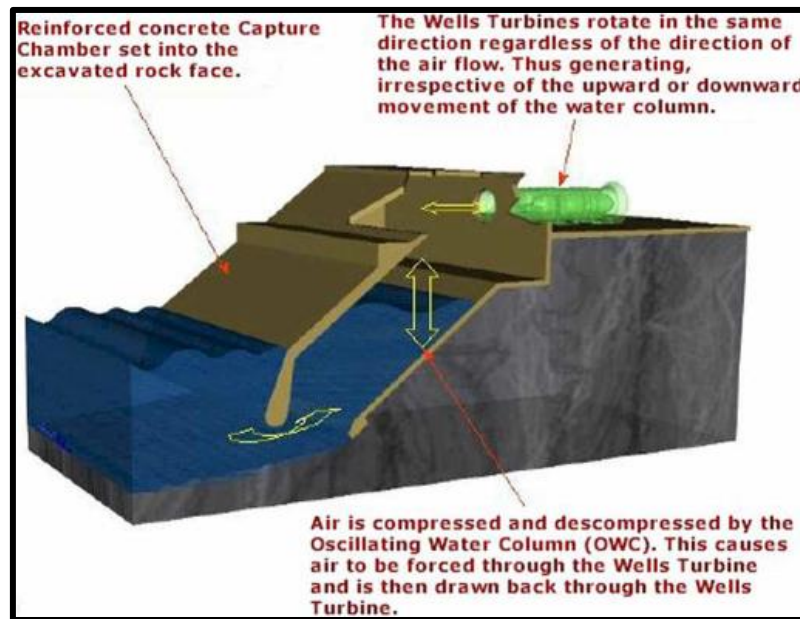


Figure 18 - Schematic of the Limpet OWC WEC [38]



Figure 19 - Wells turbine of the Limpet OWC [39]

The Pico plant is a shoreline OWC in the Azores. The electrical, power electronic and monitoring equipment was supplied by EFACEC in Portugal, while Applied Research and Technology (ART) in Inverness, Scotland supplied the mechanical equipment. It is a 400 kW rated plant equipped with a 2.3 m diameter

Wells turbine. The turbine is coupled to an asynchronous generator (see Figure 20) with two fixed guide-vane stators on either side of the rotor.

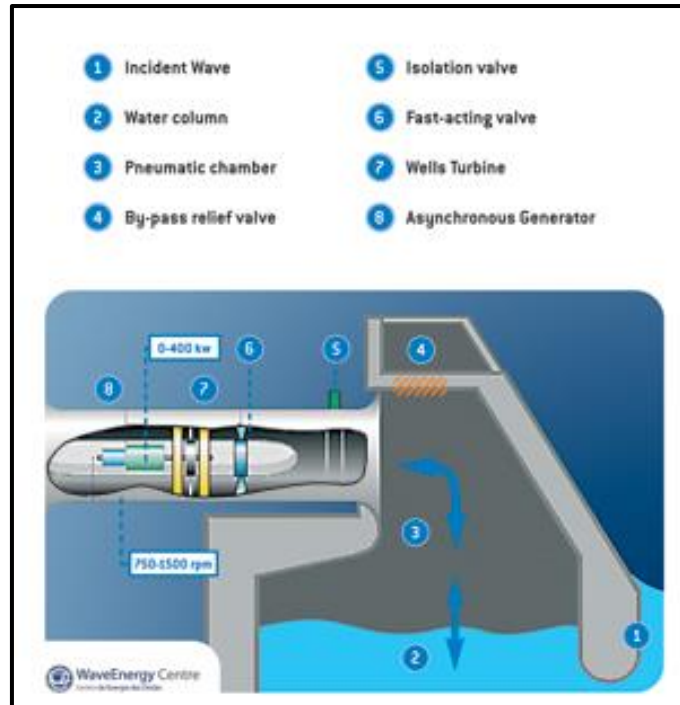


Figure 20 - Schematic of the Pico OWC WEC Power Plant [40]



Figure 21 - Posterior view of the Pico power plant [41]

The Pico plant has a pressure release valve, and a sluice-gate isolation valve which is used whenever it is disconnected for a long period of time. The fast reacting valve is used against turbine over-speed in the case of energetic seas and electrical grid fault. The Pico plant also has many sensors for the monitoring of rotational speed,

powers delivered to the grid, vibrations and oil temperature at the turbo-generator bearings, cumulative active energy produced etc.

2.2.2 Point Absorber

The Archimedes Wave Swing (AWS) is a type of point absorber WEC. It is fully submersible and envisaged to be deployed in arrays of devices rated in a few megawatts. Figure 22 shows the schematic and picture of the 2 MW pilot plant attached to a pontoon.

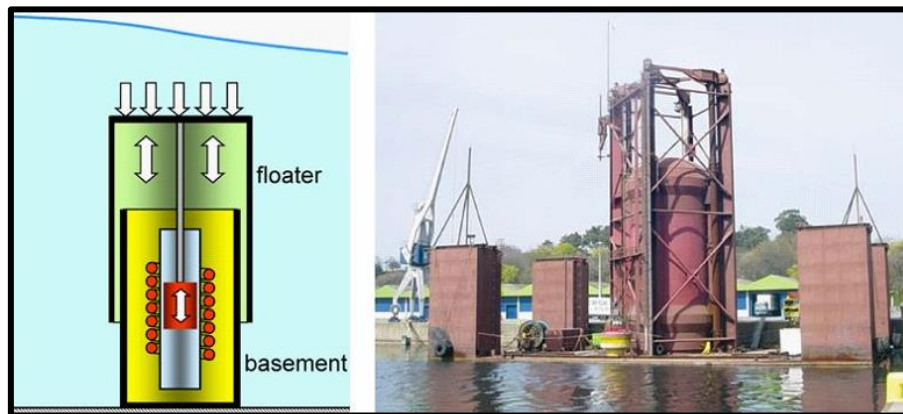


Figure 22 - Schematic (left) and Picture (right) of the AWS Point Absorber Device [42]

It consists of an air filled chamber (the silo) which is fixed to the bottom of the sea and opened at the top. This chamber is closed by another cylinder (the floater) with an airlock between the two cylinders, to prevent water flooding the silo. The floater moves up or down due to pressure increase or decrease, respectively, with the incoming wave front directly above the device. The PTO of the AWS is a permanent-magnet linear generator for conversion of the wave energy to electrical energy.

2.2.3 Attenuator

The now defunct Pelamis WEC comprises of semi-submergible cylindrically linked structures linked together by hinged joints. The full scale Pelamis WEC was installed at the European Marine Centre in Orkney (UK) and is of length 150 *m* and 3.5 *m* diameter (see Figure 13). The cylindrical structures articulate around the joints as waves travel down the length of the machine as previously shown in schematics of Figure 12. The joints induce motion during wave travel which is restricted by hydraulic rams which pump high-pressure oil through hydraulic motors via smoothing accumulators, and this in turn drives electrical generators to produce electricity. The Pelamis WEC can be installed in many offshore water depths and sea bed conditions as it is constructed, assembled and commissioned off-site on land. Its attachment/detachment electrical and moorings connections allows for an ease of dismantling for maintenance requirements, thus avoiding costly offshore operations with specialist equipment and vessels.

2.2.4 Overtopping

The Wave Dragon deployed in Northern Denmark is among a few WEC devices that do not oscillate with the sea waves. It is designed to float above water depths from 2 *m* and over. The front of the device is curved ramp, allowing oncoming waves to surge up it. There is a reservoir behind the ramp which gathers the ‘overtopping’ waters with an eventual high potential energy (compared to surrounding waters). The Wave Dragon has long reflector wings as shown previously in Figure 17. This simplifies its effectiveness as they channel the waves towards the ramp. The energy is extracted as the wave drains back into the sea via low head hydro turbines within the reservoirs.

Chapter 3

3 Sound Signals and Underwater Acoustics

Sound is propagated by the molecular transfer of motional energy [43]. Sound needs a medium to propagate in as it cannot pass through a vacuum. In acoustics, the media via which sound propagates include solid, liquid, gases and plasma. UA is concerned with the propagation of sound in water, together with the interaction of its constituent waves with the boundaries. This chapter details the fundamentals of sound, the various properties of sound in water and the principal techniques involved in the modelling of sound signals and propagation in water.

3.1 Fundamentals of Sound

When sound signals travel through any of the aforementioned media, compressional waves occur as a very small change in pressure. This pressure change is caused as a result of disturbance which communicates itself to the surrounding medium. This phenomenon is synonymous with the ripples caused by a stone thrown into water whose energy gradually dissipates with respect to the volume in a three dimensional configuration. When the medium in which the sound propagates is disturbed, the oscillations of the particles cause the pressure of the medium to deviate from its equilibrium state. A higher density of particles corresponds to a higher pressure value as depicted in Figure 23.

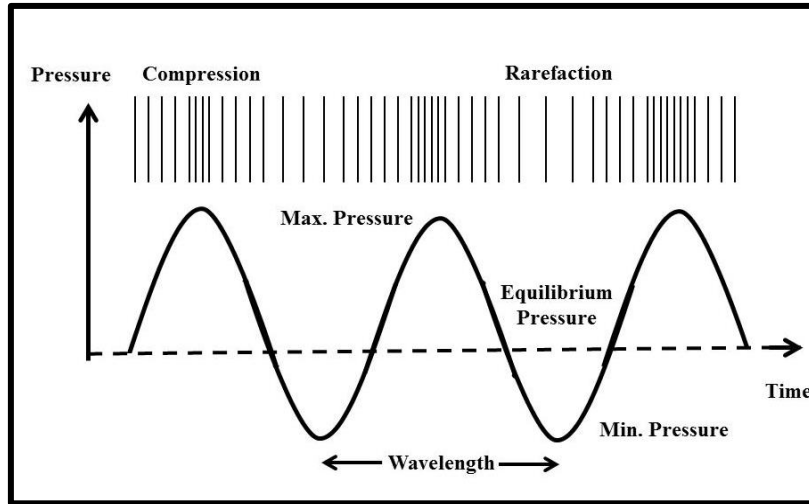


Figure 23 - Schematic of a representation of sound pressure variation. At the maximum deviation of sound from the equilibrium pressure there is compression and vice versa in the case of rarefaction.

There is always a steady-state component of pressure in any medium. When a disturbance is made to this medium, it appears as a small fluctuation in pressure. In air, the atmospheric pressure p_0 is equivalent to $10^5 Nm^{-2}$ or 760 mmHg (torr). The total pressure at any time is equal to $p_0 + p(t)$ where $p(t)$ represents the fluctuating sound wave components, and p_0 is the mean pressure component. To define the strength of the fluctuating component $p(t)$, the following eqn. (3.1.1) is used:

$$\bar{p}^2 = \frac{1}{T} \int_0^T P(t)^2 dt \quad (3.1.1)$$

In eqn. (3.1.1), T is the time period of interest and \bar{p} is the root mean square (rms) pressure. If the sound wave is harmonic, the pressure fluctuation at a point can be represented as [44]:

$$p = a \cos \omega t \quad (3.1.2)$$

$$\therefore \bar{p}^2 = \frac{1}{T} \int_0^T a^2 \cos^2 \omega t dt = \frac{a^2}{2} \quad (3.1.3)$$

$$\bar{p} = \frac{a}{2^{1/2}} = 0.707a \quad (3.1.4)$$

The range of pressure values for human hearing is $2 \times 10^{-5} - 20 Nm^{-2}$. These approximately correspond to the minimum and maximum pressure fluctuation discernible to the human ear respectively at a frequency of 1000 Hz (see Figure 24)

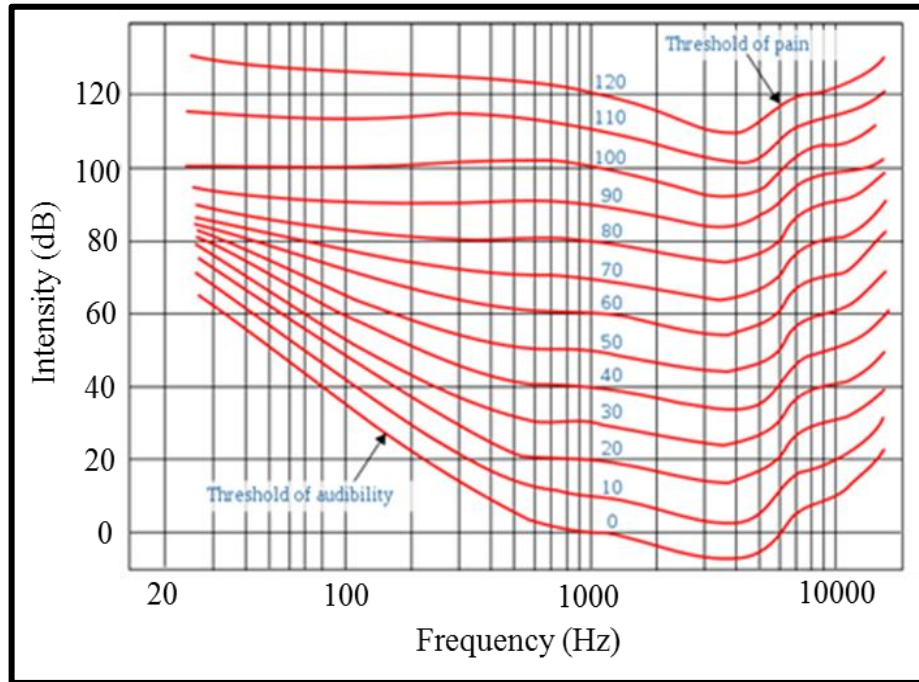


Figure 24 - The Fletcher-Munson equal-loudness contours showing the threshold of human audibility and threshold of pain for various frequency components [45].

The Fletcher-Munson equal loudness contour curve (Figure 24) was obtained in the 1930s from measurements made on many subjects. The data relates the subjective loudness of tones compared to a fixed level at 1000 Hz.

The speed, c , by which sound goes through different mediums, varies according to the properties of the specified medium and it is related to the wavelength, λ , and frequency, f , of the sound signal. It is deduced that the velocity of sound in gas is proportional to the square root of the absolute temperature given by eqn. (3.1.5a).

$$c = \sqrt{\frac{RP}{\rho}} \quad (3.1.5a)$$

$$c = \sqrt{\gamma RT} \quad (3.1.5b)$$

where γ is the ratio of the specific heat of the gas (or adiabatic index C_p / C_v , C_p and C_v are constant pressure and volume resp.), R is the specific gas constant, ρ is the density, and T is the absolute temperature. It is however difficult to establish such a simple equation for the velocity in liquid as there are no simple relationships

between all of the parameters in the equation as they all vary with temperature. Instead the equation for the velocity of sound in liquid is given as thus:

$$c = \left(\frac{B_a}{\rho_0} \right)^{1/2} \quad (3.1.6)$$

In the eqn. (3.1.6), B_a is the adiabatic bulk modulus of elasticity, and ρ_0 is the density. In the case of the velocity in solids, the equation is given as:

$$c = \left(\frac{E}{\rho_0} \right)^{1/2} \quad (3.1.7)$$

In eqn. (3.1.7), E is Young's modulus of elasticity of the solid and ρ_0 is the density of the material. The velocity in this case is largely independent on both the temperature and the pressure. It is important to note that eqn. (3.1.7) takes into account the Poisson effect (small change in cross sectional area) thus giving the Young's modulus of elasticity. However, in the case of a bulk form (restricted from moving laterally) of the solid, a bulk modulus of elasticity is substituted for the Young's modulus in eqn. (3.1.7).

Decibels (dB) and Frequency Sensitivity

Using the decibel value is a simple way of expressing ratios which makes life a bit easier in acoustics, electrical engineering and most especially when both fields combine in electro acoustics.

If $W_1 = W_2 \times n$, where n is a factor and W_1 and W_2 are values of a particular parameter e.g. power then $\log_{10}W_1 = \log_{10}W_2 + \log_{10}n$. The unit associated with the logarithmic value is known as the bel. However, for convenience, the logarithmic equation is multiplied throughout by 10 to produce the decibel (dB) i.e. $10 \log_{10}W_1 = 10 \log_{10}W_2 + 10 \log_{10}n$. Now, from this equation the difference between $10 \log_{10}W_1$ and $10 \log_{10}W_2$ is 10 dB if $n = 10$ and 20 dB if $n = 100$.

Decibel is a relative unit used to describe SPL values in acoustics. When using this unit, it is important to state whether the reference SPL value is that of air

or water. The SPL reference value in air is $20\mu\text{Pa}$ and $1\mu\text{Pa}$ in water, and as such reported as dB re $20\mu\text{Pa}$ and dB re $1\mu\text{Pa}$ respectively. In other cases, dB_{ht} (Species) can be used to report a value referenced to the ‘hearing threshold’ of a particular species.

It is important to note that sensitivity of the ear varies with frequency components. Several factors depend on these sound frequency components. These include the ability of the sound to bend around a corner, attenuation by a silencer, insulation of a wall etc. As a simple case, musical instruments generally comprise of a combination of tones with the lowest tone referred to as the fundamental, and the others integrally related to this fundamental frequency known as its harmonics. In complex cases of sounds like the case of a church bell, a karaoke singer, noises from automobiles etc., the several frequency components can be resolved by a method of Fourier transform (FT) into their respective unrelated frequency components. The FT is important for general sound analysis.

Sound Pressure Level (SPL) & Intensity

The magnitude of measured sound is commonly referred to as the sound pressure level (SPL). The SPL value of a given sound is usually obtained by the following eqn. (3.1.8).

$$SPL = 20 \log_{10} \frac{\bar{p}}{2 \times 10^{-5} Nm^{-2}} dB \quad (3.1.8)$$

where, $\bar{p} = 2 \times 10^{-5} Nm^{-2}$ (reference pressure in air), and the corresponding dB value is 0dB which corresponds to the threshold of human hearing. Typically, the maximum SPL value audible to human is 120 dB. This value corresponds to $\bar{p} = 20 Nm^{-2}$. It is important to note that these extremes are seldom encountered on the daily basis. As a matter of fact, everyday SPLs are in the range of 35 to 90dB. The reference pressure value for sound underwater is $10^{-3} Nm^{-2}$, corresponding to 0dB SPL underwater as a matter of convention like the reference value in air.

When a sound source radiates energy, the radiated energies flow in some directions and not others. Sound intensity is thus a vector quantity as it gives a measurement of the direction of the flow together with the magnitude unlike the sound pressure which is a scalar quantity. Sound Intensity level (I) is defined as the rate of change of energy per unit cross sectional area. This can be written in terms of the root mean square (rms) pressure $I = \frac{\bar{p}^2}{\rho_0 c}$, where, ρ_0 is the density of the medium, and c is the velocity of the sound in the medium. If the value for intensity is substituted in the SPL eqn. (3.1.8) for pressure (p) with values for speed and density of air,

$$SPL = 10 \log_{10} \frac{\bar{p}_1^2 / \rho_0 c}{(2 \times 10^{-5})^2 / \rho_0 c} dB \quad (3.1.9)$$

Eqn. (3.1.9) is then rewritten to give eqn. (3.1.10)

$$I = 10 \log_{10} \frac{I_1}{10^{-12}} dB \quad (3.1.10)$$

As expected, the intensity value for sound in water differs from that in air. It is $6.7 \times 10^{-9} Wm^{-2}$ with a reference pressure value of $10^{-1} Nm^{-2}$.

In the simple case of two loudspeakers connected to an amplifier, when these sound sources are coherent their corresponding SPL values in dB can be added to give a zero value SPL or twice the SPL depending on the phases of the waves. If the waves are perfectly in phase, the SPL values will double (a rise of 6 dB). If they are perfectly out of phase, they can cancel each other out therefore giving 0 dB SPL (see Figure 25).

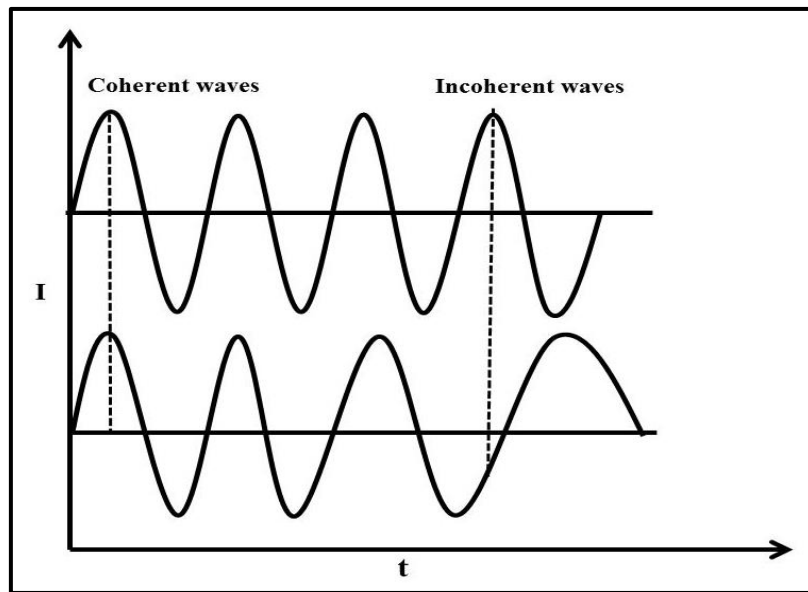


Figure 25 - Schematic of two waveforms. The initial coherent waves are in phase adding up to increase sound level. The subsequent incoherent waves are out of phase adding up and cancelling out each other to reduce sound levels.

Researchers have attempted to use this feature in cases of noise cancellation. That is a sound source with the exact SPL as the noise source but with a completely opposite phase is placed next to the noise source to cancel the noise. However, this has been met with little success as usually the primary source sound level is too high. At points where the noise source and sound source are not at equidistance, there would be an increase in noise instead of the theoretical total noise cancellation at equidistant points.

Octave and 1/3-Octave Bands

Sound signals produced by noise sources such as a car, a singing choir, a jet engine etc. all contain a wide range of frequencies. However, their relative strengths are different. Also the time-domain waveforms vary quite a lot. Because of the large amount of frequencies in these waveforms and the variation of their amplitude in time, it is not possible to analyse the variation in pressure using just a few frequencies.

To deal with the fluctuations in the amplitude, the rms value is measured over a reasonably long period of time. The frequencies can then be grouped into various frequency bands (see

Table 1) and the total strength in each frequency band can be measured. These bands are known as the octave band, and frequency bands that are three times smaller than an octave band are known as the 1/3 octave band. It is important to note that 1000 Hz is the internationally accepted reference frequency, and it is the centre frequency of one octave band.

Table 1 - Octave and 1/3 octave band centre, upper and lower frequency values

| Octave band centre frequency (Hz) | One-third octave band centre frequency (Hz) | Band frequency limits (Hz) | |
|-----------------------------------|---|----------------------------|-------|
| | | Lower | Upper |
| | 25 | 22 | 28 |
| 31.5 | 31.5 | 28 | 35 |
| | 40 | 35 | 44 |
| | 50 | 44 | 57 |
| 63 | 63 | 57 | 71 |
| | 80 | 71 | 88 |
| | 100 | 88 | 113 |
| 125 | 125 | 113 | 141 |
| | 160 | 141 | 176 |
| | 200 | 176 | 225 |
| | 250 | 225 | 283 |
| 250 | 315 | 283 | 353 |
| | 400 | 353 | 440 |
| | 500 | 440 | 565 |
| | 630 | 565 | 707 |
| 500 | 800 | 707 | 880 |
| | 1000 | 880 | 1130 |
| | 1250 | 1130 | 1414 |
| 2000 | 1600 | 1414 | 1760 |
| | 2000 | 1760 | 2250 |
| | 2500 | 2250 | 2825 |
| | 3150 | 2825 | 3530 |
| 4000 | 4000 | 3530 | 4400 |
| | 5000 | 4400 | 5650 |
| | 6300 | 5650 | 7070 |
| | 8000 | 7070 | 8800 |
| 8000 | 10000 | 8800 | 11300 |
| | 12500 | 11300 | 14140 |
| | 16000 | 14140 | 17600 |
| | 20000 | 17600 | 22500 |

Octave bands are the widest bands normally used for sound analysis. The centre frequencies are obtained by multiplying or dividing the previous centre frequencies by a factor of two ($10^{3/10}$), starting at 1000 Hz. Frequency limits of each band are obtained by multiplying or dividing of the centre frequencies by a factor of

the square root of 2 ($10^{3/20}$) [46]. Therefore, the upper frequency limit in an octave band is twice the lower frequency limit.

A sound may therefore be organised into frequency bands with each having a band level in decibels. The graph obtained from the plotting of these band levels with the corresponding decibel values as a function of frequency is called a spectrum.

The audio spectrum from approximately 20 Hz to approximately 20 kHz can be divided up into approximately 31 1/3-octave bands. If we set or define the 19th 1/3-octave band's centre frequency to be $f_{19}^{ctr} \equiv 1000\text{Hz}$, then all lower centre frequencies for 1/3-octave bands can be defined from each other using eqn. (3.1.11).

$$f_{n-1} \equiv f_n/2^{1/3} \quad (3.1.11)$$

All higher centre frequencies for 1/3-octave bands can be defined from each other using eqn. (3.1.12).

$$f_{n+1} = 2^{1/3} f_n \quad (3.1.12)$$

Then for each centre frequency the 1/6 octave frequency for each 1/3-octave band are respectively given by the formulae $f_n^{low} = f_n/2^{1/6}$ and $f_n^{high} = f_n/2^{1/6} f_n$. The percent fractional bandwidth per 1/3-octave band is constant:

$$BW \equiv \left[\frac{(f_n^{high} - f_n^{low})}{f_n^{ctr}} \right] \approx 23.2 \% \quad (3.1.13)$$

Noise Types & Weighted Sound Levels

Noise produced by a lawn mower and by a fingernail being drawn across a chalkboard may have the same SPL. However the frequency content in each varies significantly. A sound that has a uniform spectral level over the range of human hearing is termed white noise. Every frequency in the human frequency-range of white noise has an equal energy level, and as such, they appear to be rich in high frequencies only [5]. However that is not the case [47]. The perception of this richness in high frequencies is because each successive octave is twice as wide as the

preceding one. For instance, the 500 Hz octave band has a width of 354 Hz and the next octave (1000 octave band) has a width of 707 Hz. This results in a higher net energy in the high frequency components. The sound of water and wind resemble white noise. Pink noise is white noise filtered so that each octave has equal energy. This filtering is done to compensate for the increase in the number of frequencies per octave. Using a sound level meter, one can demonstrate the difference between pink and white noise. Figure 26 shows typical values for underwater sound measurement by Wenz (1962) [48].

The range of frequency for human hearing is between 20Hz to 20,000 Hz, with frequencies below the lower end known as infrasound and those above the higher end known as ultrasound. Frequency values between 1000 Hz and 4000 Hz are more discernible to humans than those at the higher or lower ends of the human frequency range. In other words, given the same SPL value, sounds containing frequency components > 4000 Hz or < 1000 Hz are more tolerable than those within this range. This is due to the physiological configuration of the human auditory system. Taking this into account, filters are normally fitted into sound meters adapting the measured human sound response to the human sense of sound. Typically, four types of filters are used to describe measure SPL levels (see Figure 27). These filters are used to increase or reduce some parts of the measured sound signal when compared to others, for measurement purposes.

Weighted sound levels dB (A, B, C and D) are levels obtained from sound meters fitted with any of the curves. They characterise measured sound with a single number, as opposed to the many readings that would be obtained using an octave or 1/3 octave band reading [50]. The A-weighting curve which is designated dB(A) is the most common curve. It follows the frequency sensitivity of the human ear at low levels. This curve filters much of the low frequency sounds it measures, similar to what the human ear does. In the same manner, the B-weighting curve follows the frequency sensitivity of the human ear at moderate levels. B-weighting curves were used in the past to measure the performance of stereos and loudspeakers. However, its limitations come into play when it is used industrially. The C-weighted curve is practically linear over several octaves and is mostly used in high sound level measurements. Although the D-frequency-weighting (like the B-frequency

weighting) is no longer in use, it was specifically designed for use when measuring high level aircraft noise.

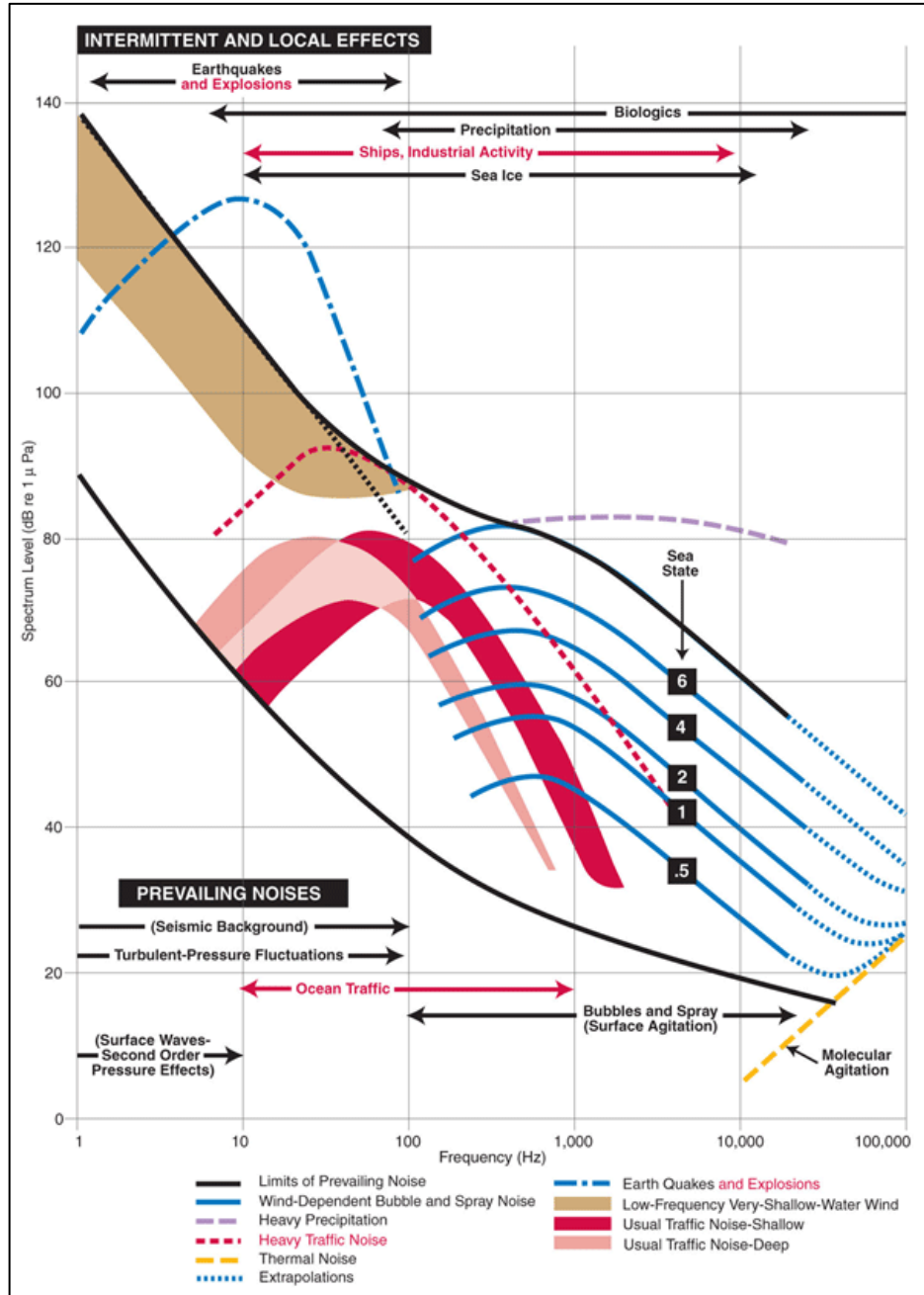


Figure 26 - Typical ocean background noise at different frequency components (Wenz curve). Underwater sound levels are given in dB re $1\mu\text{Pa}^2/\text{Hz}$ [12].

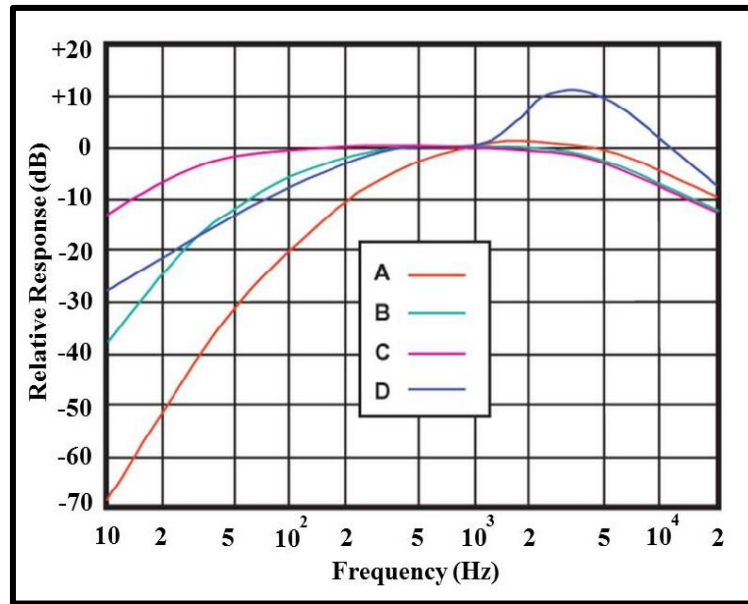


Figure 27 - Sound Level Weighting Curves A, B, C and D [49]

3.2 Underwater Acoustics

Early use of UA was for the sole purpose of intelligence for naval and nautical personnel. Traditional applications of UA involved the installation of submerged bells on lightship [51]. The sounds produced by these bells during navigation were then detected from a significant long distance by a stethoscope or a simple microphone which is mounted on the hull of the ship. If two such detecting devices were available, they were placed at opposite sides of the hull and the sounds received by each were transmitted separately to the left and right ears of an observer. This methodology was capable of assisting the avoidance of navigational dangers under conditions of poor visibility.

With advancement in technology in recent times, it has been possible to develop various types of ‘searchlight’ transducers which are capable of transmitting ultrasonic frequencies whose wavelengths in water are small when compared to the lateral dimensions of the radiating face of transducers. Narrow beams produced by these transducers are used to determine the bearing of sound reflecting targets. This is done by observing the direction of the sound beam leading to the strongest echo.

The range is measured by the time it takes a short pulse of energy to return as an echo/reflection.

Passive listening in UA involves listening to sounds at certain frequencies for specific analysis, while active UA involves the creation of sound pulses and listening to their reflections. Ultrasonic transducers and hydrophones have been most recently used in passive listening to distant ships not only for navigational purposes during poor visibility, but also for listening to enemy ships in the distance during wartime. Sound Navigation and Ranging (SONAR) has had the most research effort in UA because of its military applications. This has led to the necessity for the development of means for the efficient conversion of electrical power into high intensity beams of water-borne acoustic power and to develop a detection system capable of detecting very weak signals in the presence of masking background noise.

Ambient Noise

Ambient noise is the composite noise from all sources in a given environment. It includes sound from natural and anthropogenic sources, and varies with time and location. Natural occurrences include seismic activity and turbulence from tidal currents as well as biological noise including marine mammal vocalizations. Anthropogenic sources include vessel activity and industrial operations such as pile driving, seismic surveys, offshore drilling, etc.

The study of ambient noise in a marine environment is useful to acquire a baseline against which to compare future changes to the acoustic environment. Noise footprints of wave energy converter devices (WEC) compared with these baseline levels can also be used to determine the extent to which any new noise is likely to be detected above ambient levels [52]. Baseline ambient noise of an environment should be captured for at least 24 hours. However, for seasonal variability, which greatly influences ambient noise level, recording should be done over a year.

Linear unweighted SPL data does not allow underwater sound to be assessed biologically in a significant manner. This is because perceived noise levels of sources measured in dB_{ht} (species) are usually much lower than the unweighted levels. These

unweighted noise levels usually contain frequency components that species cannot detect, and also most marine species have high thresholds of perception of sound [53]. Table 2 illustrates an overview of the effect of noise levels on marine species.

Table 2 - Assessment criteria used in studies to assess potential impact of underwater noise on marine species

| Level in $dB_{ht}(\text{species})$ | Effect |
|------------------------------------|--|
| 0 – 50 | Low likelihood of disturbance |
| 75 and above | Mild avoidance reaction by the majority of individuals but habituation or context may limit effect |
| 90 and above | Strong avoidance reaction by virtually all individuals |
| Above 130 | Possibility of traumatic hearing damage from single event |

It is important to note that ambient noise spectral levels vary between deep and shallow water environments. Deep water is generally defined as water more than 200 m deep.

Noise from Marine/Electro-Mechanical Device

Underwater noise produced by WECs is a very important environmental impact factor that should be accounted for by WEC developers, especially to meet regulations by responsible implementing bodies [52]. It should be noted that acoustic spectra vary between shallow and deep water environments, and also amongst levels in bays, coastal waters and harbours [54]. General classification of the noise from WECs is based on their operational components, and thus the environmental impact is presumed to be minimal. However a comprehensive assessment should include the

examination of noises due to installation, operation, or decommissioning of these WEC devices.

Acoustic signatures of marine devices and machinery are composed of noise primarily from components such as turbines, generators and hydraulics, and are a combination of different noise sources within the device [55]. These components can be sub-grouped into: rotating parts like Shaft Motor Armatures, repetitive discontinuities like gear teeth armature slots and turbine blades (in Wells and Pelton turbines), explosion in cylinders in internal combustion motors, mechanical friction and cavitation and fluid flow like pumps, pipes, cylinders and valves. The first three components are associated with noises which are dominated by a fundamental frequency and harmonics of the vibration producing process, while the others produce noise with a continuous spectrum. Usually, the superposition of these two types of spectrum is observed with the tonal components clearly distinct. Other secondary noises include noise from water waves hitting these devices, vibration of mooring cables, cavitation, etc.

Noises from operating WECs are usually associated with their energy conversion mechanism, and they vary from device to device due to their respective designs. In general, the associated noise from the components of WECs tend to be continuous and it usually contains tonal (single or narrow band frequency) features, with most of the sound energy at frequencies less than a few kilohertz [56].

The temporary noise emission associated with the installation of a point absorber WEC involves the drilling or pile-driving of the fixed component to the seafloor. These noises emanate from the tugs of the power train, together with cavitation noises from the blades of the propeller. On the other hand, operational noises from point absorbers include those from the turbines, generators, electromechanical energy converters such as hydraulics, valves and pumps. Attenuator WEC devices only require vessels for deployment or decommissioning during installation as they float on the surface of sea, as opposed to the installation of point absorbers that require drilling or pile-driving. Operational noises from attenuator WECs include those from the motion of the hinges, and the interaction of water with the surface of the device. Operational noises from terminators (aka OWC) include those from the air being expelled into the air through the turbine (although

coupled into the water), and noises emanating from the impingement of the waves on the structure as a whole. Similar to the OWC WECs, operational noise from overtopping devices include impingement of waves on the device and also mechanical noise from the turbine outlet. It is important for the reader to note that the mechanism of operation of all the device types mentioned are described in the previous chapter of this thesis (Chapter 2). Typically, the installation of WECs (especially point absorbers) can involve the deployment of tens or hundreds of point absorbers which can result in a significant noise impact because the production installation of a single point absorber especially at long distances from the receiver would have very little noise impact. Spectral analysis of emitted sound signals from WECs are best characterised on a full scale unit deployed in the sea instead of test tank measurements that usually contain reverberations from the tank.

Significant noise levels for WEC devices are usually in frequency components of not more than a few kilohertz [55]. Examination of a full scale WEC was carried out in Uppsala University in Sweden by Haikonen *et al.* [57]. Transient short duration and high amplitude noise measured from this device reached an SPL value of 133 dB re 1 μPa 20 m from the device. At the marine renewable energy device testing facility in Falmouth Bay in the United Kingdom, the maximum difference in median sound level measured approximately 200 m from the WEC (during installation and without installation activities) was 34.8 dB at a frequency value of 37 Hz. A median difference of 8.5 dB re 1 $\mu\text{Pa}^2 \text{Hz}^{-1}$ between frequency values of 10 - 5,000 Hz was also estimated [58]. A point absorber on the Danish North sea coast had noise measured from it at 25 m during operation to be between 106 - 109 dB in the 15 - 250 Hz frequency range [59]. Noises recorded include a distinct tone at 150 Hz (at SPL of 121 - 125 dB) which was easily detectable during the starting and stopping of the WEC device. This tone is said to come from the hydraulic pump responsible for lifting and lowering of the absorbers in and out of the water. The fully submerged oscillating wave surge WEC, the WaveRoller, in Peniche in Portugal was characterised for its noise emission. Sound measurements were carried out 220 m and 350 m from the device using two hydrophones. One of the two hydrophones used measured broadband SPL of between 115 and 126 dB, and the other hydrophone measured SPL of between 115 and 121 dB [60]. Spectral analysis

further revealed that the fundamental frequency of the device ranged from 100 Hz to 130 Hz, with its maximum instant component being 120 dB at 120 Hz.

A comprehensive list of measured acoustic data from marine energy devices is given in the ‘review of current knowledge of underwater noise emissions from wave and tidal stream energy devices’ document[61] by the crown estates.

For other machinery components including vessels which are not WECs, noises produced by their components on-board are similar in terms of nature and intensity [62]. In a study by Erbe [63], noises from whale watching boats were recorded in the Juan de Fuca Strait and Haro Strait in southern British Columbia and north-western Washington State. It was estimated that whale watching boats produced a source sound level in the range of 145 to 169 dB re 1 uPa @ 1m and increasing with speed. Acoustic software was used to estimate zones around whale-watching boats where boat noise was audible to killer whales, where it interfered with their communication, where it caused behavioural avoidance, and where it possibly caused hearing loss.

3.3 Physics of Underwater Acoustics

For a sound signal to travel from one point to another under water, there are several constraints and transformations which it has to overcome. The effect of the movement of a sound signal from one point to another is an attenuation of the magnitude of the signal which is caused by geometric spreading and absorption loss. In sonar systems and acoustic analysis, it is important to be able to calculate propagation losses due to these factors and evaluate the effect of each of them. This subsection provides the reader with fundamental knowledge of the physics behind underwater acoustics, so as to enable the reader to easily understand the concepts and methodology behind the modelling and simulation techniques of propagation of sound signals in water. However, exhaustive details including rigorous mathematical derivations of formulae and equations are available in several acoustic and wave

propagation text books (giving distinct descriptions depending on the governing assumptions and the intended application) for example references [64-69].

Underwater Acoustic Wave Propagation

The propagation of sound in water is governed by the laws of fluid mechanics. This propagation can therefore be described by the wave eqn. (3.3.1) [16].

$$\Delta p = \frac{\partial^2 p}{\partial x^2} + \frac{\partial^2 p}{\partial y^2} + \frac{\partial^2 p}{\partial z^2} = \frac{1}{c^2(x,y,z)} \frac{\partial^2 p}{\partial t^2} \quad (3.3.1)$$

where p is the acoustic pressure of the propagating sound wave in the space (x,y,z) as a function of time t and c is the speed of sound.

For a sinusoidal wave of frequency f_0 the above wave equation becomes the *Helmholtz equation* as represented in eqn. (3.3.2)[67].

$$\Delta p + k^2(x,y,z)p = 0 \quad (3.3.2)$$

where

$$k(x,y,z) = \frac{2\pi f_0}{c(x,y,z)} = \frac{\omega}{c(x,y,z)}$$

When there is a constant velocity $c(x,y,z) = c$ in one direction(x), eqn. (3.3.1) above becomes

$$\frac{\partial^2 p}{\partial x^2} + \frac{\omega^2}{c^2} p = 0 \quad (3.3.3)$$

This has a solution shown in eqn. (3.3.4):

$$p(x,t) = p_0 \exp\left(j\omega\left(t - \frac{x}{c}\right)\right) = p_0 \exp(j(\omega t - kx)) \quad (3.3.4)$$

For propagation in the 3-D space of an isotropic medium, the solution to the wave equation for a point source is a *spherical wave* which is described as the reduced spherical wave equation. (3.3.5).

$$p(R, t) = \frac{p_0}{R} \exp\left(j\omega\left(t - \frac{R}{c}\right)\right) = \frac{p_0}{R} \exp(j(\omega t - kR)) \quad (3.3.5)$$

In eqn. (3.3.5), R is the distance from the source to the receiver. The wave fronts are spheres centred on the source ($R = 0$), and the pressure amplitude decreases as $1/R$ from its value p_0 . These pressure amplitude values are conventionally considered 1 meter away from the source.

Velocity of Sound in Sea Water

The speed of sound in fresh water is influenced mainly by the temperature of the water. However, the speed of sound in sea water is influenced by temperature and the pressure of the water. The latter is a function of the depth and salinity of the sea water. 1500 m/s is the standard velocity value used in calculations involving the transmission of sound in sea water. This value comes from the equation derived from experimentally measured data by Kinsler *et al.* [68]. This corresponds to the velocity of surface sea water having a temperature of 13°C and a salinity of 35 parts per thousand and it is typical of those measured in the surface waters overlying the continental shelves in middle latitude. The equation of this speed of sound in water is given in eqn. (3.3.6) below.

$$c = 1400.35 + 5.02t - 0.052t^2 + (1.39 - 0.012t)S + 0.017d \quad (3.3.6)$$

In eqn. (3.3.6) above, c is the velocity in metres per second, t is the temperature of the water in °C, S is its salinity in parts per thousand, and d is the depth below the surface in metres. The density of sea water using the above characteristic values is 1026.4 kg/m³ and the corresponding standard impedance is $\rho_0 c = 1.54 \times 10^6 \frac{kg}{m^2} sec$.

Figure 28 depicts the oceanographic variables temperature, salinity and pressure on the velocity of sound in the ocean. It is important to note here that the pressure being referred to here is that of the weight of the overlying ocean water weight (equilibrium pressure).

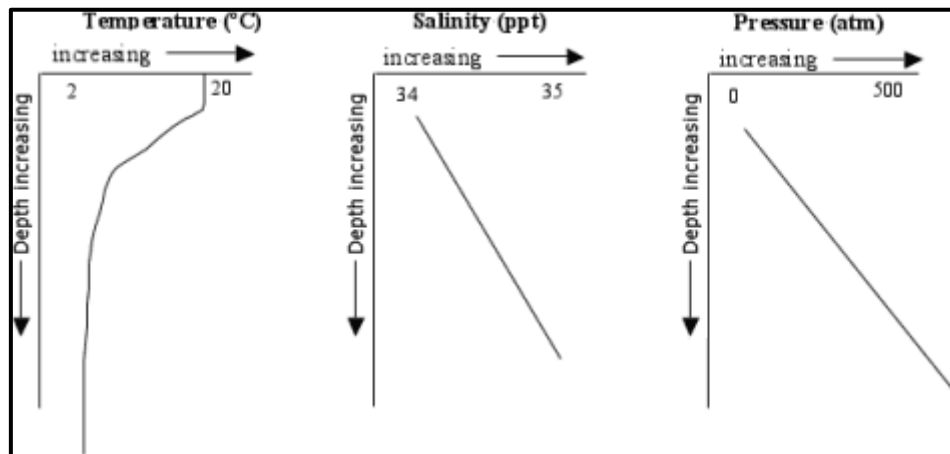


Figure 28 - Depth profiles from the open ocean of temperature, salinity and density.
 Courtesy: University of Rhode Island.

From Figure 28 it can be deduced that there is a rapid change in temperature value closer to the ocean surface down to a low temperature at the bottom. Pressure value also changes immensely from 0 atmosphere at the surface to 500 at the bottom. However, there is very little change in salinity from the surface to the bottom.

3.4 Underwater Acoustic Recording and Monitoring Systems

Acoustic Monitoring Systems

Acoustic monitoring systems usually involve two kinds of systems which are a surface deployed hydrophone connected to a digital recorder on board a vessel, or an autonomous subsea recording device that is tethered to a mooring point, or resting on the seafloor.

In an experiment by Holmes *et al.* [70], Remus (a low noise tow vehicle) was used as an autonomous underwater vehicle (AUV). The receiver was placed onto the AUV with the noise source coming from the moving ship. This gave a system with

the full versatility of a moving source and moving receiver without the expense of a second ship making this system very cost effective. In another study, Wursig and Greene [71] used calibrated sound recordings taken over a 4-day period from a quiet anchored boat at distances 80 – 2000 m from aviation fuel delivery activities at the Aviation Fuel Receiving Facility (AFRF) in Hong Kong. Hayes *et al.* [72] have used laboratory analysis of recordings to track and locate vocalizing animals. Three buoys were deployed in triangular formation at 1.8km spacing and light bulb implosions were localized to an accuracy of 60m at the array centre.

Digital Signal Processing (DSP)

Representing acquired analogue (raw) signals in a digital format, and using digital signal processors to analyse, modify and derive information from these signals are the basic concepts of digital signal processing (DSP). The processing of signals includes detecting and removing noise from signals, obtaining the spectrum of the data and transforming the data set to other formats for ease of compatibility. DSP leads to reliable accuracy which is determined by the number of data bits, excellent reproducibility (involves copying and reproducing a recorded digital signal several times without destroying the quality of the original signal), and flexibility and superior performance which involves implementing complex filters algorithms.

The base standard for modern commercially available digital recording systems is to sample at 48 kHz with a 24-bit resolution giving a frequency bandwidth of up to 24 kHz with a dynamic range greater than 16 million (2^{24}) discrete values in amplitude [52]. This is because the highest signal frequency that can be recovered from digitized data is equal to half of the sample rate which is known as the Nyquist Criterion.

3.5 Underwater Acoustic Modelling and Simulation

Computer based simulation of AE has emerged as a very important branch of underwater acoustics due to the high financial costs of test operations [73], and there are many models freely available online [74] with each providing its own range of applications.

Some properties of the seabed such as the propagation speed, compressional attenuation and density among others contribute to the spread in shallow waters significantly, making it interesting to perform a quantitative estimation of their values [75]. Numerical algorithms can be used to model the physical laws defining propagation of sound in underwater environments and compute its transmission loss as the sound spreads away from a source. An Ideal simulation must address the following:

1. A satisfactory knowledge of important medium features.
2. A mathematical model encapsulating most of the physical features of the phenomenon under study.
3. Identifying mathematical parameters and the way these should be embedded in simulation.
4. Test of the results generated through the discretized model of the problem.

Now, many of the issues stated above can take part simultaneously in the mathematical modelling of a natural sound pattern. However, not all can be taken into consideration due to the limitations of present understanding. This therefore leads to different methods of modelling based on different degrees of freedom [73]. It is important to note that as much as it is ideal to incorporate parameters such as velocity, wave number, frequency, depth range, as well as specification of the acoustic source, medium type, ambient noises, bathymetry and sea bed properties, it is more important to know what parameters possess special importance with regards to the type of simulation. For example, in a deep water model with a source far away from the sea bed and surface, most of the aforementioned parameters will lose their

direct effects as parameters such as reflection, refraction and bending of acoustic wave are not very relevant.

In the case of the simulation of sound propagation as regards wave energy devices (WEC), the choice of a specific acoustic model to apply must take into account the characteristics of the deployment site and operational principles [56]. This sub section deals with the types of mathematical models used in the modelling of sound propagation in water, with the differences between the models based on theoretical treatment of volumetric propagation. The aim of this section however is not to provide exhaustive details on the rigorous mathematical derivations of the equations behind these models which are given in reference [76], but to provide a comprehensive overview of the available models. This provides the reader with a guide to a selection criterion for selected application of each model.

Acoustic Propagation Models

There are essentially five types of underwater acoustic modelling methods including Ray Theory (RT), Fast Field Program (FFP), Normal Mode (NM), Parabolic Equation (PE), and most recently Finite-Element (FE) solutions of the full wave equation. We discuss the NM and PE models in this section as the RT is directed at computationally efficient high frequency component ray tracing, which is not of interest in this thesis.

FE and NM are concerned with the modelling of low frequency components in shallow waters. They are the most computationally intensive models; however, they have the highest fidelity amongst all models. FE models most accurately predict the reverberation and Transmission Loss (TL) in shallow water [77] when compared to the others, as they (other models) share a common approximation (neglect) of the energy scattered from the interface at angles close to normal, and neglect of multiple scattering in some cases. The FE method is used in the modelling of the propagation of UA in this thesis, and as such is discussed further in subsequent chapters of this thesis.

The Normal Modes Method starts off by applying the concept of vibrations in an idealized ocean model. The medium is homogeneous, bounded above by a free surface and below by a perfectly flat disk. The sound waves are considered flat and the speed of sound constant.

These models assume that the acoustic field can be decomposed into normal modes and eigen-functions which are obtained from the Helmholtz wave equation. This accounts for the boundary conditions of the medium being described. NM theory is particularly interesting to describe sound propagation in shallow waters and it is easily adaptable to multiple layers. Typical shallow-water environments are found on the continental shelf for water depths less than 200 m.

Several normal-mode models exist which are used for predicting acoustic transmission-loss in the ocean. However, typical difficulties include numerical instabilities for certain types of sound-speed profiles [78]. The Kraken NM program [79] written in Matlab with a Graphical User Interface (GUI) [80] is one of a few NM models that is robust, accurate, and efficient. The program for this model was written by Mike Porter of the Heat, Light & Sound Research, for the Centre for Marine Science and Technology, at the Curtin University of Technology in Perth, Western Australia. This program is used to model marine environments that are range-independent, range-dependent or fully 3-dimensional. The earliest model of the Kraken NM was developed from a set of algorithms by Pekeris [81] for a simple two-layer model (ocean and sediment) with constant sound speed in each layer. It is important to note that the SACLANTCEN Normal Mode Acoustic Propagation (SNAP) model is very similar to the Kraken Model [80] as they produce similar results when run on the same problem because they use the same algorithm. However, the Kraken model has a large number of options which provides an advantage to a user familiar with the software, although not so much for users without experience.

The Parabolic Equation (PE) method assumes that energy propagates at speeds close to a reference speed (either the shear or compressional speed). It is used to effectively simulate range dependant low frequencies in shallow and deep water sonar environments. In the PE method, a generalised Wentzel-Kramers-Brillouin (WKB) approximation is used to solve the depth-dependent equation derived from

the normal mode solution in Multipath Expansion Models. This method models high frequency, range- independent deep water sonars effectively. In a recent study by Soheilifar *et al.* [73], the parabolic method was employed in MATLAB routines to simulate acoustic wave propagation. The simulation output was compared with an ideal mathematical model and the error value obtained was 18.4%, the bed attenuation coefficient having been neglected in the simulation.

In the fast field theory which is also known as wavenumber integration, the normal mode approach is basically used to separate the wave equation parameters, after which the Hankel function expression is replaced by the first term in the asymptotic expansion. In the early stages FFP theoretical models did not allow for environmental range dependence, however, a computationally intensive method using Green's function method to solve the one-way wave equation in a stratified ocean environment was introduced [76]. A model which uses an approach of hybrid combination of wavenumber integration and Galerkin boundary elements has also been used. This approach extended the fast field theory to range-dependent environments. In recent times the FFP approach has been modified to accommodate acoustic pulse propagation in the ocean. Application of this approach includes the specification of arbitrary source time series instead of the more conventional time-harmonic sources used in frequency-domain solutions of the wave equation [76]. This is done by directly marching the formulation in the time domain. More PPF approaches towards the solution of the wave equation are given in the reference [76].

Table 3 clearly specifies the domain of application of the aforementioned underwater acoustics modelling types.

Table 3 - Sound propagation models and their respective application domain. Table is an adaptation of Paul C. Etter's professional development short course on underwater acoustics modelling and simulation.

| Model Type | Application Mode | | | | | | | |
|-----------------------|---------------------------|-----------------|-------------------|-----------------|------------------------|-----------------|-------------------|-----------------|
| | Shallow Water Environment | | | | Deep Water Environment | | | |
| | Low Frequency | | High Frequency | | Low Frequency | | High Frequency | |
| | Range Independent | Range Dependent | Range Independent | Range Dependent | Range Independent | Range Dependent | Range Independent | Range Dependent |
| Finite Element Method | ● | ● | ● | ● | ● | ● | ● | ● |
| Parabolic Equation | ● | ● | ○ | ○ | ● | ● | ● | ● |
| Normal Modes | ● | ● | ● | ● | ● | ● | ● | ○ |
| Fast Field Program | ● | ○ | ● | ○ | ● | ○ | ● | ○ |
| Ray Theory | ○ | ○ | ● | ● | ● | ● | ● | ● |

● Modelling approach is applicable both physically and computationally
 ● Modelling approach is not practical in both cases
 ○ Modelling approach is limited in accuracy of execution

Table 3 depicts a summary of the domains of applicability of underwater acoustic propagation models. Frequency components less than 500 Hz are considered low frequency components, and those above 500 Hz are considered high frequency components. The table is adapted from Paul Etter's underwater acoustic modelling and simulation. An exhaustive summary of underwater acoustic propagation models, together with their techniques and range dependency is given in the reference [76].

3.6 Finite Element Modelling and Comsol

Underwater acoustic numerical techniques and codes for WEC noise simulation (as in this thesis) require the implementation of the following features to closely delineate the underwater acoustic domain and propagation characteristic of these devices:

- The implementation of a near field water/seabed in the frequency domain around the WEC device. This region is usually no more than a couple of hundred meters. FE model code, comsol, which is a user-friendly Multiphysics platform, adequately resolves frequency components in this region for close approximation to the real solution. This is done via discretization of the domain into small discrete elements. The physical equations within the acoustics module are solved using the finite element method, with higher-order element discretization in combination with state-of-the-art solvers. It is important to note that in other analysis or simulation scenarios, NM code could be coupled with the FE code to predict long range acoustic propagation [82]. With the increase in technology in recent times, computational powers have increased and so has the limitation in terms of discretization of large domains.
- The implementation of a perfectly matched layer (PML) to truncate the computational domain via absorption of outgoing acoustic waves is required. This mimics an infinitely extended domain. The flexibility and robustness of the Acoustics modelling module of comsol allows for the implementation of this PML.
- The propagation domain also requires a large variety of boundary conditions for adequate representation of the physical parameters. Comsol offers boundary conditions such as wall types, impedance conditions, radiation, symmetry, periodic conditions etc. for modelling open boundaries as well as conditions for applying different kinds of sources.

Chapter 4

4 Marine Energy Devices and Marine Mammals

Today, a large number of marine based energy devices are being deployed rapidly across coastal areas of the world's oceans to harness the huge natural energy and power potential provided by nature. These devices produce acoustic signals at sound pressure levels (SPL) across a range of frequencies that could sometimes interfere with the livelihood of marine animals in the direct vicinity of these devices. The sound signals produced by these devices exhibit different propagation characteristics including attenuation, reverberations, scattering etc. depending on several factors. These factors include the interaction of the sound signals with the bathymetry of the bottom surface (which varies with geological properties), as well as the sea surface.

This chapter presents finite element (FE) models that simulate the emission and propagation of acoustic signals produced by marine devices in an infinite truncated idealised medium. The estimated SPL of the received sound signals at certain distances away from the source are compared with the audiogram (audible threshold for standardized frequencies) of the *harbour seal*. This chapter contributes to the overall thesis because it considers the implication of bottom surface boundary effect on emitted acoustic signals from marine devices during propagation from source to receiver.

4.1 Introduction

Underwater acoustic applications are generally grouped into two categories, military and civilian. Military applications are further sub-divided into two main categories according to their mode of functioning [67]. The first involves *active sonars* which transmit signals and receive echoes to detect submerged submarines and to also detect landmines. The second military application involves passive sonars designed to intercept noise radiated by a target vessel. Civilian underwater acoustics is a more modest sector of industrial and scientific activities. They are predominantly passive and used for environmental study and monitoring, as well as the development of offshore engineering and industrial fishing.

Researchers use underwater acoustic modelling to assess the impact of underwater noises on marine species as well as the environment [83]. Noise impact models have been used to predict the impact of low frequency noise (< 500 Hz) from mechanical noise sources on fish (cod) [84]. Several acoustic propagation models which model acoustic signals produced by wave energy devices in shallow water environments have been studied [56, 75] and their effect on marine mammals are characterised.

The bottom surface of oceans and lakes critically affect the operation of underwater acoustic systems [85], and also plays an important role towards the propagation and attenuation of sound signals.

4.2 Marine Mammals, Energy Devices & Noise

Marine animals including sea mammals such as cetaceans rely hugely on sound for adequate movement, defence, communication, feeding and to detect predators and prey in their natural habitat. Sound signals (especially low frequency signals) travel a lot further in water compared to electromagnetic radiation and light. Four zones of noise influence [86] have been defined for marine animals with respect

to the position of noise source and the distance from the subject (marine animal) of interest. These zones include audibility, responsiveness, masking and hearing loss. It is important to note that this chapter focuses on the audibility zone of the selected marine species, as it seeks to establish the ‘detection’ of sound signals by the marine animals especially the harbour seal.

In the Irish coastal waters, *Phoca vitulina* or the harbour seal (also known as the common seal) is one of two seal species that are native. They establish themselves at terrestrial colonies (or haul-outs) along all coastlines of Ireland [87], and historically, these haulout groups tend to be found at the hours of lowest tides. Audiograms for harbour seals have been determined by several researchers including Tougaard *et al.* [88]. They show good underwater hearing from very low frequencies (tens and hundreds of Hz) to high frequencies (thousands of Hz). They can detect sounds as low as about 55 dB re 1 μ Pa over a range of frequencies. Here, we compare our model results (for sounds produced by a point absorber marine based energy device) to the harbour seals’ audiogram using data presented by Tougaard *et al.* [88]. Marine energy devices are generally installed from a couple of meters to hundreds of meters from the shores of coastal lines. The deployment distance from these shores depends on the type of marine energy device and the location where they are being deployed. Some marine energy devices generate SPLs of about 120 dB re 1 μ Pa from mostly low to mid frequency values (measured 1 metre from the source). A recent report in 2013 [89] showed that typical marine energy devices such as the wave energy Pico Plant in the Algarve in Portugal and the SeaRay, west point, Puget sound, in the United States of America generate levels as high as 120 dB re 1 μ Pa.

4.3 Model Description

Acoustic forward models were used to estimate the SPL of signals emitted by marine energy devices. The dominant frequencies for these signals are usually low (0.1 - 1 kHz) [52, 55, 59] and they travel far away from the source as opposed to higher frequencies which attenuate faster. Details of the acoustic spectral emitted by

these types of WEC devices are given in chapter 3. The models consist of monopole point sound sources which are used to represent typical marine energy devices submerged in a shallow ocean environment. These sound sources emit omnidirectional spherical acoustic signals in an idealized isotropic ocean waveguide. This medium is characterised by a spreading loss of $1/r^2$, where r is the radius of the sound source to the receiver. The sound source is represented by eqn. (4.3.1).

$$-n \cdot \left(-\frac{1}{\rho_0} \nabla p + q \right) + \left(\frac{ik}{\rho_0} + \frac{R(|r|)}{\rho_0} \right) = \frac{(ik + R(|r|) - i(k \cdot n)) p_0 e^{-i(k \cdot r)}}{\rho_0} \quad (4.3.1)$$

An incoming wave with sound pressure amplitude p_0 is described by the term on the right hand side of eqn. (4.3.1), and the direction is given by the vector k . $R(|r|)$ is equal to $1/(2r)$ for the case of the cylindrical wave and r is the radius from the source to the boundary. The default for the vector k is the inward normal vector, $-n$, and this is the natural direction for waveguides and similar structures. The sound source (power point source) is described by eqn. (4.3.2), where P_{ref} is the reference pressure and c is the sound speed.

$$\nabla \cdot \frac{1}{\rho} (\nabla p - q) - \frac{k^2 p}{p} = 2 \sqrt{\frac{2\pi P_{ref} c}{\rho}} \quad (4.3.2)$$

The first of the two model types, model (a) without bottom surface interface shown in Figure 29 (a), is characterised by a simplified range-independent iso-velocity water media. This is assumed because spatial variation of sound speed in shallow water are typically small, and their effect on sound propagation are generally much smaller than the effect of interactions with the bottom surface [90]. It is bounded by pressure release (free) perfectly reflecting boundaries. There is no restoring force on these boundaries, resulting in the polarity (phase change) of the incident wave being the same as the reflected wave. The bottom surface boundary is a reasonable approximation to a penetrable seafloor at low grazing angle [82]. The second model type, model (b) (Figure 29 (b)), with bottom surface interface, is different from model (a) as it is characterised by a solid bottom surface. It has a fluid-structure interface between the liquid and the solid bottom surface.

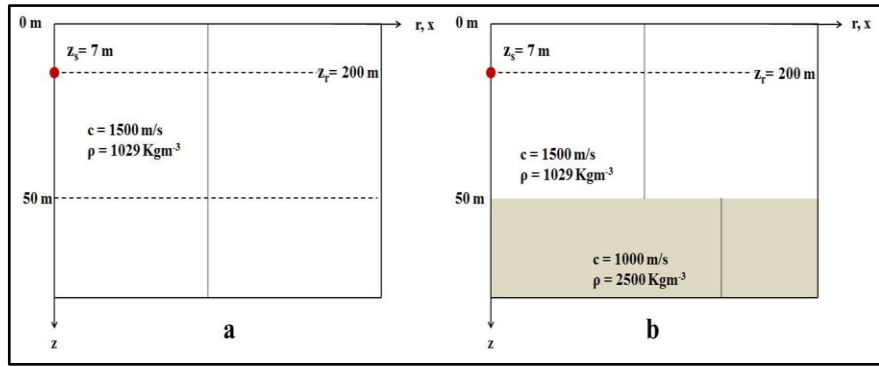


Figure 29 - Waveguide models with pressure release surface (a), and solid bottom surface (b)

From Figure 29, c and ρ represent the sound speed and density in the media respectively, z_s and z_r represent the source depth and receiver depth respectively, with the values given in Table 4. The acoustic media are characterised by other factors that are susceptible to varying parameters such as temperature and salinity.

Table 4 - Parameters of the acoustic medium used in the simulation

| Parameter | Value |
|---|-------|
| Water Depth [m] | 50 |
| Source Depth [m] | 7 |
| Water Density [Kg m^{-3}] | 1029 |
| Sound Speed in Water [ms^{-1}] | 1500 |
| Bottom Surface [Kg m^{-3}] Density | 2500 |
| Bottom Surface Sound Speed [ms^{-1}] | 1000 |

Table 4 gives typical values for sound source/receiver models for an acoustic medium in a real life scenario. The original problem is discretized by approximating the Partial Differential Equation (PDE) using the finite element method (FEM) and boundary conditions. This was solved using the steady-state stationary solver in the Fourier domain in Comsol Multiphysics [11]. To model sound waves, the wave eqn. (4.3.3) derived from the developed linearized one-dimensional (1-D) continuity equation is used [91].

$$\frac{\partial^2 p}{\partial t^2} + \nabla \cdot \left(-\frac{1}{\rho_0} \nabla p + q \right) = 0 \quad (4.3.3)$$

Eqn. (4.3.3) represents the acoustic wave equation, where:

p : is the acoustic pressure

ρ_0 : is the fluid density

q : is an optional dipole source

The acoustic pressure (p) can then be replaced by a time-harmonic wave, i.e. $p = P_0 e^{i\omega t}$, and this is substituted into eqn. (4.3.3) above to get the Helmholtz eqn. (4.3.4) shown below.

$$\nabla \cdot \left(-\frac{1}{\rho_0} \nabla p + q \right) - \frac{\omega^2 p}{c^2} = 0 \quad (4.3.4)$$

where:

$\omega = 2\pi f$: is the angular frequency

c : is the speed of sound

Equation (4.3.4), which is the wave equation in the frequency domain, is used to compute the frequency response of the model using the comsol stationary parametric solver [91]. To allow for adequate convergence of the solution, free triangular mesh elements (see Figure 30) which adequately captures the random motion of these signals especially in regions of high gradient were used to resolve the wavelength of the smallest sound signal into fractions. The maximum mesh size was given as: $\text{mesh}(h)_{max}[m] = \lambda/8$ where $(\lambda)[m] = c/f$, with time scale[s] = $1/s$, $c [ms^{-1}]$ is speed of sound and $f[Hz]$ is frequency.

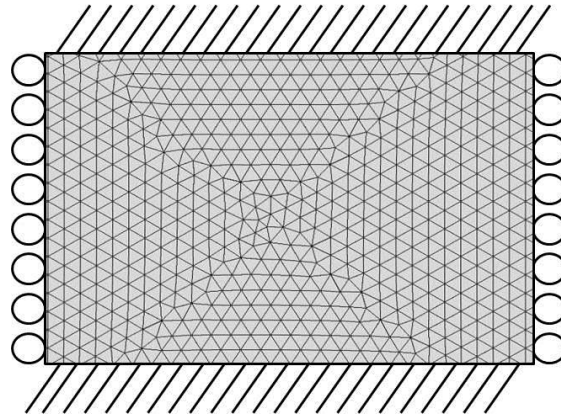


Figure 30 - Truncated acoustic-aquatic domain mesh.

An important property for time-harmonic acoustic analysis is the frequency. Therefore for accurate convergence of the solutions, it is important that the wavelength be resolved in the mesh. The rule of thumb is that the maximum mesh element should be a fraction of the wavelength. The length scale for the model is given as:

$$\text{wavelength } (\lambda) = c/f \quad (4.3.5)$$

Therefore,

$$\text{mesh size}(h) = \lambda/8 \quad (4.3.6)$$

Where:

c : is the speed of sound [ms^{-1}]

f : is the frequency value [Hz]

$$\text{Time Scale} = 1/f \text{ [s]} \quad (4.3.7)$$

4.4 Results and Discussions

Sound pressure levels of frequency components were estimated from distinct points away from the sound source(s) for models (a) and (b), with and without bottom surface interface respectively, and multiple sound sources. The result from model (a) without the bottom surface influence is shown in Figure 31. It shows that SPL values attenuate proportionally with an increase in distance for all frequency values. This is evidential to the spreading loss mechanism exhibited by isotropic media when there are no influences by the scattering of waves or interaction with the boundaries. Results from model (b) with bottom surface interface (shown in Figure 32) is characterised with reverberation and interaction of sound signals during propagation due to the solid bottom surface. Therefore it is difficult to establish a linear decrease of SPL with distance for this model when compared to the model (a) without the influence of a bottom surface interface.

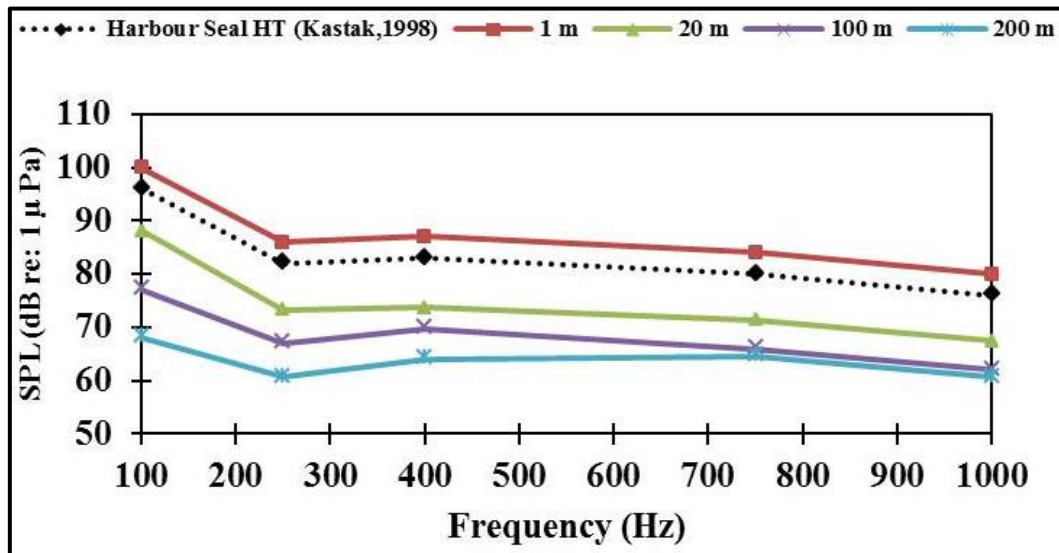


Figure 31 - Sound pressure level values from sound source of model without bottom surface interface influence

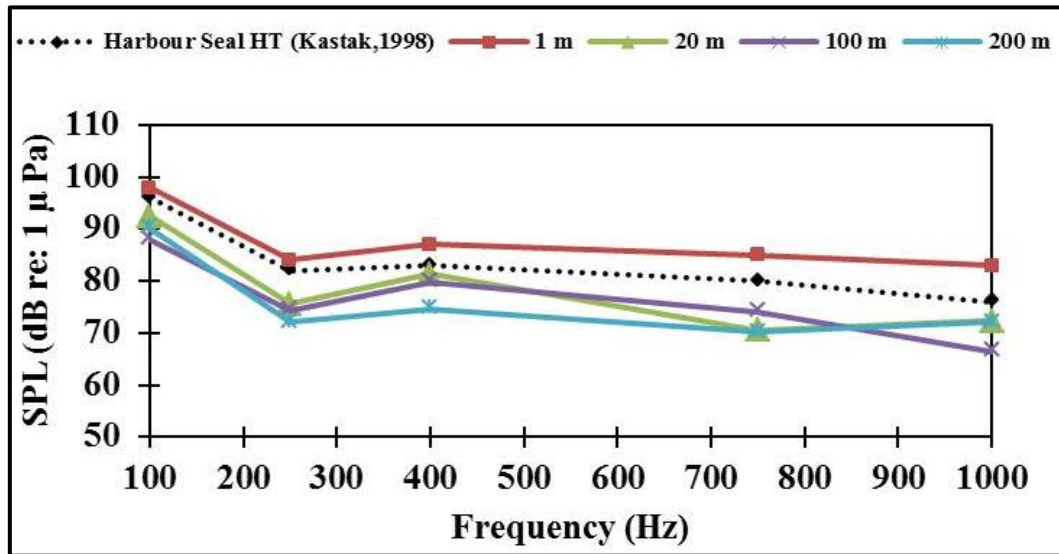


Figure 32 - SPL value from sound source of model with bottom surface influence

Figure 31 and Figure 32 also depict that the audiogram of the harbour seal is above the SPL values for all frequencies at 20 meters from the sound source. This means that harbour seals which are approximately 20 meters and beyond the sound source do not receive these sound signals. In other words, the signals' SPLs are below their hearing threshold for these frequency values. However, for the model (b) with a bottom surface interface it is difficult to state this relationship, as there is no gradual or steady decrease in SPL at incremental distances away from the source.

Figure 33 shows the models with and without the influence of the bottom surface for 3 different frequency values covering the typical range of frequency components emitted by these devices. The interaction of the sound signals with the bottom surface causes reverberation of the sound signals as can be seen from the graphs. Sound signals impinge off the solid bottom surface of the acoustic medium and the extent of the reverberations depends on several factors including the individual frequency component. It can be deduced that the higher the frequency component, the higher the scattering effect as a result of the surface bottom interface. It is important to note that marine energy devices can be set as an array of multiple devices, with the combined SPL values exceeding that of a single device.

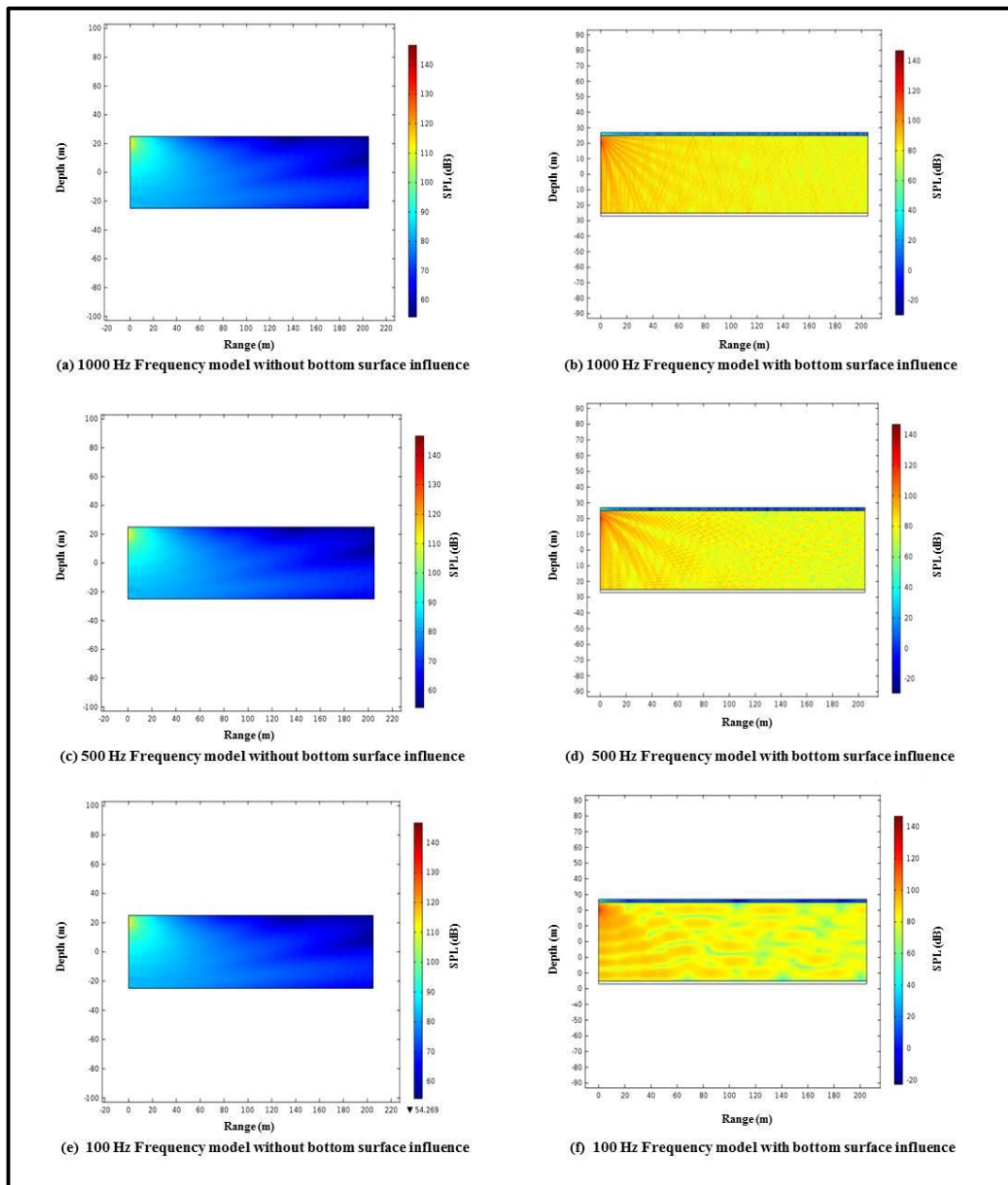


Figure 33 - Models with and without bottom surface influences

Figure 34 shows the sound propagation result of multiple (three) sound sources in the model with bottom surface interface influence. This is representative of a real life scenario of an array of WEC devices, with the configuration of the WEC devices depicted in Figure 34.

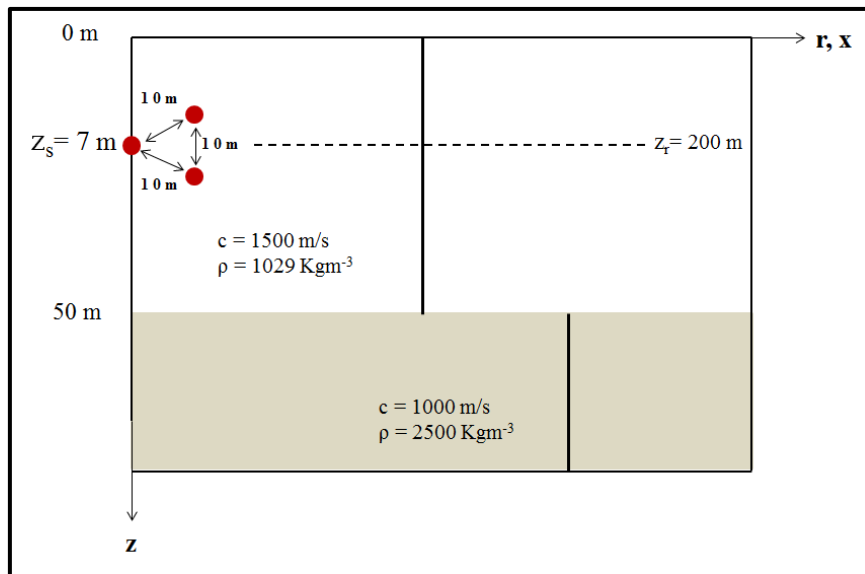


Figure 34 - Schematic showing configuration of multiple deployed WEC.

The result (Figure 35) shows an effective increase in the overall SPL value of the combination of the noise from the sound sources up to 10 dB. When compared to the results obtained from the other models, it is observed that the overall SPL value rises above the hearing threshold of the harbour seal for all distances.

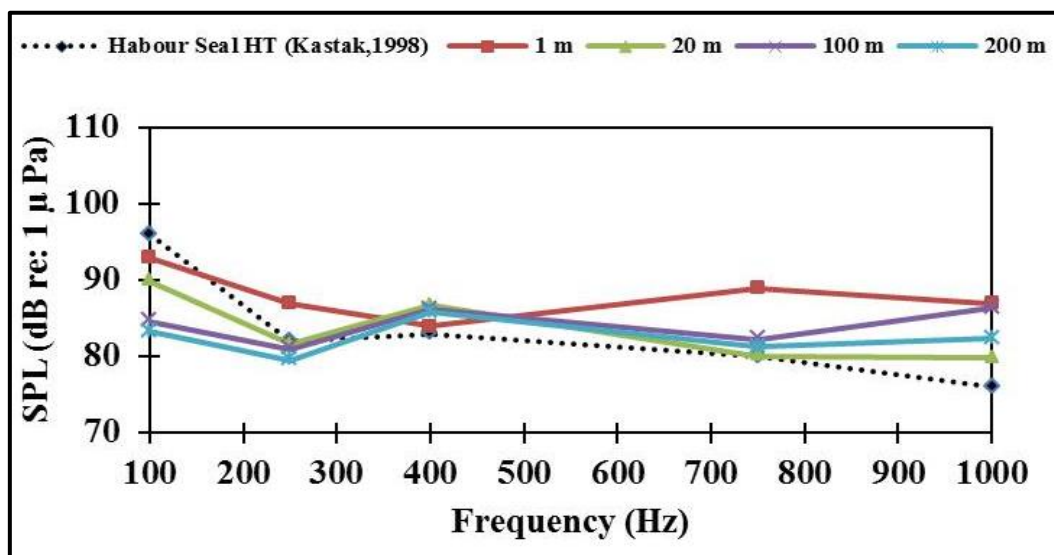


Figure 35 - SPL values from multiple sound sources of model (b) with bottom surface influence

4.5 Conclusion

Sound signals comprising of low frequency components emitted from point absorber marine energy devices were simulated. These devices were modelled as point sources in the acoustic domain as their components mainly generate tonal noise of low frequencies. An acoustic medium with and without the inclusion of a bottom surface interface, together with single and multiple sound sources were modelled for the propagation of these sound signals. The bottom surface interface interacted with these sound signals resulting in their reverberation off the bottom surface and interaction with each other. Sound pressure level values of 100 Hz frequency components decreased by up to 30 dB re 1 μ Pa from 1 m to 200 m from the device, in the model without bottom surface influences. This difference in SPL values however decreased to up about 10 dB re 1 μ Pa in the model with bottom surface influence. This showed a linear decrease of SPL with distance for the model without the bottom surface influence when compared to the model with an influence of bottom surface interface.

The models with bottom surface interface expressed complexity in sound propagation compared with the models without a bottom surface. These models show variability in angle from the source as well as local increases in SPL values with increasing distance. The models without bottom surface interface generally show SPL values decreasing monotonically with increasing distance from the source, similar to spreading law assumptions. An overall increase in the overall SPL value of frequency components of up to 10 dB was also estimated due to the increment in the number of sound sources representing an increase in number of devices. These analyses highlight considerations to be taken during acquisition of sound signals from the operating vicinity of WECs, as it shows the influences of bottom surface on the propagation of sound signals from source to receiver, and an increment in the number of devices deployed.

Chapter 5

5 Noise from Ferries and the Potential Effect of Sea State on their Propagation: A Dublin Bay Port Area Study

This chapter presents analysis of acoustic data of underwater sound emitting vessels (USEV) recorded during operation in the Dublin Bay Port Area. Investigations were carried out to assess the magnitudes of these underwater sounds, and also the potential effect of changes in tidal states on these sound signals and their propagation. Power spectral densities (PSD) and 1/3 octave band sound pressure levels (SPL) were computed for frequencies between 50 - 500 Hz and 50 - 1000 Hz, respectively. During the presence of these vessels in the study site, broadband SPL values for a range of frequency components were calculated to be between 94 - 121 dB (re 1 μ Pa) at a distance of 200m from the vessels. These values decreased by 5 - 21 dB during their absence. The strongest sound level recorded at this site was during the departure of vessels from the dock at 200 m from the recording system. The SPL value calculated during this operational period at 315 Hz frequency was 121 dB re 1 μ Pa²/Hz. Associated components' spectral of the vessels were also identified, and the effect of difference in heights of tidal ranges (Neap/Spring) on this site was investigated.

5.1 Introduction

Shipping activities contribute significantly to the overall noise composition of most underwater environments [92]. It is important to note that the effect of oceanographic conditions, such as tidal changes, on the underwater soundscape of USEV has seldom being researched in literature. The acoustic signatures of these USEV are primarily composed of sounds from their components such as engine, propeller propulsion systems, generators and hydraulic components (including pumps and valves). Recent studies indicate that the magnitudes of underwater acoustic signals can be affected by tidal states (Neap and Spring tides) [93-95], thus it can be inferred that tidal states are likely to influence acoustic propagation conditions of sound emissions from USEV between sound source and receiver. The periodic nature of surface waves are huge influences on the magnitude of sounds from these USEV as they are likely to exhibit periodicity [96]. The physical properties of the ocean bottom surface and the type of sound signals produced are also important estimable parameters in underwater sound analysis [97].

Studies on vessel operations across the globe show a statistical steady growth in vessel traffic over the past few decades [98]. Due to the surge in global trade, commercial ships and ferries have not only increased in number and operations but in sophistication, sizes and propulsion power. In fact, it has been reported that the total gross tonnage of ships in recent times between 1965 and 2003 has quadrupled and that number of ships doubled [99] thus drastically increasing the underwater noise contribution of shipping activities in the marine ocean environment. Acoustic signal components produced by these ships propagate as far as hundreds of kilometres from their sources especially in deep water (> 200 m) environments.

Underwater acoustics from shipping activities dominate the low to mid frequency (10 Hz – 1 KHz) acoustic spectral components in the marine environment [98, 100-102]. Previous studies have shown that differences in vessel types including vessel design [103] and operational conditions [71, 99] account for the distinctions in frequency components emitted by these vessels. Typical noise spectrum levels

decrease with increasing frequency from about 140 dB re 1 $\mu\text{Pa}^2/\text{Hz}$ at 1 Hz to about 30 dB re 1 $\mu\text{Pa}^2/\text{Hz}$ at 100 kHz [71, 83], with distant shipping traffic being one of the most dominant noise sources in most areas for frequencies of around 100 Hz [104].

In this chapter underwater acoustic signals from shipping vessels are recorded, stored, conditioned and analysed. These acoustic signals are emitted from shipping activities in the Poolbeg Marina site of the Dublin bay region. The schedule of these activities which include departure and arrival of these shipping vessels from the port were obtained from the Irish Port Company. These roll in roll off (Ro-Ro) ferries have a length of approximately 166m, beam of 23m, displacement tonnage of 17464 gross tonnage (GT), and deadweight tonnage of 6790. The effect of oceanographic conditions such as Neap and Spring tides, and sound source/receiver distances on the acoustic signals recorded is investigated.

5.2 Methodology

Site Information

Acoustic recordings were carried out at the Dublin Poolbeg Marina site (see Figure 36). This site is a busy port environment located on the lower Liffey estuary covering a wide area of 5 km². It is geographically placed at latitude 53°20'39' and longitude -6°12'59''.

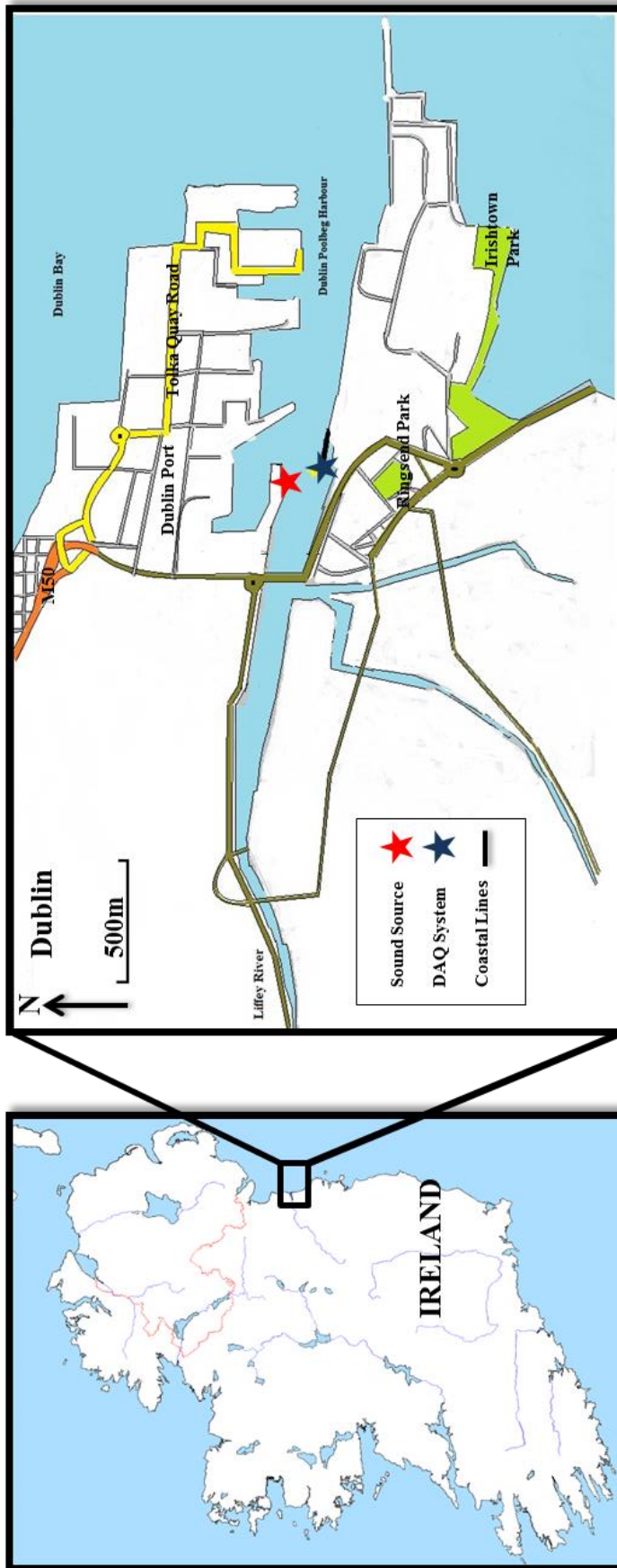


Figure 36 - Map of the Dublin bay region in Ireland showing the hydrophone deployment area and the ship docking area in relation to the lower Liffey.

The study site is restricted to the public, and activities here comprise mainly of the entry and exit of the Ro-Ro ferries and a few fishing and recreational boats together with some occasional ferries a couple of kilometres away. The site is home to benthic communities, shellfish, marine birds as well as some marine mammals including harbour seals, all contributing to the ambient noise of the site. Other noise contributing sources include migrating salmon and sea trout and anthropogenic aquacultures and recreational activities [105]. The water depth in the immediate vicinity of the monitoring data acquisition system (DAQ) and the channel width are approximately 8m and 260 m respectively. And is characterised with macro-tidal waves of mean tidal range of 2.75 m and an average mean spring and neap tide of 3.6 m and 1.9 m, respectively [106].

Equipment and Deployment

Figure 37 shows the schematic of the signal processing approach utilised. Acoustic signals recorded by the hydrophone are amplified using a preamplifier. The amplified signals are then digitally converted and stored on a computer for further signal processing and analysis. The hydrophone used (H2a series, Aquarian audio products, United States) has a range of 1 Hz to 100 kHz with a sensitivity of -190 dB re 1V/ μ Pa (+/- 4 dB), with a flat response frequency range of 20 Hz to 4 kHz. It has an optimal performance operating depth of 80 meters with a horizontal omnidirectional polar response. The preamplifier (PA2-PIP, Aquarian audio products, United States) has a gain of 20 dB with the A/D recorder used to record sounds at 24-bit/44.1 kHz in a WAV format.

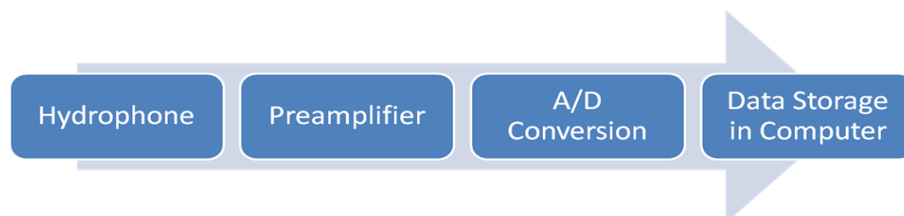


Figure 37 - Schematic of the Data Acquisition System

A moored hydrophone system suspended by a buoy was the adopted technique for the DAQ deployment in this study (see Figure 38). This system is preferred to other systems such as vessel-based surveys, and the drifting systems employed in other studies [93, 107, 108 , 66, 109, 110] for the acquisition of data, due to its long term deployment advantages. This deployment technique also allows data acquisition of a range of tidal cycles, weather conditions, and operational states.

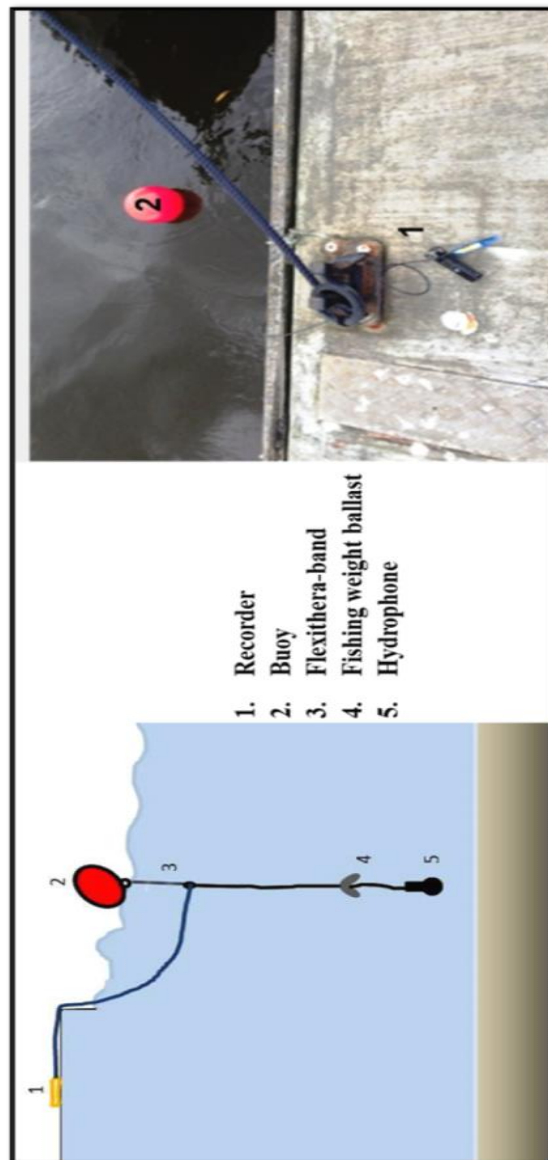


Figure 38 - Schematic of the hydrophone system (left) and the actual system on the pontoon (right) with the hydrophone submerged in water.

The overall system consisted of the hydrophone, a spar buoy, fishing weight ballasts and some surgical tubing as illustrated in Figure 38. The spar buoy was used to restrict the hydrophone from the motion of the waves, whilst the ballasts and

surgical tubing compensated the tidal movement and cable strumming of the hydrophone by the waves respectively. This was useful in preventing hydrostatic pressure which contaminates the recording as the hydrophone moves up and down in the water column with surface wave motion, as they generate high levels of low frequency noise which dominates the overall noise levels recorded. The overall structure of this system aids in the elimination of high current noise like flow noise, swell noise, cable strumming characterised by static hydrophone systems.

Underwater acoustic recording systems have to have sufficient autonomy and be properly rugged to withstand the harsh ocean environment, especially for long-term deployment. This requires paying attention to the power supply (or battery life) and the data storage capacity. In this study, the limitations of the power supply were overcome by using a self-powered hydrophone. In the case of the data storage capacity, an ‘on/off’ system, whereby recordings are stopped and started at certain times, was initiated. This helps in capturing only relevant acoustic data thus maximising the storage capacity of the system.

Data Collection

Acoustic data was collected on several days during the summer months of July, August and September of 2014. This includes recordings of the arrival, berthing and departure of these vessels at several distances away from the hydrophone at different tidal states shown in Figure 39.

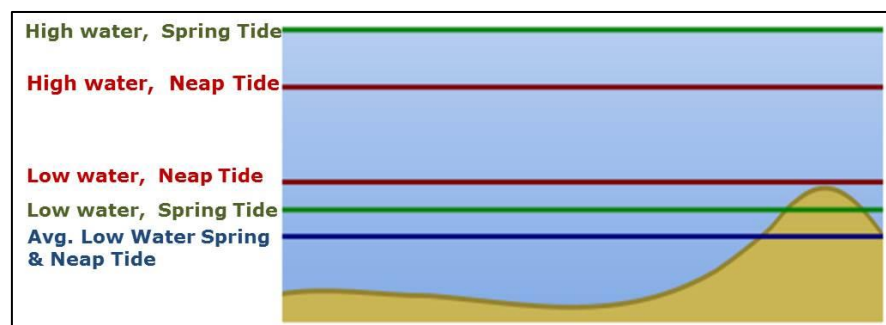


Figure 39 - Tidal states at the site. Data were collected during spring and neap tides, at low and high water levels.

Sea state conditions during these recording dates were approximately 2 on the Beaufort scale. This condition is characterised with wind speeds of about 2 m/s resulting in small ripples and very small wavelets in the water. Sea surface temperature values were 14.5 °C on average with no rain. During spring tides, tidal heights ranged between 3 - 3.41 m at high tides and 1.05 - 1.26 m at low tides during recordings. At Neap tides, tidal heights ranged between 1.02 - 1.24 m at low tide and between 2.65 - 3.20 m at high tide. The hydrophone was suspended from the pontoon at a depth of 6 m at the upper part of the estuary. This was determined with consideration of the dependence of depth to frequency and is complimentary to the depth along the propagation distance, and the draft of the vessel which is 5.6 m. Typically there is a stronger dependence on depth per frequency in the uppermost part of the water column, in particular within one quarter of an acoustic wavelength of the water surface [111].

The decision to collect data from this site was mainly influenced by the fact that the arrival and departure of these particular types of vessels are predictable and constant, as they have scheduled times, and they dock closest to the measuring system. Other factors include the ease of accessibility to the site by the author as other research activities by the university are being taken place there, together with its proximity to the university.

During the arrival of these vessels, berthing and manoeuvring activities are carried out by employing their draught and propulsion systems and thus producing a variety of sound signals. This is prior to the offloading and on-loading of freights and cargo from the rear of the ships.

Noise Analyses & Data Presentation

The results in this chapter are presented to allow the display of smooth underwater acoustic data, and as such are reported in two forms. The PSD outlines the distribution of power of the average signal values as a function of their frequency contents. It is calculated in a 1 hertz frequency band with units of decibels (dB re 1 $\mu\text{Pa}^2/\text{Hz}$). The other form is the SPL, which is a logarithmic measure of the rms

acoustic pressure in the 1/3 octave band with units of decibels (dB re 1 μ Pa), and 1 μ Pa is taken to be reference pressure value of sound underwater. These units are usually important for analysis of underwater acoustic data with variance in pressure levels of various frequency components [95].

The technique adopted for the analysis of the results is similar to that used by Würsig *et al.* [71]. Several recordings lasting from 3 to 20 minutes were stored in the digital audio tape (DAT) recorder and were then transferred to a PC for further analysis. The recordings were based on a selection criterion of vessel distance from the hydrophone, and its operation (arrival, departing and berthing). Sectioning of the recordings was based on tags that were placed on each recording, these tags helped to distinguish the type of information that was to be deduced from a particular recording at different times. These sections were backed up by other forms of information like video recording and ‘time tagging’ at relevant times.

The PSD data was calculated using 16 samples of one second each. These samples were analysed and averaged using a Matlab Hanning fast Fourier transform (FFT) window. This was done with a 50% overlap to give ~ 8 seconds of averaged data. These provided steady enough results for the complete capture of wanted sounds, and are just long enough to avoid the averaging out of varying sounds as time passes. The frequency resolution (Δf) is expressed as $N = f_s T$, with f_s been the sampling frequency, where N is the number of samples and T the time segment thereby giving a 1.67 Hz resolution.

5.3 Results & Discussion

In this study, SPL values are presented for 1/3 octave band centred frequency components (represented simply as ‘Frequency in Hz’ therein the results), with a lower and upper frequency limit of 50 and 1000 Hz, respectively. The PSD values are presented with a lower and upper frequency limit of 50 and 500 Hz, respectively. The main sources of acoustic signals from vessels come from cavitation effects of propeller blades, and swirl sounds from underneath the hull during full sail. The sounds from these propeller propulsion systems create continuous broadband noise

with high frequency components. These sounds are very complex to analyse and vary rapidly depending on speed, type and depth of operation. Other sources that make up the acoustic spectra of these vessels include those that generate tones of discrete frequency components. These include the numerous machinery devices placed within the hull of the vessels like the engines, hydraulic systems and generators. These components transmit mechanical vibrations into the water via the hull of the vessels.

Noise Levels during Arrival and Departure of Vessels

Figure 40 (a) and (b) present the results of the PSD and the SPLs respectively at distances of 200 m and 300 m during departure of a vessel as well as their respective normalised graphs (Figure 41 (a) and (b)). From the graphs (Figure 40 (a) and (b)) it can be seen that as the vessel pulls away (during departure) at different distances from the hydrophone, the overall SPL and PSD levels of all frequency contents decrease. There is a gradual decrease in SPL levels as frequencies increase because these vessels produce less noise at higher frequencies. At higher frequencies (> 1 kHz), the sounds received are indicative of the background environment rather than sound from these vessels.

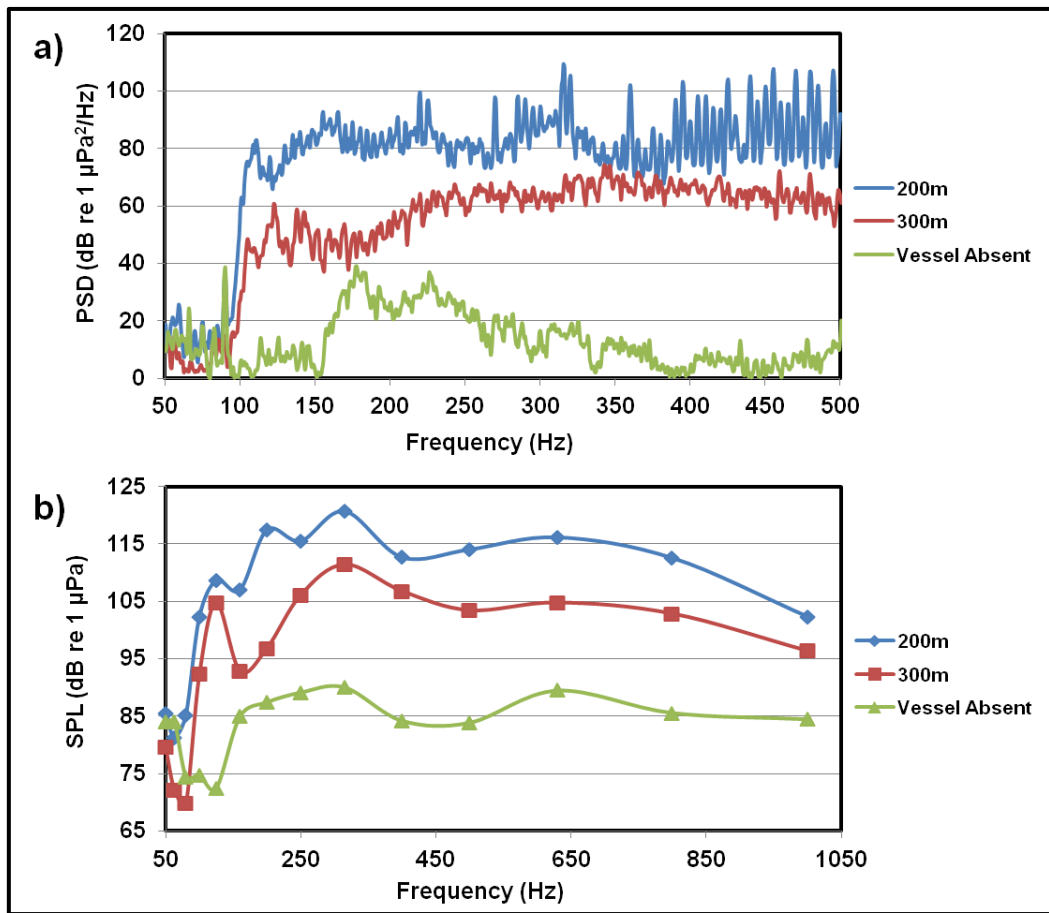


Figure 40 - Graph of (a) narrowband PSD and (b) 1/3 octave band centred frequencies SPL of vessel departing the Dublin Poolbeg marina.

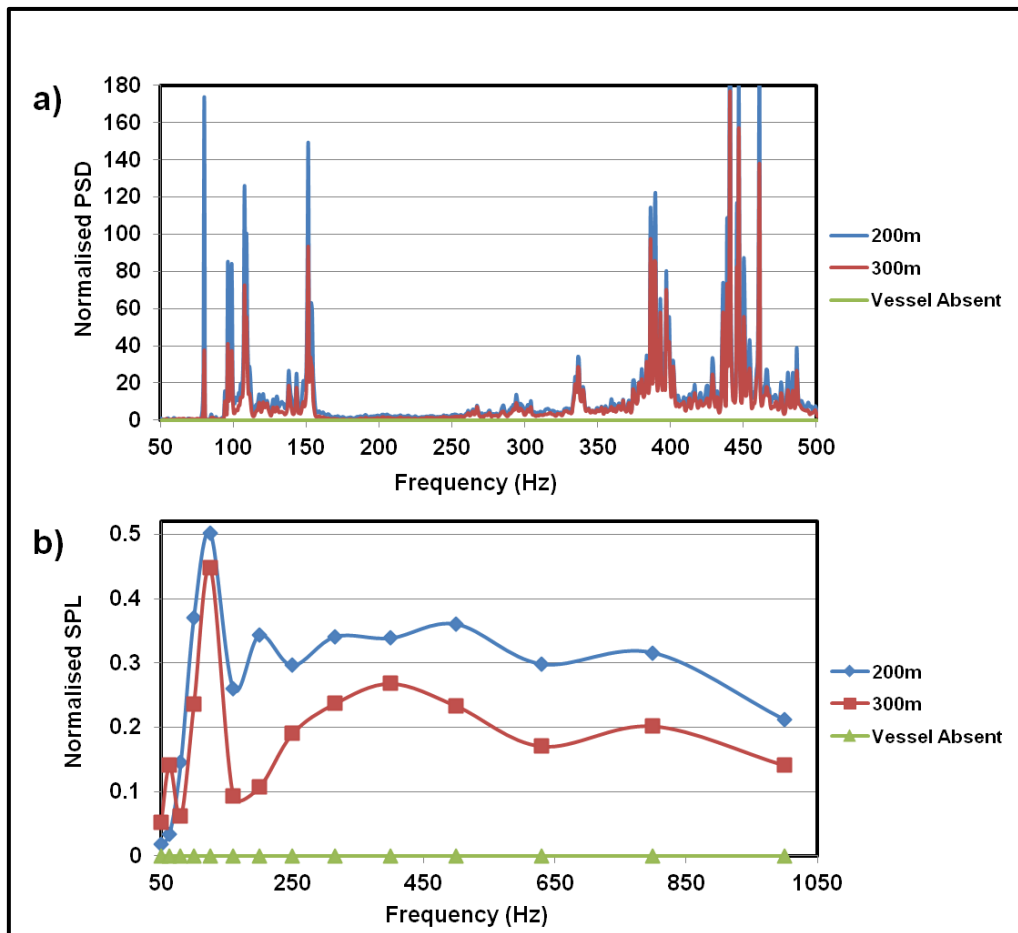


Figure 41 - Normalised data for vessel departure against the absence of vessel

Figure 40 shows the PSD and SPL values at approximate distances of 200 m and 300 m from the recording system of vessel departing the Dublin Poolbeg marina. In Figure 40 (a) spectral components at 200 m distance are also identified at 300 m. In Figure 40 (b) similar frequency components are detected at 200 m and 300 m, with different amplitude values. The highest levels at 200 m are 120 dB and 109 dB recorded at the 315 Hz 1/3 octave centred frequency SPL and PSD spectrum level respectively. A decrease to 111 dB and 66 dB corresponds to the same frequency components as the vessel pulls away at a further distance of 300 m. This frequency content and its harmonics are features likely corresponding to vessel propulsion system producing cavitation sounds with bottom surface reflection and interaction in this shallow water environment. This is subject to change with depth of source and

receiver, bottom reflection properties, as well as water column properties [112]. This observation is further expressed in Figure 42 (a) and Figure 42 (b) which show the Short Time Fourier Transform (STFT) time-frequency analysis of the vessel when it is absent from the site, and as it pulls away from the dock respectively. It can be seen that the amplitude of its frequency components decrease over the time period of about 6 minutes.

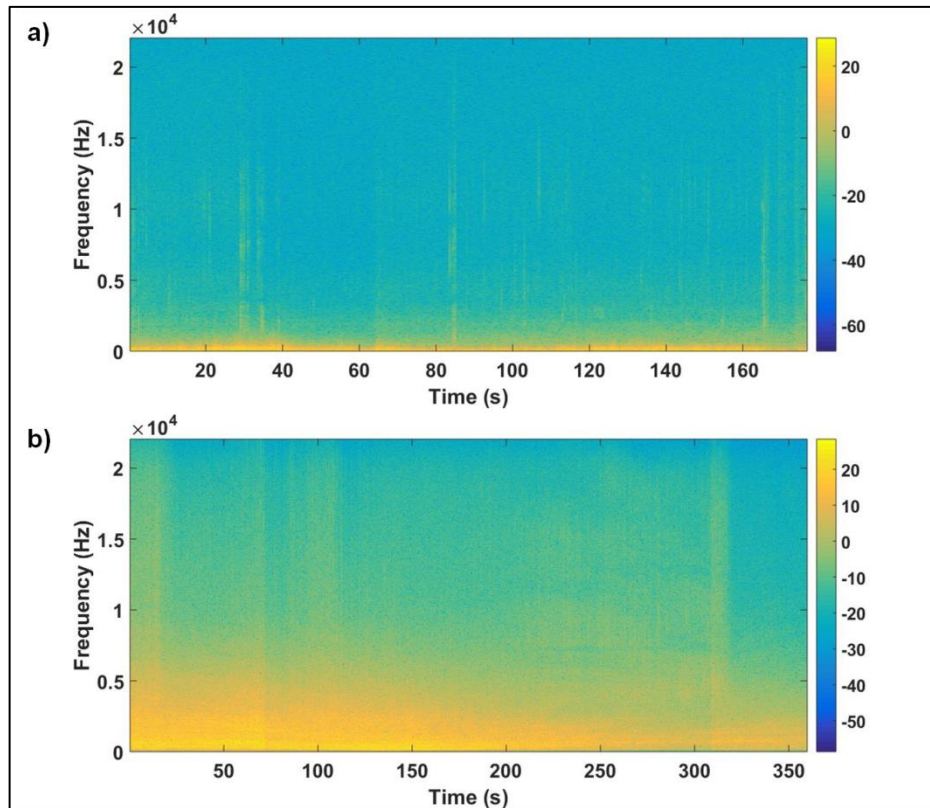


Figure 42 - Spectrogram of the short-time Fourier transform of the (a) ambient noise when the vessel is absent from the site and (b) noise radiated as the vessel pulls away from the dock for 350 s.

Figure 42 (b) shows the spectrogram of the vessel pulling away. It illustrates a decrease in sound amplitude as a function of time as the vessel pulls further away from the recording system. At times 0 to 50 seconds, the intensity of the lower frequency amplitudes can be seen to be much more than those after about 200 seconds. This decrease in amplitude of the lower frequency components correlates to a sound propagation loss [53] as expected, with an increase in distance from the sound source to the receiver.

The spectral analyses for the acquired sound signals from the vessel during arrival at the dock (in place of departure) are presented in Figure 43 (a) and (b), as well as their respective normalised graphs (Figure 44 (a) and (b)). There appears to be no significant difference in terms of the overall average sound levels at 200 m and 300 m from the recorder this time. This similarity in overall sound spectral is attributed partly to the decrease in sound level from the full forward propulsion system as it approaches the dock. This system (including components for berthing and turning around) emits lower amplitude SPL values compared to when in full sail, thus producing a similar sound level at both distances from the recording system.

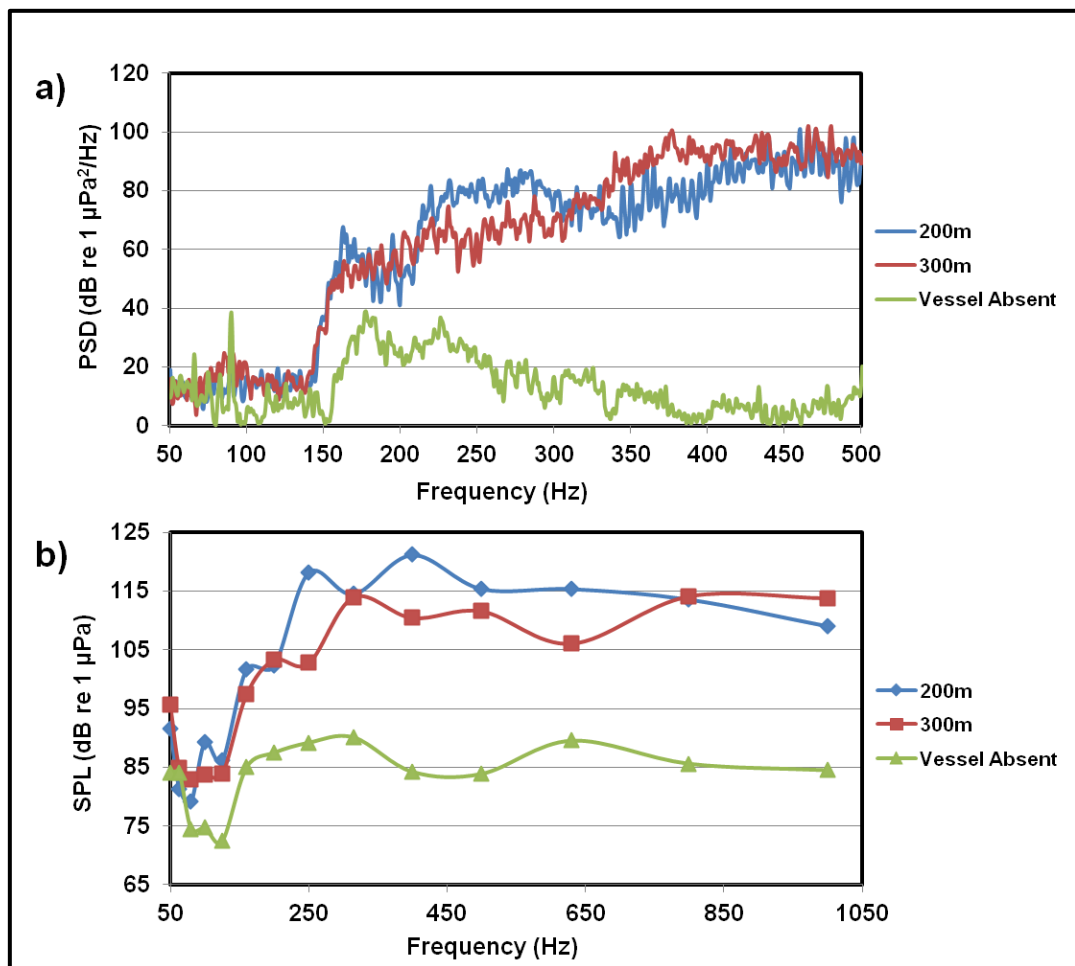


Figure 43 - Graph of (a) narrowband PSD and (b) 1/3 octave band centre frequencies SPL of vessel arriving and berthing the Dublin Poolbeg marina.

Figure 43 depicts the PSD and SPL estimated at distances of 200 m and 300 m from the recording system of vessel arriving and berthing the Dublin Poolbeg marina. In Figure 43 (a) some spectral components observed at 300 m are absent at 200 m, indicating alteration in the sound emitted due to different activities. In Figure 43 (b) similar sound amplitudes are detected at the different distances.

The sounds from the machinery components including the engine do not change, and thus their amplitude values at both distances are approximately the same also. Therefore at 300 m from the recorder the average broad band SPL acquired was about 101 dB, and about the same level was received at a closer distance of 200 m.

Again it is paramount to note that acoustic signals from components of USEV are distributed throughout a very wide band of frequency range due to variable complexities. These acoustic sources are diverse, and each given source changes its acoustic output with regards to the instantaneous operational condition such as speed, water depth, manoeuvring type, bathymetry [113] etc.

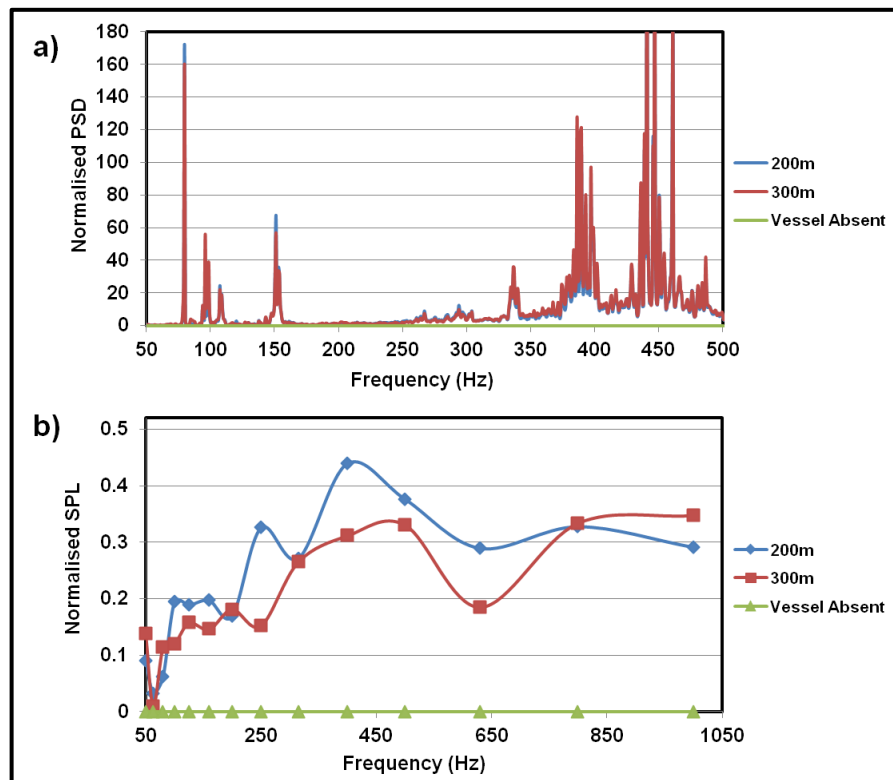


Figure 44 - Normalised data for vessel arrival against the absence of vessel

Tidal Influences on Noise Levels

The tidal effect (Neap & Spring) on vessel sound and its propagation is presented in Figure 45 (a) and (b) and there appears to be very little to no variation in SPL values between the spring and neap tides in lower frequency components. At higher frequency components, there also seems to be very little to no variation in terms of PSD and SPL values between both tidal seasons.

Acoustic signal propagation is usually influenced by the sea surface height (SSH) and roughness in the shallow water environment, especially for higher frequency components. However, theoretically, the energy of low frequency components (with higher wavelengths) is not affected in the shallow water environment by these factors. This is consistent with the little to no difference in sound signals received between the spring and neap tidal states as shown in Figure 45. It is expected that there would be an increase in the effect of SSH on energy loss during propagation with higher frequency components.

The Rayleigh parameter estimates the effect of sea surface on the loss of acoustic energy compared to the effect of the bottom surface. If the value of this number is much less than 1, it implies that losses of sound energy due to surface scattering are small, and are likely to be far less significant compared to the bottom losses due to interaction with the seabed [90]. The Rayleigh parameter for the deployed site is thus estimated as:

$$R = 2\pi H_{rms} \sin\theta / \lambda \quad (5.3.1)$$

where R is the dimensionless Rayleigh parameter, H_{rms} the rms wave height, θ the grazing angle between the path of the sound and the surface and λ the acoustic wavelength. Given the shallow water environment where low frequency ($\lambda > 1.5$ m) signals with moderate wave height ($H_{rms} \approx 1$ m) propagate at small grazing angles ($\sin \theta \approx 1$ m), the Rayleigh parameter is estimated to be approximately 0.42 [90]. This suggests that energy loss due to the surface is not significant (because R is less than 1) when compared to that of the bottom surface. Energy losses due to SSH

would become significant compared to that of the bottom loss as R becomes greater than 1.

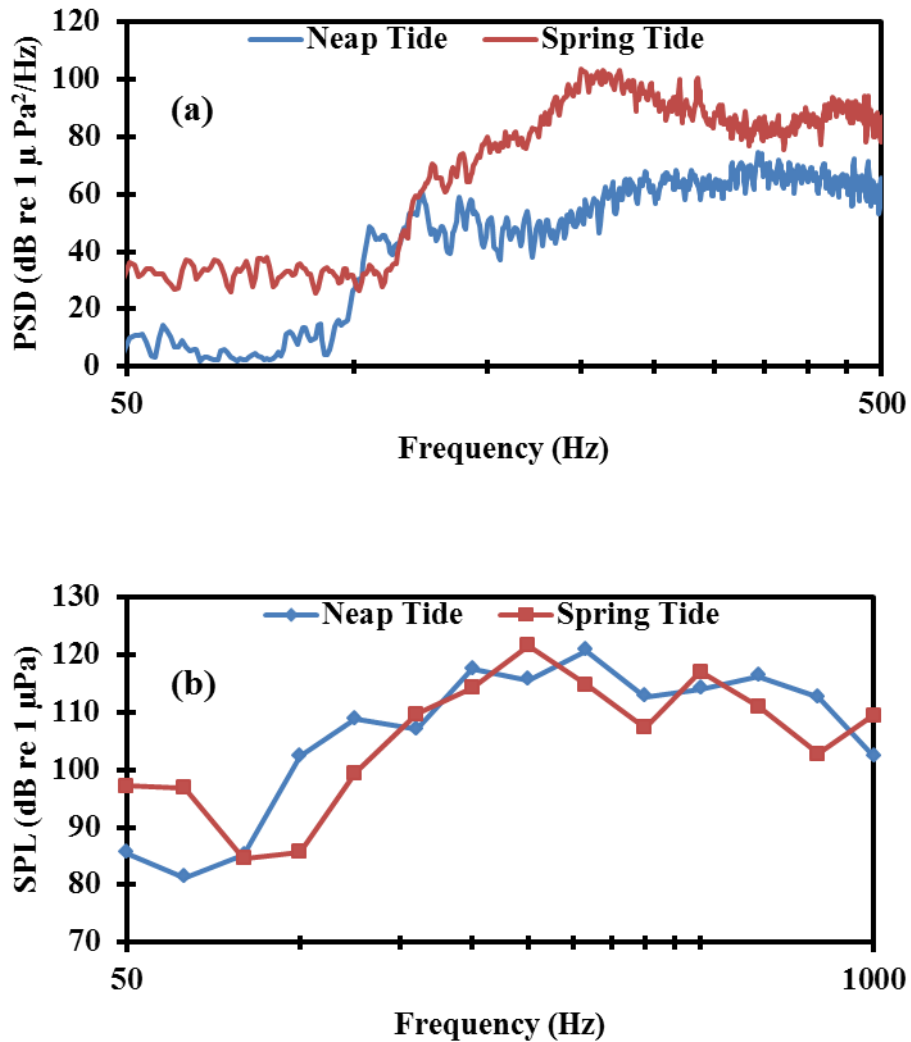


Figure 45 - Graph of (a) narrow-band PSD and (b) 1/3 octave band centre frequencies SPL of vessel activities during spring and neap seasons. Here, the variations in the tidal heights of both seasons show an insignificant effect on the sound signal amplitudes; this might be attributed to the use of a static hydrophone system.

In theory one would expect lesser attenuation of sound levels from source to receiver in spring tides when compared to neap tides given the higher water levels of the former (see Figure 39). This is because if there is a significant difference of at least a few meters in tidal levels between the seasons, and/or higher frequency

components above ~3 kHz, there is likely to be a sea surface effect on the sound propagation due to the Rayleigh parameter [114]. However, the overall variation in tidal heights between these seasons is not significant enough in our study, i.e. the overall differences in tidal heights does not seem to influence the sound propagation significantly.

A conclusive study to ascertain the effect of tidal season on the propagation of sound signal would require a significant variation of tidal heights of tens of meters between both seasons, and the collection of data over a long period of time.

Ambient Noise vs. Vessel Noise

As a conclusive analysis to this study, the contribution of these vessels to the ambient noise of the site was established. Ambient noise in this area during the absence of these vessels in the direct vicinity was measured to have broadband SPL values between 68 - 95 dB for various frequency components. These values (illustrated in Figure 46) increased by approximately 5 – 21 dB during the presence of the vessels at a distance of 200 m. Similar variations were observed for the PSD values for both narrow and broadband sounds.

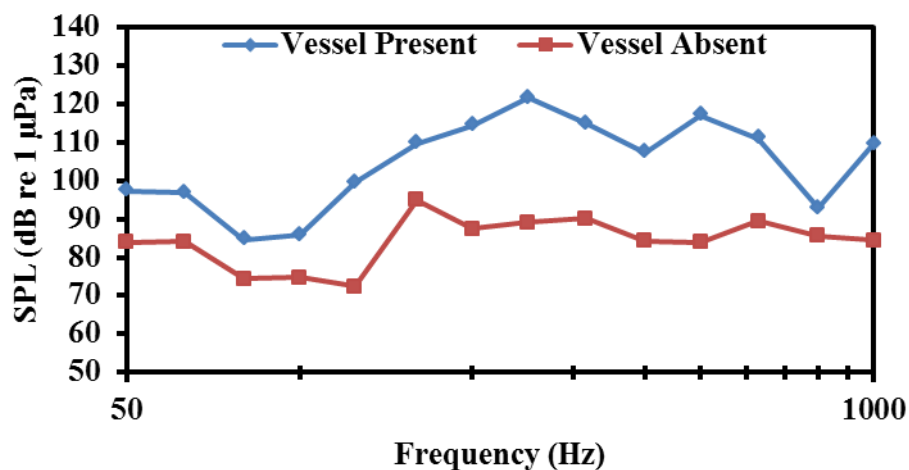


Figure 46 - Underwater 1/3 octave band centre frequencies SPL, for low tidal conditions, during the presence and absence of vessels. Similar values are obtained at high tidal conditions. Overall SPL values for low frequency components increases significantly during the presence of these vessels as supposed during their absence.

5.4 Conclusion, Recommendations & Future Work

In this chapter acoustic data in the form of spectrograms and spectral densities associated with selected underwater acoustic emitting vessels was analysed. Analyses of this data include spectral analysis of the sound signals from components of the vessels, and the effect of the acoustic propagation condition (tidal states) on the received sound levels from the sound source. This effect could not be definitively established in this study due to small variations of tidal heights together with the period of data collection. The higher Rayleigh parameter of 0.46 was estimated for the sea surface at spring tide, which indicated that there was no significant sea surface effect on the sound propagation. Further data collection over a very long period of time (years) is recommended before a conclusive statement could be made.

Frequency changes from the operation of the different components of the vessel indicated differences in their amplitudes during different activities. Highest PSD and SPL values were recorded 200 m from the vessel. These values were approximately 109 and 120 dB at the 315 Hz 1/3 octave centred frequency PSD and SPL spectrum level respectively. There were corresponding decreases of about 43 and 9 dB respectively, at a further distance of 300 m from the vessel as it moves away from the hydrophone.

A quantitative analysis however is recommended to determine noise spectra of every individual component. The average broadband SPL measured at a longer distance was the same at a shorter distance during arrival and berthing of vessels. This suggests that the magnitude of sound signals from the propulsion system and other components employed during turning around and berthing are similar, as they produce low average SPL broadband sounds even at a shorter distance from the hydrophone.

SPL and PSD values for both narrow and broadband sounds were compared for ambient (absence of the vessels) and presence of the vessels from the site. These values were generally lower for the absence of the vessels compared to those

acquired during their presence. These values (for frequency components 50 - 1000 Hz) increased variably by 5 to 21 dB during the presence of vessels as opposed to their absence. More research is currently on-going at the same site to identify all other sources of noise further down the bay as well as in its immediate environs. The result acquired from this study will be fused into a future study to analyse the correlation of the sound signals emitted by both the vessels and WEC devices. Thus, results obtained would serve as input data to an ideal ocean model with variable parameters. This will facilitate further work on the creation of acoustic signatures for underwater noise generating devices to use against emitted acoustic spectra to monitor devices' health and condition.

It is paramount to note that underwater noise in a shallow water environment is very difficult to monitor and analyse. Future recommended study involves the acquisition and analysis of underwater acoustic noise emitted by these vessels under full sail to establish their individual signatures. Simulation of acoustic emitting sources is also considered to characterise the changing acoustic propagation condition between emitter and receiver.

Chapter 6

6 Modelling and Analysis of Underwater Acoustic Signals Emitted by Marine Energy Devices

Assessment of the ‘health’ of marine based electro-mechanical devices where certain types of failure modes (e.g. damaged bearings, hydraulic faults, electrical arcs, vibrations) occur is essential for companies involved in the renewable ocean energy and marine technology sectors. This directly impacts on the operation and management costs of ocean based systems, specifically impacting on efficiency / yield, reliability, and maintenance costs. This chapter presents the modelling and simulation of sound signals emitted by point absorber WEC device. One third octave band centred frequency signals in a dominant 100 Hz to 1000 Hz range were used to estimate the propagation loss as a function of range. Estimated SPL values from FE models with different surface interfaces were compared to data values from the WEC device in literature. Rough surface interfaces in the FE models were seen to contribute significantly towards the propagation loss of the sound signals in an acoustic domain. It was estimated that an increase in the root mean square (rms) height of the rough surface led to a significant increase in sound attenuation and propagation loss. This study contributes to the knowledge of parameter effects in an acoustic environment, which is useful in the understanding and informed prediction and performance of idealized underwater acoustic models. It demonstrates and gives an insight of the contribution of the bottom surface roughness on the attenuation of sound pressure level values.

6.1 Introduction

Assessment of the ‘health’ of marine based electro-mechanical devices where certain types of failure modes (e.g. damaged bearings, hydraulic faults, electrical arcs, vibrations) occur is essential for companies involved in the renewable ocean energy and marine technology sectors. This directly impacts on the operation and management costs of ocean based systems, specifically impacting on efficiency / yield, reliability, and maintenance costs.

In shallow water environments, attenuation/transmission loss by the bottom surface, scattering, wave interactions and boundary effects are important factors in understanding acoustic signal propagation. Attenuation of underwater acoustic signals is caused mainly by their geometric spreading. Other factors causing attenuation include surface interactions and the absorption of sound in sea water. The absorption of sound in sea water with an absorption co-efficient (α) is dependent on temperature, frequency, depth, salinity and acidity [115]. Underwater acoustic models are important when it comes to the understanding and estimation of both active and passive sound navigation and ranging.

An idealized predictive medium for modelling and simulation of underwater sound propagation incorporates the spreading, absorption, and scattering loss mechanisms exhibited by underwater acoustic signals during propagation. Ray theory, normal modes, parabolic equations and couple modes are all current methods used to simulate underwater acoustic propagation and loss. Most of the aforementioned methods, however, neglect scattered energy from the interfaces at angles which are close to normal [77], thereby underestimating the effect of incident waves close to normal angle on sound analysis. This makes the finite element (FE) analysis method one of the benchmarks for approximation as discretization density increases as discussed in chapter 3. In this chapter Comsol FE acoustics module is used. This package is capable of coupling different physical domains such as the solid and fluid domains, and can achieve a solution that approaches the exact solution of the Helmholtz equation.. Acoustic field measurement data from full scale operating WECs in the Lysekil and Wave Energy for a Sustainable Archipelago

(WESA) project at Uppsala University and University of Turku, respectively, were utilized in this study. These data (obtained from literature by Haikonen *et al.* [57]) were measured 1 m from the full scale point absorbers with directly driven linear generators. These measured spectra data were used as real life input data towards generating the propagation loss in SPL values as sound travels from source to receiver. This chapter evaluates the effect of bottom surface roughness on the propagation loss of these sound signals from the emitting source to receiver. The results show the effect of varying surface interface roughness on the sound signal emitted by the wave energy device, and its attenuation with range from source to receiver.

6.2 Wave Energy Converter and Noises

The Acquisition of acoustic signatures for WEC devices from their associated primary operational components such as turbines, generators, hydraulic components (pumps and valves), moving parts such as hinges and actuators, without actual field measurements is not trivial. Secondary noise sources associated with these devices include noises from cable vibration, cavitation noises and noises from water impinging on these devices.

To quantify the noise radiated by WECs, ambient noise present at the site in the absence of any WEC is usually characterised in both ebb and flood conditions [93, 95]. One of the earliest noise measurements in the direct vicinity of an operational WEC was carried out in the Bristol Channel on marine current turbines. An SPL value of 166 dB re 1 μ Pa at 1m from the source (using a simple spreading law) was measured. It is important however to take caution during the interpretation of this effective source level (using the spreading law), since there might be interference effectively leading to large fluctuations in sound pressure level at short distances from the source [116]. A full scale point absorber, the Danish Wavestar WEC, was measured to emit 106 - 109 dB re 1 μ Pa in the 125 Hz to 250 Hz frequency range, which was 1 - 2 dB above ambient levels in October of 2012. The

highest sound signal emitted by this device was at 150 Hz frequency with a corresponding SPL value of between 121 - 125 dB. This was present from the hydraulic pump of the device during start-up and shut-down of the converter [61]. Harmonic acoustic components associated with the rotational speed of turbine and the impulsive noise associated with increased air pressure within the air chamber, were obtained from a wave energy oscillating water column device in Portugal in 2010. SPL values measured for the harmonic at different rotational speeds of the turbine blades was highest at 126 dB re 1 μ Pa 10m from the device [117].

The characteristic noises emitted by WECs differ between different WEC types. In the full scale point absorber type WEC which is represented by the point source in this study, noise types include transient noises originating from the activities of the translator and stator components as demonstrated by Haikonen *et al.* [118]. The amplitudes of the sound signals emitted by these components are dominant at frequencies below 1000 Hz ranging between 118 and 155 dB re 1 μ Pa, with peak amplitudes at 100 Hz and 300 Hz.

6.3 Finite Element Modelling and Simulation

The FE analysis involves finding the solution to the Helmholtz eqn. (6.3.2) which stems from the reduction of the wave eqn. (6.3.1). In this chapter, only a summary of the derivation of the equation is provided. Full details are contained in reference [119].

$$\frac{1}{\rho_0 c^2} \frac{\partial^2 p}{\partial t^2} + \nabla \cdot \left(-\frac{1}{\rho_0} \nabla p + q \right) = 0 \quad (6.3.1)$$

In eqn. (6.3.1), p is the acoustic pressure, ρ_0 the fluid density and q an optional dipole source with unit of acceleration. A time-harmonic wave $p = p_0 e^{i\omega t}$ is substituted into eqn. (6.3.1) to obtain the Helmholtz eqn. (6.3.2).

$$\Delta p + k^2 p = 0 \quad (6.3.2)$$

Eqn. (6.3.2) describes a harmonic wave equation propagating in a medium with an assumption of no dissipation of energy. P is the sound pressure amplitude and k is the wave number which is related to angular frequency $\omega = 2\pi f$ and speed of sound c_s as shown in eqn. (6.3.3)

$$k = \frac{\omega}{c_s} \quad (6.3.3)$$

The homogeneous Helmholtz equation is thus derived by substituting (6.3.3) into (6.3.2) to give eqn. (6.3.4).

$$\nabla \cdot \left(-\frac{1}{\rho_0} (\nabla p) \right) - \frac{\omega^2 p}{\rho_0 c_s^2} = 0 \quad (6.3.4)$$

Sound signals radiate from a point source with the energy emitted at a given time diffusing in all directions as described by eqn. (6.3.5)

$$\nabla \cdot \frac{1}{\rho_c} (\nabla p_t - q) - \frac{k^2 p_t}{\rho_c} = 2 \sqrt{\frac{2\pi P_{ref} c_c}{\rho_c}} \quad (6.3.5)$$

From eqn. (6.3.5), P_{ref} is the reference pressure, p_t is the time varying pressure, and c is the speed of sound in the medium.

Pressure Release Surface & a Perfectly Matched Layer

The upper boundary for the acoustic domain was modelled as a pressure-release surface [120]. This boundary surface assumes a Dirichlet boundary condition (soft boundary with pressure = 0 when imposed on the partial equation) and a Pierson/Moskowitz spectrum (empirical relationship of frequency energy in the ocean) at 10.3 m/s. To reduce reflections at the boundaries, the absorbing boundary condition (ABC) perfectly matched layers were used to truncate the infinite domain. In Comsol, perfectly matched layers (see Figure 47) are used to formulate the problem to limit the geometric domain of the solution.

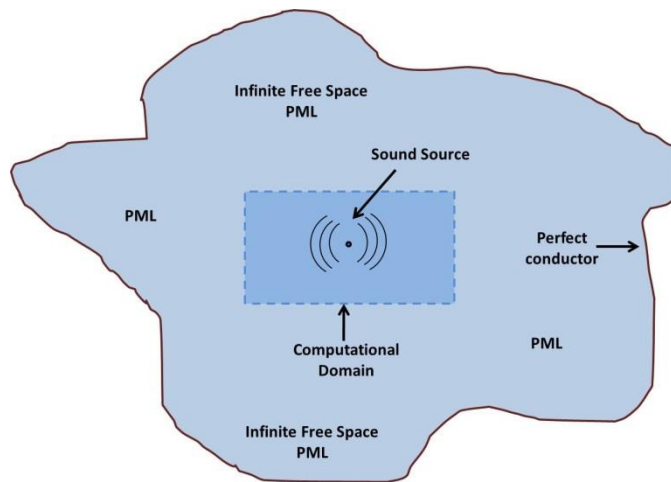


Figure 47 - Geometry showing the absorbing boundary condition (ABC), perfectly matched layer (PML).

In reality, the object of interest is located in a vast geometric domain. This increases the processing time. In order to solve this problem, perfectly matched layers are used which mimic the original environment but also reduces the geometric boundary, i.e. no waves are reflected or scattered from those boundaries, and thus do not affect the original solution [121]. These layers were at least twice the size of the largest wavelength.

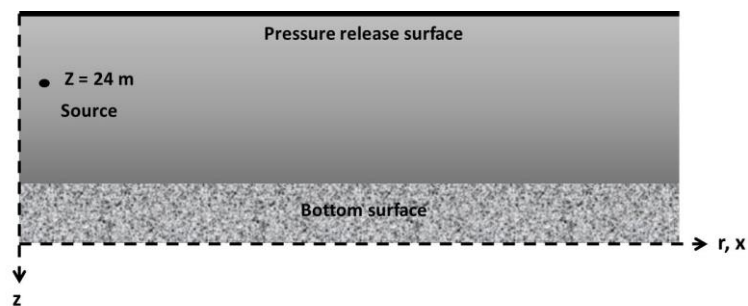


Figure 48 - Computational domain depicting bottom surface and pressure release surface.

Domain Description

Sound is assumed to propagate spherically in a free homogeneous acoustic medium from a point source. The mix winter Pekeris water sound speed profile is used together with other parameter values shown in Table 5.

Table 5 - Acoustic parameters and properties used in the models

| Parameter/Material | Value |
|--------------------|--|
| Water | Density (ρ), 1029 [kg/m ³] Sound speed (c), 1500 [m/s] |
| Bottom Sediment | Density (ρ), 2500 [kg/m ³] Sound speed (c), 1700 [m/s] |
| Source depth | 24 [m] |

Theoretical plots of frequencies against range are shown in Figure 49 (a) and (b) for the Spherical spreading and attenuation loss of sound signals in an acoustic medium using the simple propagation loss (PL) eqn. (6.3.6). This formula is widely used to evaluate the performance of underwater acoustic systems [120].

$$- PL = - 20 \log R - \alpha R \quad (6.3.6)$$

From eqn. (6.3.6), R is the range from the sound source and α is the attenuation coefficient which is calculated using the temperature, depth, salinity and acidity parameters.

Figure 49 depicts the theoretical propagation loss of the amplitude of signals with respect to range and frequency components (extended frequency and range values is given in appendix 8.2). Higher frequencies attenuate very quickly, with very low frequencies having the capacity to travel further. However, more idealised propagation models require the incorporation of other propagation parameters including interfaces generating multiple concurrent paths, scattering and other parameters contributing to the attenuation of sound signals. Figure 50 shows a schematic of the bottom surfaces included in the models in this chapter. The rough surface bottom features together with the material properties contribute to the attenuation of sound signals in the acoustic medium. These models thus incorporate

these other parameters (not included in the theoretical propagation loss model) in their estimates for the propagation loss of sound.

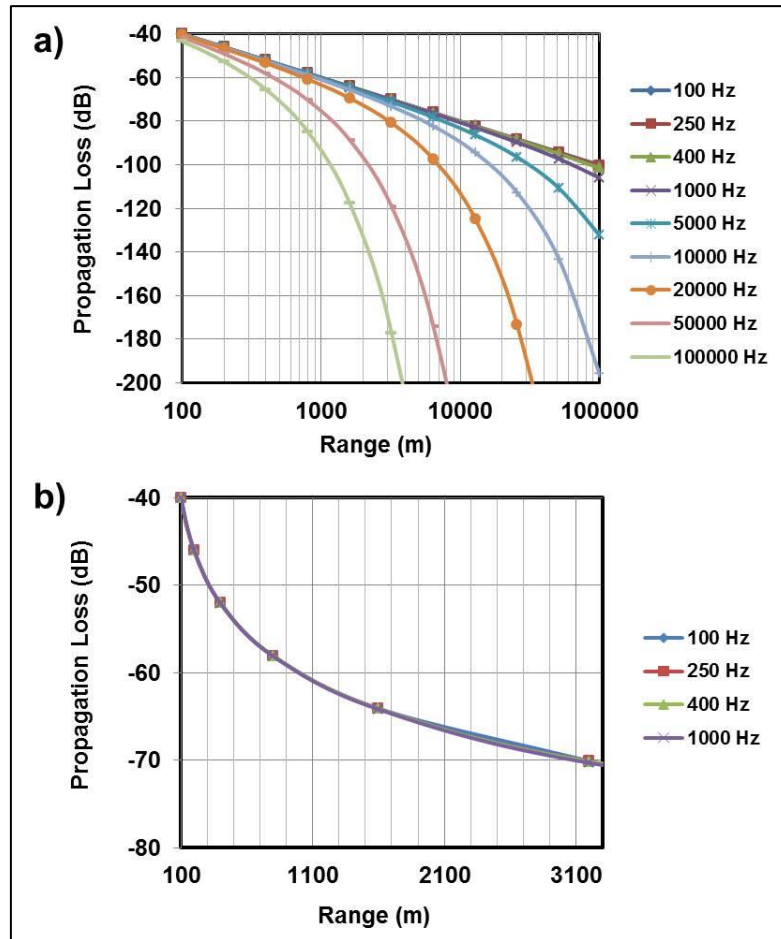


Figure 49 - Theoretical propagation loss - $PL = -20 \log R - \alpha R$ of (a) frequencies as a function of range from 0.1 – 100 km and frequencies of 0.1 – 100 kHz, and (b) 0.1 – 3.1 km and frequencies 0.1 – 1 kHz. Using Francois and Garrison absorption coefficient (α) with conditions: Temperature = 10⁰C, Salinity = 35 p.s.u. and depth = 24 m.

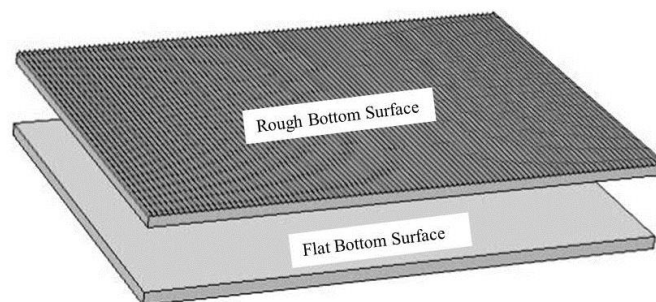


Figure 50 - Solid bottom Surfaces of Models. Four types of rough surfaces used with roughness values equal to fractions of the RMS wavelength values.

6.4 Results

Analysis was carried out amongst four different models. Model 1 is assumed to be the control model with no surface interface roughness, models 2, 3 and 4 have an increasing surface interface roughness height values. These roughness values correspond to a fraction of the root mean squared (rms) value of their respective frequency wavelengths (λ_{rms}). Initial simulations involved testing a range of test roughness values. Then based on empirical observations, this range of values was whittled down to a quartet of values. These fraction values are λ_{rms} , $0.5 \lambda_{\text{rms}}$ and $0.25 \lambda_{\text{rms}}$ of the frequency components for models 2, 3 and 4 respectively. One third Octave band centred frequencies 100 Hz, 250 Hz, 500 Hz and 1000 Hz were used. It is important to note that these frequency values cover the range of frequency values for which the amplitudes of the sound signals normally emitted by the WEC device under study are most dominant.

6.4.1 Analysis of FE Models

Analysis on the FE models show a general decrease in sound pressure levels (SPL) as the sound signals propagate away from the source. Figure 51 shows the SPL values for the four different models for a 3000m range at 100 Hz, 250 Hz, 500 Hz and 1000 Hz frequency values. It is observed that as frequency values increases, the rate of attenuation of SPL increases. This is consistent with the previously described theoretical analysis and other sound propagation investigations [11].

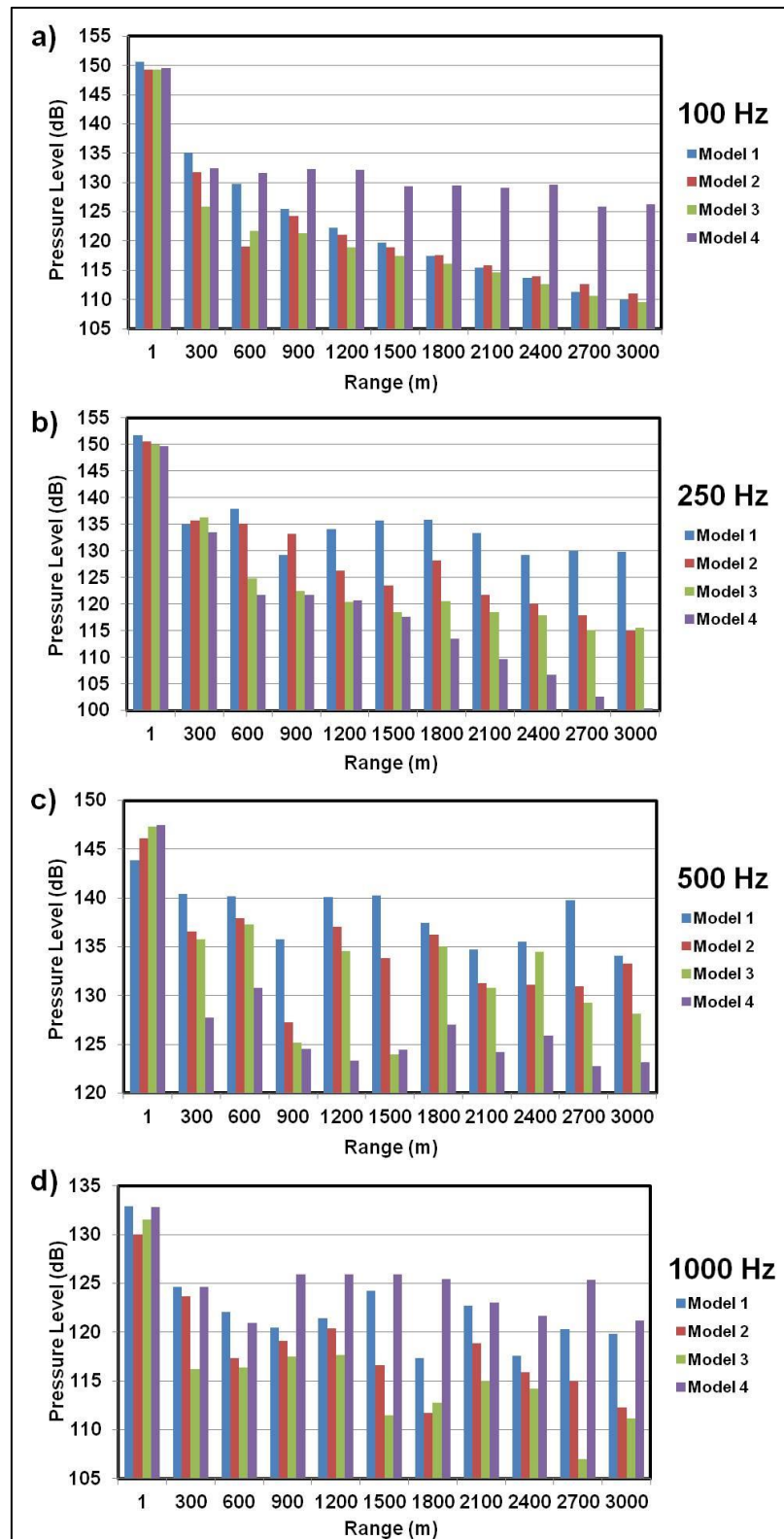


Figure 51 - Attenuation of sound as a function of frequency and range for the different models. Models exhibit the same characteristics as theoretical models with respect to frequency against range.

From Figure 51, it is observed that the models (2, 3 & 4) with the rough surface interfaces attenuate more sound signals than the model (1) with the flat surface interfaces. Model 4 with the largest surface roughness attenuates more sound signals than models 2 & 3 with smaller surface roughness interfaces. However, it is important to note that for a very low frequency component with relatively high surface roughness value (see Figure 51, 100 Hz), there appears to be no correlation of the attenuation of sound signal to surface roughness. This is attributed to the very high ratio of surface roughness to wavelength values, resulting in an increase in the overall SPL value instead of a decrease.

6.4.2 Analysis of Data from Literature

The underwater noise from the WECs possesses two main operational noises which include the noise when the translator is moved past the stator in the generator, and when the translator hits the end stop springs in the top or bottom in the generator (see Appendix 1). Evaluation of sound propagation loss of 1/3 octave centred frequency sound signals, emitted from the point absorber device when the translator hits the stop springs was estimated at 100 m and 1000 m from the sound source, in the 100 Hz to 1000 Hz range. A summary of the WEC and ambient noise types and spectra data of the different noises from the devices are presented in Appendix 2 and 3, respectively.

These real life acoustic data from the WEC device was part of a study by Haikonen *et al.* [118]. The parameters such as depth of the device for the acquisition of the data from the WEC are similar to those incorporated into the models in this study. Figure 52 shows attenuation of sound signals emitted by the WEC in the 100 Hz to 1000 Hz frequency range. The signals in this range have the greatest amplitude.

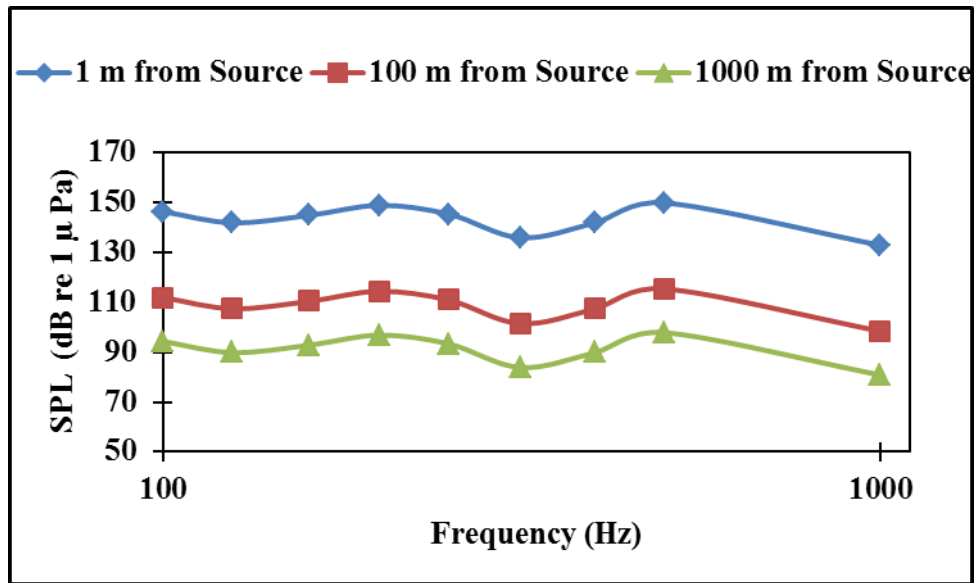


Figure 52 - Propagation loss of 1/3 Octave band centred frequency from a point absorber WEC. Sound source is at a depth of 24 m and the dominant frequency amplitudes are in the 100 Hz to 1000 Hz frequency range.

It can be seen from Figure 52 that the overall SPL values decrease as the sound signals propagate away from the source. The propagation loss eqn. (6.3.6) was used in the estimation of the values at the different point. However, it is important to note that the attenuation loss coefficient was not accounted for during extrapolation due to lack of availability of the attenuation loss factors from the site during measurement.

Comparative analysis of values obtained from models 1, 2 & 4 was carried out against estimated literature (Haikonen *et al.*) SPL values from the device. From Figure 53, model 1 represents the model with no bottom surface interface roughness, model 2 has smaller sized roughness when compared to model 4 with larger sized roughness values. Figure 53 depicts the values estimated at 900 m, 3000 m and 1500 m distances from the sound source. Model 4 provides a closer fit to the estimated (from literature) measured values from the WEC device in terms of attenuation effect. This indicates that the increased roughness of the interface of model 4 contributes significantly to the propagation loss of the sound signals.

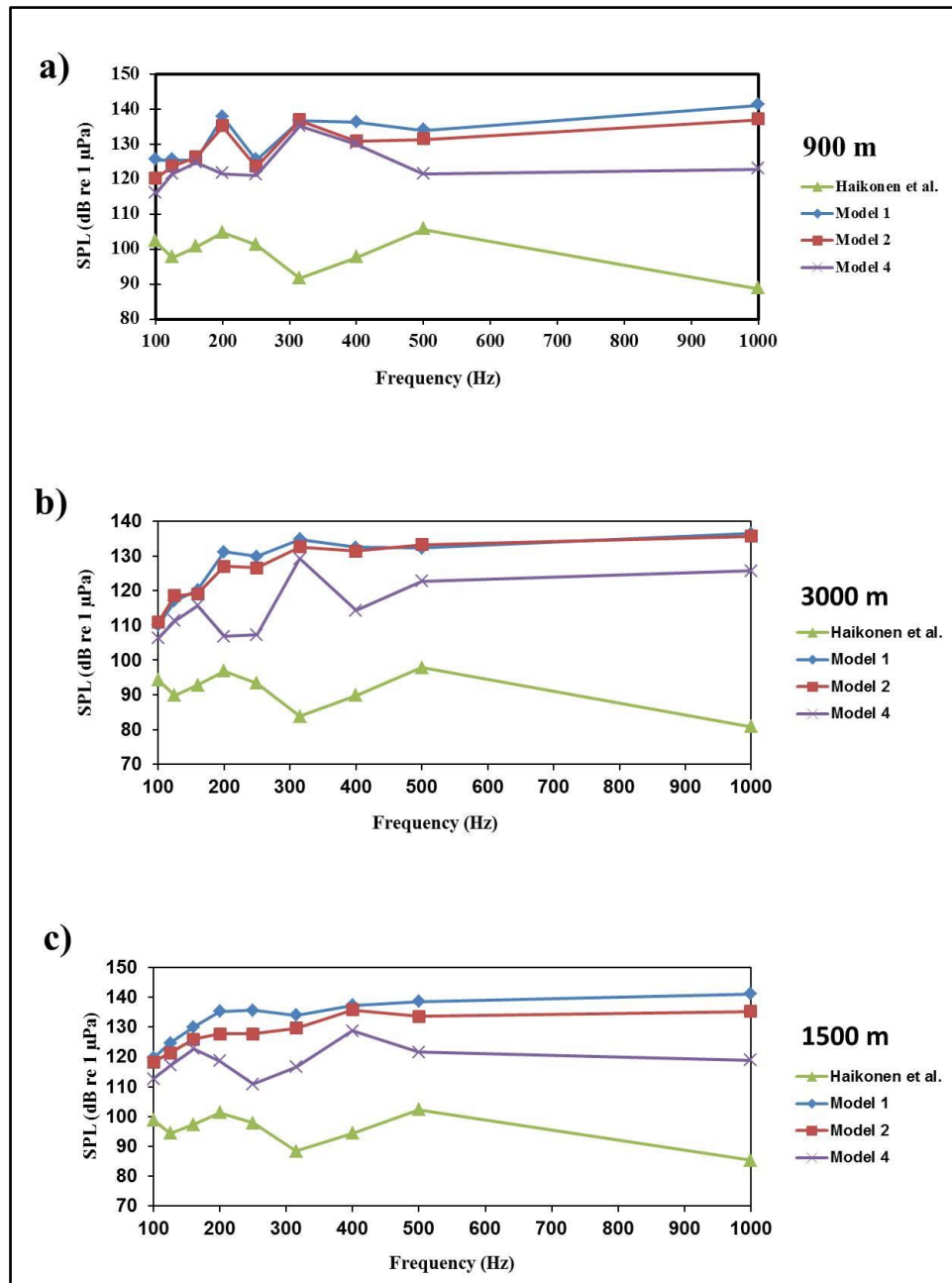


Figure 53 - Propagation loss of models 1, 2 & 4 against estimated values from literature (Haikonen *et al.*). Model 4 with rough surface interface exhibits more attenuation of sound signals and gives closer results to actual experimental values estimated from the literature.

6.5 Conclusion

The modelling and simulation of acoustic wave propagation in an acoustic environment with different surface roughness interfaces was carried out in this chapter. Spreading loss, attenuation loss due to domain properties such as temperature and density, together with losses due to scattering and interaction of waves were incorporated into the models. Results showed an increase in attenuation of sound signals as frequencies increased in the models, which is consistent with theoretical calculation of attenuation as a function of distance and frequency components. Control models (without bottom surface roughness) showed a steady decrease in SPL values of up to 40 dB (at 100 Hz) in a 3.6 km range from source to receiver. However, this propagation loss value is reduced for the models with bottom surface roughness by up to 20 dB due to reverberations and interactions of the signals. Increase in surface roughness values amongst the models showed an increase in attenuation with an increase in rms bottom roughness value. At a distance of 3 km from the source for example, the difference in estimated SPL values between models with different bottom surface roughness values was up to 3 dB for the 100 Hz frequency signals, and up to 10 dB for the 1 kHz signals.

6.6 Limitations of Modelling

Most modelling and simulations are carried out in a 2-D domain due to computational power constraints. Implementation of a 3-D domain for simulation suggests a more idealistic representation. However 2-D acoustic modelling gives a very sound knowledge of the characteristics of the sound propagation scenario. Sound directionality is an important factor for the modelling of sound. Sound sources are generally represented by sources which radiate signals in an omnidirectional pattern. However, this is not the case with most sound emitting sources. Incorporation of different sound speed profiles in underwater acoustic models also has an effect towards the analysis of sound propagation and loss.

Chapter 7

7 Conclusion & Future Work

This thesis explores the methodology involved in the acquisition of acoustic signals from underwater noise emitting machinery. This assists in the creation of a unique ‘acoustic fingerprint’ for these devices, to enable a non-invasive means of monitoring their health. It is important to note that ships comprise of many conventional acoustic emitting components, thus facilitating a benchmark acoustic emitting source for the implementation of acoustic data acquisition, analyses and presentation techniques and methodology. Sound acquisition from ships as opposed to WECs is also not trivial due to the rapid change in designs, and constraints in the ease of sound data accessibility and availability of WECs, as they are only an emerging technology.

The thesis also focuses on the development and simulation of numerical models that represent these noise emitting machinery in an aquatic domain. These models are concerned with the propagation of the acoustic signals, together with the effect of the bathymetry on their propagation and attenuation. The realistic forward acoustic models within a limited frequency range provide an insight of the application of current utilization of FEM in the evaluation of sound propagation in underwater acoustic propagation systems. It is important to note that the number of elements solved for which relates to the meshing of all domains, and thus the overall number of degrees of freedom are crucial in obtaining the best and most accurate results in the fastest manner. This therefore provides a limitation in terms of geometric extension and frequency components analyses with current computer configuration, which would be improved upon in the future with the emergence of more sophisticated and inexpensive computing power.

7.1 Summary

Chapter 1 of this thesis introduces the essence of the overall research project, by presenting the need for newer alternative forms of energy. It explains the environmental impact of the burning of fossil fuels to obtain energy, and presents the benefits of the adoption of renewable sources of energy. It outlines the need for the exploration of the ocean as a source of renewable energy along with other types of renewable energy sources including wind, and the urgency to adopt these energy sources for future sustainability.

Chapter 2 gives the state of the art research into this new renewable energy source. It introduces the concept of harnessing of ocean energy, and the conversion of this energy by wave energy devices. It demonstrates the principles of operation of these devices and their classification criteria, together with their respective power output. The chapter goes further to show the various types of devices that currently exist in the marine sector and where they are being deployed.

Chapter 3 introduces the reader to the basics of sound. It explains how sound waves need a medium to propagate, together with the physical parameters used to describe sound. The chapter goes on to focus on underwater sound signals, and the physical properties that influence sound propagation in water. It finishes off with the introduction of the various techniques involved in the modelling of sound signals in water, especially low frequency sound signals which is the main focus of UA. It goes on to briefly describe the suitability of each numerical model as regards their application when it comes to modelling, together with their advantages and their shortcomings.

Chapter 4 presents an initial modelling and simulation technique to investigate the effect of underwater sound signals emitted by WEC devices on marine animals. This model has a sound emitting source representing a wave energy device, and takes into account boundary conditions such as the bathymetry of the deployment site, properties of the propagation media, type of spreading of the acoustic signal and the interaction with the surface and bottom interfaces of the acoustic environment. A key finding from the chapter suggests that a sensor placed very close a noise emitting device might not necessary capture the adequate information needed. Therefore, an optimum position which is not too far or close to the device has to be established.

Chapter 5 outlines the experimental methodology involved in the acquisition of

sound signals from a noise emitting source. It gives details on the consideration of the kind of sensor used and all the signal processing and analysis procedures involved in establishing a unique acoustic emission from different noise emitting sources. These raw analogue signals are captured using appropriate underwater sensor and DAQ, before they are digitized and stored prior to being analyzed. The presented data detail the frequency components of the sound data together with the dominating (high amplitude) frequency components. The methodology employed for the acquisition of the acoustic data was compared to other methods and the advantages expressed.

Chapter 6 builds on the modelling and simulation technique employed in chapter 4, and incorporating findings from chapter 5 to create a more robust and realistic ocean model. This chapter presents the simulation and analysis of field measurements of acoustic signatures of marine based noise generating devices using the FE Method. A key feature of this model as opposed to most models is that it does not neglect scattered energy from the interfaces at angles which are close to normal, thus making it a benchmark for approximation as discretization density increases.

7.2 Contribution of Thesis

Acoustic emission is routinely used in the manufacturing engineering industry to monitor the condition of complex electro-mechanical machinery. This thesis introduces a novel conceptual approach by which a similar methodology is used for the condition monitoring of marine based electro-mechanical devices.

In summary:

- It takes a mature manufacturing technology, AE, and applies it in the marine environment. It has specifically examined the feasibility of acoustic emission for marine deployed devices, with an emphasis on energy conversion devices. The methodology for acquiring the acoustic spectra information associated with this noise-emitting machinery such as WECs is introduced and explored in chapter 5.
- It has also explored several issues relating to the practical design and deployment of an AE system in the marine environment. These include variation in the acoustic medium (i.e. density, temperature) and some of the impacts on marine mammals. It explored the

evaluation of the effect of sound signals produced by marine devices on marine animals, by introducing a methodology to estimate impact of sounds on marine life. This includes the comparison of emitted sound signals from a WEC device to the audiogram of marine mammal in chapter 4.

- A computer simulation that will act as a design aid for acoustic emission systems for these applications was presented in chapter 6. This model included the physical parameters affecting the propagation from source to receiver. These include the bottom/top surface influences of the acoustic domain on the attenuation of sound signals. The boundary conditions for the model were also defined.

These materials have been published, or the revised version submitted (in the case of *article 2*) to the following conferences and journals:

1. *Article 1 in the Renewable Energy & Power Quality Journal (RE&PQJ), April 2014.*
2. *Article 2 in the Journal of Ocean Engineering, June 2015.*
3. *Article 3 in the Asian Conference on Sustainability, Energy & the Environment Official Conference Proceedings (ACCESS), June 2015.*

7.3 Future Work

This work developed a methodology to acquire acoustic signals from noise emitting marine machinery. A follow up would include the acquisition of several ‘unique acoustic fingerprints’ from ‘several’ WEC devices at different oceanographic and operational conditions. This fingerprint data should then be tagged and stored. Regular acquisition of acoustic emissions from this machinery should then be carried out, and the acquired data compared to the original to monitor the ‘health’ of the devices. This should be done in the following sequence:

- Acquisition of acoustic signals from different noise emitting machinery under different normal oceanographic and operational condition.

- Tagging and storing of this data.
- Regular acquisition of data from the machinery for comparison with the stored data to monitor their health.
- Fault detection, prediction or classification using deviation of the acquired data from the original stored data during normal operation.
- Recommendations on the necessary actions to be taken.

Another area to develop on the work carried out in this thesis is the modelling aspect of the overall project. Future enhancement of the model would include the following;

- The implementation of multiple noise sources representing an array of noise generating machinery.
- Importing of a real life bathymetry mapping for the bottom surface of the model to represent a more realistic scenario.
- Implementation of coastal ocean dynamics applications radar (CODAR) data for large scale and temporal oceanic modelling [122].
- Implementation of a 3-Dimensional modelling and simulation domain for more realistic results.

Chapter 8

8 Appendices

8.1 Appendix 1

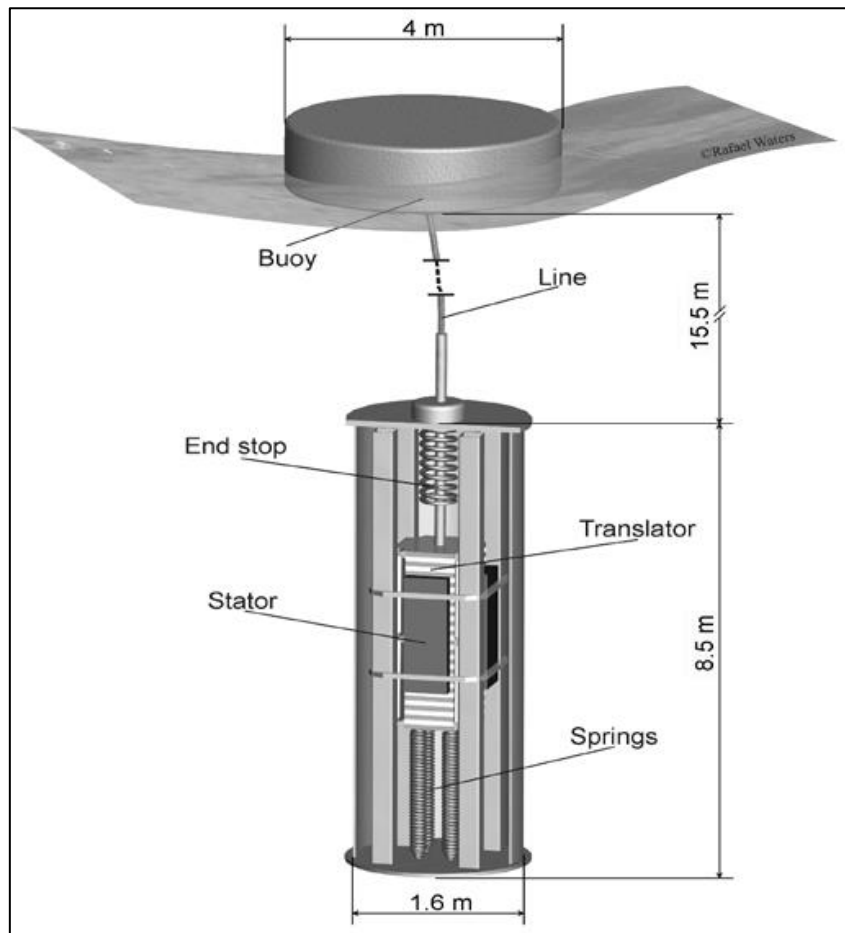


Figure 54 - Representation of a direct driven linear WEC [57]

8.2 Appendix 2

Table 6 - Summary of WEC and ambient noise measurements. Shown are noise type: Moving Translator (MT) and End Stop Hit (ESH), Significant Wave Height (SWH), overall sound pressure level (SPL), noise duration, ambient noise level (ANL), estimate range for the noise to reach ambient noise levels [57].

| WEC | Noise Type | SWH (m) | Overall SPL (dB re 1 μ Pa) | duration (s) | ANL (dB re 1 μ Pa) | Estimated Range (m) |
|------|------------|---------|--------------------------------|--------------|------------------------|---------------------|
| L12 | MT | 0.5 | 144 | 1.3 | 89 | 5400 |
| L12 | MT | 1.5 | 155 | 1.3 | 101 | 4000 |
| WESA | MT | Low | 118 | 1.5 | 104 | 10 |
| WESA | MT | High | 131 | 1.3 | 116 | 10 |
| L12 | ESH | 1.5 | 160 | 0.2 | 101 | 8600 |
| WESA | ESH | Low | 149 | 0.3 | 104 | 1000 |
| WESA | ESH | High | 159 | 0.2 | 116 | 735 |

8.3 Appendix 3

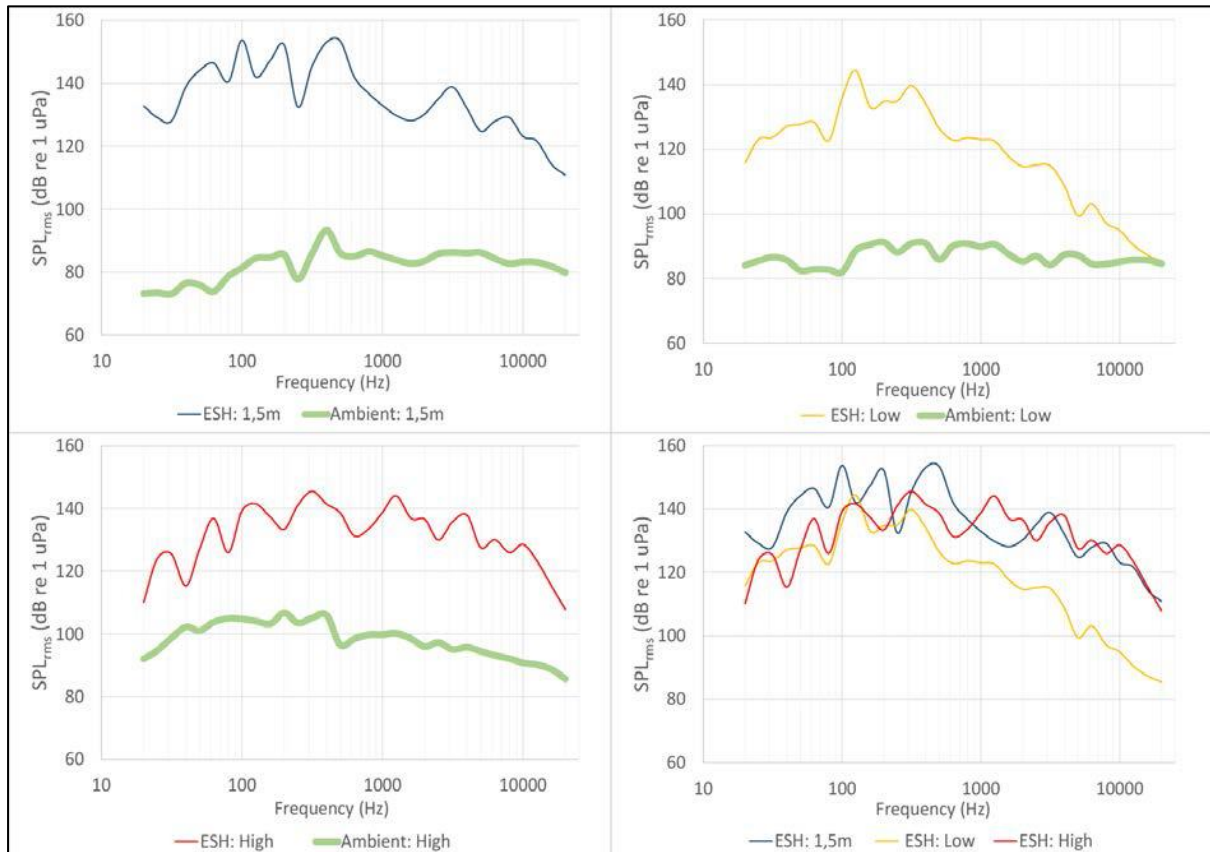


Figure 55 - Spectrums of the ESH noise from the L12 and WESA. Frequency (Hz) on the x-axis and sound pressure level root mean square (dB re 1 μ Pa) on the y-axis. (a) L12 ESH noise in SWH 1.5m (blue line) and ANLs in SWH 1.5m (green line). (b) WESA ESH noise in Low (SWH 1.5 \pm 0.15m) (yellow line) and ANLs in Low (green line). (c) WESA ESH noise in High (SWH 2.5 \pm 0.5m) (red line) and ANLs in High (green line). (d) Comparison between all ESH: L12: SWH 1.5 (blue line), WESA: Low (yellow line) and WESA: High (red line) [57].

References

- [1] I. Dincer, "Renewable energy and sustainable development: a crucial review," *Renewable and Sustainable Energy Reviews*, vol. 4, no. 2, pp. 157-175, 2000.
- [2] I. Burton, "Report on Reports: Our Common Future: The World Commission on Environment and Development," *Environment: Science and Policy for Sustainable Development*, vol. 29, no. 5, pp. 25-29, 1987.
- [3] B. Drew, A. Plummer, and M. N. Sahinkaya, "A review of wave energy converter technology," *Proceedings of the Institution of Mechanical Engineers, Part A: Journal of Power and Energy*, vol. 223, no. 8, pp. 887-902, 2009.
- [4] M. Leijon, H. Bernhoff, M. Berg, and O. Ågren, "Economical considerations of renewable electric energy production—especially development of wave energy," *Renewable Energy*, vol. 28, no. 8, pp. 1201-1209, 2003.
- [5] D. Brown and J. Jorgensen, "Machine-condition monitoring using vibration analysis," *B&K Application Notes BO*, pp. 0209-11, 1990.
- [6] Z. Hameed, Y. Hong, Y. Cho, S. Ahn, and C. Song, "Condition monitoring and fault detection of wind turbines and related algorithms: A review," *Renewable and Sustainable Energy Reviews*, vol. 13, no. 1, pp. 1-39, 2009.
- [7] P. Charles, J. K. Sinha, F. Gu, L. Lidstone, and A. Ball, "Detecting the crankshaft torsional vibration of diesel engines for combustion related diagnosis," *Journal of Sound and Vibration*, vol. 321, no. 3, pp. 1171-1185, 2009.
- [8] D. Gu and B. Choi, "Machinery Faults Detection Using Acoustic Emission Signal, Acoustic Waves—From Microdevices to Helioseismology, Prof. Marco G. Beghi (Ed.), ISBN: 978-953-307-572-3," *InTech*, verfügbar von: www.intechopen.com, 2011.
- [9] M. Ali and D. Mba, "Observation of Acoustic Emission in A Hydrodynamic Bearing," in *The 2nd International Conference on Technical Inspection and TINDT October Teheran Iran*, 2008.
- [10] D.-E. Lee, I. Hwang, C. M. Valente, J. Oliveira, and D. A. Dornfeld, "Precision manufacturing process monitoring with acoustic emission," *International Journal of Machine Tools and Manufacture*, vol. 46, no. 2, pp. 176-188, 2006.

- [11] T. Kim, J. Lee, S. Cho, and T. Kim, "Acoustic emission monitoring during laser shock cleaning of silicon wafers," *Optics and Lasers in Engineering*, vol. 43, no. 9, pp. 1010-1020, 2005.
- [12] University of Rhode Island. (2002 - 2015, 30/09/2016). *Discovery of Sound in the Sea*.
- [13] J. C. Goold, "Acoustic assessment of populations of common dolphin *Delphinus delphis* in conjunction with seismic surveying," *Journal of the Marine Biological Association of the United Kingdom*, vol. 76, no. 03, pp. 811-820, 1996.
- [14] I. El-Thalji, I. Alsyouf, and G. Ronsten, "A model for assessing operation and maintenance cost adapted to wind farms in cold climate environment: based on Onshore and offshore case studies," in *European Offshore Wind Conference Proceedings*, Stockholm, Sweden, 14-16 September 2009.
- [15] D. Ross, *Power from the Waves*. Oxford University Press, USA, 1995.
- [16] S. H. Salter, "Wave power," *Nature*, vol. 249, no. 5459, pp. 720-724, 1974.
- [17] A. Clément *et al.*, "Wave energy in Europe: current status and perspectives," *Renewable and Sustainable Energy Reviews*, vol. 6, no. 5, pp. 405-431, 2002.
- [18] M. A. Delucchi and M. Z. Jacobson, "Providing all global energy with wind, water, and solar power, Part II: Reliability, system and transmission costs, and policies," *Energy Policy*, vol. 39, no. 3, pp. 1170-1190, 2011.
- [19] L. Mofor, J. Goldsmith, and F. Jones, "OCEAN ENERGY: Technology Readiness, Patents, Deployment Status and Outlook," *Abu Dhabi*, 2014.
- [20] *Ocean Energy: State of the Art*. Available: [Online], http://si-ocean.eu/en/upload/docs/WP3/Technology%20Status%20Report_FV.pdf (Accessed: 27th April 2015).
- [21] J. Cruz, *Ocean wave energy: current status and future perspectives*. Springer Science & Business Media, 2007.
- [22] M. Mohamed and S. Shaaban, "Optimization of blade pitch angle of an axial turbine used for wave energy conversion," *Energy*, vol. 56, pp. 229-239, 2013.
- [23] C. C. Mei, "Power extraction from water waves," *Journal of Ship Research*, vol. 20, pp. 63-66, 1976.
- [24] T. Stewart, "The influence of harbour geometry on the performance of OWC wave power converters," Ph. D. Thesis, The Department of Civil Engineering, The Queen's University of Belfast, UK, 1993.

- [25] S. Raghunathan, C. Tan, and O. Ombaka, "Performance of the Wells self-rectifying air turbine," *Aeronautical Journal*, vol. 89, no. 890, pp. 369-379, 1985.
- [26] M. Inoue, K. Kaneko, T. Setoguchi, and S. Raghunathan, "The fundamental characteristics and future of Wells turbine for wave power generation," *Science of Machine*, vol. 39, no. 2, pp. 275-280, 1987.
- [27] L. Gato and A. d. O. Falcao, "Aerodynamics of the wells turbine: Control by swinging rotor-blades," *International Journal of Mechanical Sciences*, vol. 31, no. 6, pp. 425-434, 1989.
- [28] J. H. Horlock, *Axial flow turbines*. Butterworth, 1966.
- [29] S. Raghunathan, "A methodology for Wells turbine design for wave energy conversion," *Proceedings of the Institution of Mechanical Engineers, Part A: Journal of Power and Energy*, vol. 209, no. 3, pp. 221-232, 1995.
- [30] T. Setoguchi, K. Kaneko, H. Taniyama, H. Maeda, and M. Inoue, "Impulse turbine with self-pitch-controlled guide vanes for wave power conversion: guide vanes connected by links," *International Journal of Offshore and Polar Engineering*, vol. 6, no. 1, pp. 76-80, 1996.
- [31] S. Raghunathan and W. Beattie, "Aerodynamic performance of contra-rotating Wells turbine for wave energy conversion," *Proceedings of the Institution of Mechanical Engineers, Part A: Journal of Power and Energy*, vol. 210, no. 6, pp. 431-447, 1996.
- [32] G. Machine. *Wavebob*. Available: [Online], <https://dublin.sciencegallery.com/book/export/html/11698> (Accessed 16 December 2014).
- [33] M. C. Current. *On Truth at Kent State & Safe Renewable Energy Solutions* Available: [Online], <https://mendocoastcurrent.wordpress.com/tag/pelamis-wave-power/> (Accessed: 29th April 2015).
- [34] D. Dzhonova-Atanasova, R. Popov, and A. Georgiev, "Challenges of Marine Power in the Balkan Region," *Balkan Journal of Electrical and Computer Engineering*, vol. 1, no. 2, 2013.
- [35] R. D. (2013). *Oceanlinx wave power turbines - wave energy from down under*. Available: [Online], <http://www.alternativeconsumer.com/2013/08/22/oceanlinx-wave-power-turbines-wave-energy-from-down-under/> (Accessed 13 October 2016).

- [36] O. EI. (2016). *Marine and hydrokinetic technology glossary*. Available: [Online], http://en.openei.org/wiki/Marine_and_Hydrokinetic_Technology_Glossary (Accessed: 13 October 2016).
- [37] *Wave Dragon*. Available: [Online], <https://stateofgreen.com/en/profiles/wave-dragon-aps> (Accessed: 29 April 2015).
- [38] WordPress. *Renewable energy*. Available: [Online], <https://baonguyen1994.wordpress.com/>, (Accessed: 15 December 2016).
- [39] WordPress. *A Nuclear Investment: The Future of Nuclear Energy in the US*. Available: [Online], <https://energycrWoSs2012.wordpress.com/>, (Accessed: 15 December 2016).
- [40] U. D. Commons. *Energy and the Environment - A Coastal Perspective*. Available: [Online], <http://coastalenergyandenvironment.web.unc.edu/>, (Accessed: 15 December 2016).
- [41] Tethys. *Pico oscillating water column WEC power plant*. Available: [Online], <https://tethys.pnnl.gov/annex-iv-sites/pico-oscillating-water-column>, (Accessed: 16th October 2016).
- [42] E. Enferad and D. Nazarpour, *Ocean's Renewable Power and Review of Technologies: Case Study Waves*. INTECH Open Access Publisher, 2013.
- [43] R. D. Ford and J. Morgan, "Introduction to Acoustics," ed: Pergamon, 1971.
- [44] C. H. Hansen, "Fundamentals of acoustics," *Goelzer, B., H. Hansen, CH, Sehrndt, GA (eds.) Occupational Exposure to Noise: Evaluation, Prevention and Control. World Health Organization, Geneva, 2001*.
- [45] Wikibooks. *"Threshold of Hearing and Pain"*. [Online]. Available: http://en.wikibooks.org/wiki/Acoustics/Threshold_of_Hearing/Pain. [Accessed: 30 April 2015].
- [46] M. P. Norton and D. G. Karczub, *Fundamentals of Noise and Vibration Analysis for Engineers*. Cambridge University Press, 2003.
- [47] Vernier. *"Sound Level Meter," Venier Software & Technology*. [Online]. Available: <http://www2.vernier.com/booklets/slm-bta.pdf> [Accessed: May 1st, 2015].
- [48] G. M. Wenz, "Acoustic ambient noise in the ocean: spectra and sources," *The Journal of the Acoustical Society of America*, vol. 34, no. 12, pp. 1936-1956, 1962.
- [49] C. E. Baukal Jr, *The John Zink Hamworthy Combustion Handbook: Volume 1-Fundamentals*. CRC Press, 2012.

- [50] E. H. Berger, *The noise manual*. Aiha, 2003.
- [51] Discovery. "The First Practical Uses of Underwater Acoustics: The Early," *Discovery of Sound in Sea*. [Online]. Available: <http://www.dosits.org/people/history/early1900/> [Accessed: May 1st, 2015].
- [52] M. Austin, N. Chorney, J. Ferguson, D. Leary, C. O'Neill, and H. Sneddon, "Assessment of Underwater Noise Generated by Wave Energy Devices," Oregon Wave Energy Trust.
- [53] J. Nedwell, "Measurements of Baseline Underwater Noise and Vibration in Sruwaddacon Bay, Co. Mayo, Eire," Subacoustech Enviromental Report No. E270R0103, 2010.
- [54] R. Urick, "J.(1975). Principles of Underwater Sound," ed: New York: McGraw-Hill.
- [55] S. Patrício, A. Moura, and T. Simas, "Wave energy and underwater noise: State of art and uncertainties," in *OCEANS 2009-EUROPE*, 2009, pp. 1-5: IEEE.
- [56] S. Patrício, C. Soares, and A. Sarmento, "Underwater noise modelling of wave energy devices," *Proc. 8th European Wave and Tidal Energy Conference*, pp. 1020-1028, 2009.
- [57] K. Haikonen, J. Sundberg, and M. Leijon, "Characteristics of the operational noise from full scale wave energy converters in the Lysekil project: estimation of potential environmental impacts," *Energies*, vol. 6, no. 5, pp. 2562-2582, 2013.
- [58] J. K. Garrett, M. J. Witt, and L. Johanning, "Underwater sound levels at a wave energy device testing facility in Falmouth bay, UK," in *The Effects of Noise on Aquatic Life II*: Springer, 2016, pp. 331-339.
- [59] J. Tougaard, "Underwater Noise from a Wave Energy Converter Is Unlikely to Affect Marine Mammals," *PloS one*, vol. 10, no. 7, p. e0132391, 2015.
- [60] E. Cruz, T. Simas, and E. Kasanen, "Discussion of the effects of underwater noise radiated by a wave energy device–Portugal," in *Proceedings of the 11th European Wave and Tidal Energy Conference*. [https:// www. researchgate. net/publication/281775636_Discussion_of_the_effects_of_the_underwater_noise_radiated_by_a_wave_energy_device_-Portugal](https://www.researchgate.net/publication/281775636_Discussion_of_the_effects_of_the_underwater_noise_radiated_by_a_wave_energy_device_-Portugal), 2015.
- [61] S. R. Paul Lepper, Victor Humphrey, Micheal Butler, "Review of current knowledge of underwater noise emissions from wave and tidal stream energy devices.," The Crown Estate, 2013.

- [62] M. M. Services. [Online]. *Renewable Energy and Alternate Use Program, U.S. Department of the Interior*. [Accessed: October 20th, 2016]. Available: <http://ocsenergy.anl.gov>.
- [63] C. Erbe, "Underwater noise of whale-watching boats and potential effects on killer whales (*Orcinus orca*), based on an acoustic impact model," *Marine Mammal Science*, vol. 18, no. 2, pp. 394-418, 2002.
- [64] H. Medwin and C. S. Clay, *Fundamentals of Acoustical Oceanography*. Academic Press, 1997.
- [65] D. Farmer, "Fundamentals of Acoustical Oceanography," *Eos, Transactions American Geophysical Union*, vol. 79, no. 34, pp. 408-408, 1998.
- [66] H. Medwin and J. E. Blue, *Sounds in the sea: From ocean acoustics to acoustical oceanography*. Cambridge University Press, 2005.
- [67] X. Lurton, *An introduction to underwater acoustics: principles and applications*. Springer, 2002.
- [68] L. E. Kinsler, A. R. Frey, A. B. Coppens, and J. V. Sanders, "Fundamentals of acoustics," *Fundamentals of Acoustics, 4th Edition, by Lawrence E. Kinsler, Austin R. Frey, Alan B. Coppens, James V. Sanders, pp. 560. ISBN 0-471-84789-5. Wiley-VCH, December 1999.*, vol. 1, 1999.
- [69] J. DeSanto, "Theoretical methods in ocean acoustics," in *Ocean Acoustics*: Springer, 1979, pp. 7-77.
- [70] J. D. Holmes, W. M. Carey, J. F. Lynch, A. E. Newhall, and A. Kukulya, "An autonomous underwater vehicle towed array for ocean acoustic measurements and inversions," in *Oceans 2005-Europe*, 2005, vol. 2, pp. 1058-1061: IEEE.
- [71] B. Würsig and C. Greene Jr, "Underwater sounds near a fuel receiving facility in western Hong Kong: relevance to dolphins," *Marine Environmental Research*, vol. 54, no. 2, pp. 129-145, 2002.
- [72] S. A. Hayes, D. K. Mellinger, D. A. Croll, D. P. Costa, and J. F. Borsani, "An inexpensive passive acoustic system for recording and localizing wild animal sounds," *The Journal of the Acoustical Society of America*, vol. 107, p. 3552, 2000.
- [73] R. Soheilifar, A. M. Arasteh, J. Rasekhi, and A. G. Urimi, "A computer simulation of underwater sound propagation based on the method of parabolic equations," in *Proceedings of the WSEAS International Conference on Applied Computing*

- Conference*, 2008, pp. 91-97: World Scientific and Engineering Academy and Society (WSEAS).
- [74] Acoustics. "Ocean Acoustics Library". [Online]. Available: <http://oalib.hlsresearch.com/>. [Accessed: May 8th, 2015].
- [75] E. de Sousa Costa and E. B. Medeiros, "Mecánica Computacional, Volume XXIX. Number 22. Interdisciplinary Topics in Mathematics (C)," 2010.
- [76] P. C. Etter, *Underwater acoustic modeling and simulation*. CRC Press, 2013.
- [77] M. J. Isakson and N. P. Chotiros, "Finite element modeling of reverberation and transmission loss in shallow water waveguides with rough boundaries," *The Journal of the Acoustical Society of America*, vol. 129, no. 3, pp. 1273-1279, 2011.
- [78] P. Alexander, A. Duncan, and N. Bose, "Modelling sound propagation under ice using the Ocean Acoustics Library's Acoustic Toolbox," in *Acoustics 2012 Fremantle: Acoustics, Development and the Environment*, 2012, vol. 400, pp. 1-7.
- [79] A. J. Duncan and A. L. Maggi, "A consistent, user friendly interface for running a variety of underwater acoustic propagation codes," *Proceedings of ACOUSTICS 2006*, pp. 471-477, 2006.
- [80] M. B. Porter, "The KRAKEN normal mode program," DTIC Document 1992.
- [81] C. L. Pekeris, "Theory of propagation of explosive sound in shallow water," vol. 27, ed: Geol. Soc. Amer. Mem., 1948.
- [82] F. B. Jensen, W. A. Kuperman, M. B. Porter, and H. Schmidt, *Computational ocean acoustics*. Springer Science & Business Media, 2011.
- [83] C. Erbe, R. McCauley, C. McPherson, and A. Gavrilov, "Underwater noise from offshore oil production vessels," *The Journal of the Acoustical Society of America*, vol. 133, no. 6, pp. EL465-EL470, 2013.
- [84] T. P. Lloyd, V. F. Humphrey, and S. R. Turnock, "Noise modelling of tidal turbine arrays for environmental impact assessment," in *Proceedings of the 9th European Wave and Tidal Energy Conference, Southampton, UK*, 2011.
- [85] A. Ivakin, "Modelling of sound scattering by the sea floor," *Le Journal de Physique IV*, vol. 4, no. C5, pp. C5-1095-C5-1098, 1994.
- [86] W. J. Richardson, C. R. Greene Jr, C. I. Malme, and D. H. Thomson, *Marine mammals and noise*. Academic Press, 2013.
- [87] M. Cronin, C. Duck, O. Cadhla, R. Nairn, D. Strong, and C. O'keeffe, "An assessment of population size and distribution of harbour seals in the Republic of Ireland during

- the moult season in August 2003," *Journal of Zoology*, vol. 273, no. 2, pp. 131-139, 2007.
- [88] J. Tougaard *et al.*, "Harbour seals on Horns Reef before, during and after construction of Horns Rev Offshore Wind Farm," *Vattenfall A/S*, 2006.
- [89] S. P. Robinson and P. A. Lepper, "'Scoping study: Review of current knowledge of underwater noise emissions from wave and tidal stream energy devices'," The Crown Estate, 2013.
- [90] A. Farcas, P. M. Thompson, and N. D. Merchant, "Underwater noise modelling for environmental impact assessment," *Environmental Impact Assessment Review*, vol. 57, pp. 114-122, 2016.
- [91] C. Multiphysics, "Comsol Multiphysics Modelling Guide 3.2," ed, September 2005, pp. 26 - 35.
- [92] I. Gloza, "Ship's underwater noise measurements using sound intensity method," *Hydroacoustics*, vol. 12, pp. 53-60, 2009.
- [93] M. Broudic, N. Croft, M. Willis, I. Masters, and C. Sei-Him, "Comparison of underwater background noise during Spring and Neap tide in a high tidal current site: Ramsey Sound," *Proceedings of Meetings on Acoustics*, vol. 17, no. 1, p. 070104, 2014.
- [94] M. R. Willis, M. Broudic, C. Haywood, I. Masters, and S. Thomas, "Measuring underwater background noise in high tidal flow environments," *Renewable Energy*, vol. 49, pp. 255-258, 2013.
- [95] M. B. Miles R Willis, Ian Masters, "Ambient Underwater Noise in High and Low Energy Flow Conditions," ed. Rome: 4th Int. Conf. Wind Turbine Noise. National Research Council of Italy (CNR), 2011.
- [96] C. Bassett, J. Thomson, B. Polagye, and K. Rhinefrank, "Underwater noise measurements of a 1/7 th scale wave energy converter," in *OCEANS 2011*, 2011, pp. 1-6: IEEE.
- [97] O. W. Ikpekha, F. Soberon, and S. Daniels, "Modelling the propagation of Underwater Acoustic Signals of a Marine Energy Device Using Finite Element Method," presented at the International Conference on Renewable Energies and Power Quality, Cordoba, Spain, 2014.
- [98] L. L. Mazzuca, "Potential effects of low frequency sound (LFS) from commercial vessels on large whales," Thesis Submitted to University of Washington, 2001.

- [99] M. F. McKenna, D. Ross, S. M. Wiggins, and J. A. Hildebrand, "Underwater radiated noise from modern commercial ships," *The Journal of the Acoustical Society of America*, vol. 131, no. 1, pp. 92-103, 2012.
- [100] M. Pricop, V. Chitac, F. Gheorghe, T. Papzara, V. Oncica, and D. Atodiresei, "Underwater radiated noise of ships' machinery in shallow water," in *Conference on Manufacturing Engineering, Quality and Production Systems*, Romania, 2010.
- [101] S. Lee, Y. Lee, S. Kim, J. Park, and J. Rak, "Measurement of Low Frequency Ambient Noise using Screened Hydrophone in Shallow Water," in *Proceedings of Symposium on Ultrasonic Electronics*, 2010, vol. 31, no. 2010, pp. 421-422.
- [102] J. Hildebrand, "Sources of anthropogenic sound in the marine environment," in *Report to the Policy on Sound and Marine Mammals: An International Workshop. US Marine Mammal Commission and Joint Nature Conservation Committee, UK. London, England*, 2004.
- [103] M. F. McKenna, S. M. Wiggins, and J. A. Hildebrand, "Relationship between container ship underwater noise levels and ship design, operational and oceanographic conditions," *Scientific Reports*, vol. 3, 2013.
- [104] J. A. Hildebrand, "Anthropogenic and natural sources of ambient noise in the ocean," *Marine Ecology Progress Series*, vol. 395, no. 5, 2009.
- [105] C. Briciu-Burghina, T. Sullivan, J. Chapman, and F. Regan, "Continuous high-frequency monitoring of estuarine water quality as a decision support tool: a Dublin Port case study," *Environmental monitoring and assessment*, vol. 186, no. 9, pp. 5561-5580, 2014.
- [106] Z. Bedri, M. Bruen, A. Dowley, and B. Masterson, "Environmental consequences of a power plant shut-down: A three-dimensional water quality model of Dublin Bay," *Marine Pollution Bulletin*, vol. 71, no. 1, pp. 117-128, 2013.
- [107] J. G. Proakis, E. M. Sozer, J. A. Rice, and M. Stojanovic, "Shallow water acoustic networks," *Communications Magazine, IEEE*, vol. 39, no. 11, pp. 114-119, 2001.
- [108] S. P. Robinson *et al.*, "Measurement of underwater noise arising from marine aggregate dredging operations.," MALSF Report, Submitted to Loughborough University, 2011.
- [109] M. Purcell, A. Vasudevan, and D. Gregg, "Real-time sensor signal capture from a harsh environment," in *Distributed Simulation and Real Time Applications (DS-RT), 2012 IEEE/ACM 16th International Symposium on*, 2012, pp. 36-43: IEEE.

- [110] H. Kolar *et al.*, "The design and deployment of a real-time wide spectrum acoustic monitoring system for the ocean energy industry," in *OCEANS-Bergen, 2013 MTS/IEEE*, 2013, pp. 1-4: IEEE.
- [111] S. Robinson, P. Lepper, and R. Hazelwood, "Good Practice Guide for Underwater Noise Measurement," *National Measurement Office, Marine Scotland, The Crown Estate*, 2014.
- [112] M. J. Wilmut, N. R. Chapman, G. J. Heard, and G. R. Ebbeson, "Inversion of Lloyd Mirror Field for determining a source's track," *Oceanic Engineering, IEEE Journal of*, vol. 32, no. 4, pp. 940-947, 2007.
- [113] A. Zak, "Ship's Hydroacoustics Signatures Classification using Neural Networks [in] J. I. Mwasiagi (ed.) Self Organizing Maps—applications and novel algorithms design," ed: INTECH, 2011.
- [114] L. Brekhovskikh and I. Lysanov, "Fundamentals of ocean acoustics, AIP series in modern acoustics and signal processing," ed: Springer, New York, 2003.
- [115] F. Fisher and V. Simmons, "Sound absorption in sea water," *The Journal of the Acoustical Society of America*, vol. 62, no. 3, pp. 558-564, 1977.
- [116] S. Richards, E. Harland, and S. Jones, "Underwater noise study supporting Scottish Executive Strategic Environmental Assessment for marine renewables," *QinetiQ Ltd. Farnborough, Hampshire*, 2007.
- [117] C. S. Sofia Patricio, "Analysis of underwater noise data from the Pico Wave Power Plant as a complementary tool to analyse operational phenomena," in *Proceedings of the 11th European Conference on Underwater Acoustics*, Edinburgh, 2012, pp. 289-296.
- [118] K. Haikonen, J. Sundberg, and M. Leijon, "Hydroacoustic measurements of the radiated noise from Wave Energy Converters in the Lysekil project and project WESA," in *Proceedings UA 2013*, 2013, pp. 199-209.
- [119] F. Ihlenburg, *Finite element analysis of acoustic scattering*. Springer Science & Business Media, 1998.
- [120] B. Katsnelson, V. Petnikov, and J. Lynch, *Fundamentals of shallow water acoustics*. Springer Science & Business Media, 2012.
- [121] Comsol Multiphysics, "Acoustics module user guide version 4.2," in *User's manual*, ed, 2011.

- [122] L. Alberotanza, "Active and passive remote sensors as a new technology for coastal and lagoon monitoring," *Aquatic Conservation: Marine and Freshwater Ecosystems*, vol. 11, no. 4, pp. 267-272, 2001.